Distribution Agreement

In presenting this thesis or dissertation as a partial fulfillment of the requirements for an advanced degree from Emory University, I hereby grant to Emory University and its agents the non-exclusive license to archive, make accessible, and display my thesis or dissertation in whole or in part in all forms of media, now or hereafter known, including display on the world wide web. I understand that I may select some access restrictions as part of the online submission of this thesis or dissertation. I retain all ownership rights to the copyright of the thesis or dissertation. I also retain the right to use in future works (such as articles or books) all or part of this thesis or dissertation.

Signature:

_____ _____

[Lisa Jean McLay] Date

CHARACTERIZATION OF FACTORS AND MECHANISMS OF VIRULENCE OF ARENAVIRUSES THROUGH MUTATIONAL ANALYSIS

By

Lisa Jean McLay
Doctor of Philosophy

Graduate Division of Biological and Biomedical Sciences
Immunology and Molecular Pathogenesis

_____
Hinh Ly, Ph.D.
Advisor

_____
Yuying Liang, Ph.D.
Committee Member

_____
Aftab Ansari, Ph.D.
Committee Member

_____
Eric Hunter, Ph.D.
Committee Member

_____
Andrew Gewirtz, Ph.D.
Committee Member

_____
Paul Rota, Ph.D.
Committee Member

Accepted:

_____
Lisa A. Tedesco, Ph.D.
Dean of the James T. Laney School of Graduate Studies

_____
Date

CHARACTERIZATION OF FACTORS AND MECHANISMS OF VIRULENCE OF ARENAVIRUSES THROUGH MUTATIONAL ANALYSIS

By

Lisa Jean McLay
B.S., Salem State College, 2005

Advisor: Hinh Ly, Ph.D.

An abstract of
a dissertation submitted to the Faculty of the
James T. Laney School of Graduate Studies of Emory University
in partial fulfillment of the requirements for the degree of
Doctor of Philosophy
Graduate Division of Biological and Biomedical Sciences
Immunology and Molecular Pathogenesis
2013

ABSTRACT

CHARACTERIZATION OF FACTORS AND MECHANISMS OF VIRULENCE OF ARENAVIRUSES THROUGH MUTATIONAL ANALYSIS

By Lisa Jean McLay

Arenaviruses are one of the most neglected tropical pathogens. The most prominent human pathogen belonging to this group is Lassa Fever virus (LASV), which is responsible for ~5,000 - 10,000 deaths and ~2 million infections annually. Mutational analysis of arenaviral proteins may provide insight into the pathological mechanisms of these viruses.

A related arenavirus, Pichinde virus (PICV), is capable of causing a disease in guinea pigs that mimics LASV infection in humans. We have sequenced two strains of PICV with different disease phenotypes in infected guinea pigs. The P2 strain causes a mild disease from which the animals quickly recover. The P18 strain results in a highly virulent disease, which results in death. While the phenotypes are vastly different, relatively few sequence changes exist between them.

We have developed reverse genetics systems for both the P2 and P18 strains of PICV, which have allowed us to generate recombinant viruses. Through mutational analysis, we have identified sequence changes in the L polymerase that contribute to the increased pathogenesis of P18. Three amino acid changes in the C terminus of L are required for increased virulence of the P18 strain by increasing the rate of viral genome replication, indicating that the rate of viral genome replication is an important factor in arenavirus pathogenesis.

We have also developed a LASV minireplicon system in order to perform mutational analysis of the LASV nucleoprotein (NP). We have shown that LASV NP contains a cap-binding domain in its N terminus that is required to initiate viral RNA transcription. We have also shown that LASV NP contains a 3'-5' exoribonuclease domain in its C terminus that is required to mediate type-I interferon inhibition. We therefore propose a novel mechanism of immune evasion in which the NP protein degrades viral RNAs that would otherwise be detected by innate immune sensors, therefore allowing these viruses to replicate to high levels in infected patients.

Collectively, this work characterizes two important viral factors (NP and L polymerase) required for arenaviral replication, transcription and immune evasion. This information will aid in the development of vaccines and therapeutics against arenaviral hemorrhagic fever.

CHARACTERIZATION OF FACTORS AND MECHANISMS OF VIRULENCE OF ARENAVIRUSES THROUGH MUTATIONAL ANALYSIS

By

Lisa Jean McLay
B.S., Salem State College, 2005

Advisor: Hinh Ly, Ph.D.

A dissertation submitted to the Faculty of the
James T. Laney School of Graduate Studies of Emory University
in partial fulfillment of the requirements for the degree of
Doctor of Philosophy
Graduate Division of Biological and Biomedical Sciences
Immunology and Molecular Pathogenesis
2013

ACKNOWLEDGEMENTS

Firstly, I would like to thank my advisor, Dr. Hinh Ly, for welcoming me into his lab and taking me under his wing. Thank you for your encouragement and patience, and especially for your enthusiasm. You were always smiling, even on the stressful days. Also, thank you for being accommodating when things in our lab were changing, and for working with me to find a way for me to continue my studies and complete my dissertation. Equally, I would like to thank Dr. Yuying Liang, who was heavily involved in my PhD work, and provided excellent experimental guidance and advice. Again, thank you for your encouragement and patience, and for never turning me away from your office when I had questions.

To Dr. Aftab Ansari, I cannot express my gratitude for everything you have done. Thank you for welcoming me into your lab and making it possible for me to finish my dissertation work here at Emory. Thank you for your guidance and advice. Most of all, thank you for your kindness, and for your steadfast support.

I would like to thank Dr. Tristram Parslow for your unflagging support. Your kind words are more appreciated than you know.

I would like to thank my committee members for their guidance and expert advice. I could not have asked for a better committee.

To Dr. Shuiyun Lan, I owe you so many thanks. You took me under your wing and taught me everything in the lab. Thank you for your guidance, your teaching, your patience, and most of all, your friendship. I am so glad to have had the opportunity to work with you.

To my labmates, I love you all. Dr. Zhongtao Xin, you will always be my lab "big brother". Jingming Liu, I don't think I ever saw you without a smile on your face. You are truly missed. Dr. Sushma Bhosle, I will always value our friendship. Dr. Yuhong Liang, your smile is infectious, and you never failed to bring some sunshine to the lab. To Dr. Naveen Kumar, you could always make me laugh, and are a true friend. Dr. Luan Dao, you would always sit and go over my data with me, even though it was completely unrelated to your project. Thank you for that, and your invaluable friendship. To Dr. Jialong Wang, my buddy, I will forever miss our late nights in the lab, our guinea pig room conversations, and learning to moonwalk with you. You will always have a friend in me. To my "girls", words cannot express how grateful I am for your friendship. Dr. Katie Carroll, we have been through a lot of ups and downs together, and you were always there when I needed you. Dr. Suganthi Suppiah, you are one of the kindest people I know, and I am so glad that we became friends. Thank you for your encouragement. Jill Seladi, you will always be one of my great friends, and I want to thank you for your "medicinal" support as well. You always know how to make me feel better! To Shamika Danzy, I don't even know where to begin. You have been there to pick me up every time things got tough. You are one of my most treasured friends. I cannot say thank you enough for your strength, understanding, and support. That and you give the best hugs.

While I have thanked the members from my lab, I am lucky enough to have an "adoptive" lab family to thank as well. To Anne Mayne, thank you for your assistance and understanding. Martha Simmons, I have enjoyed our conversations, and your kindness. Dr. Siddappa Byareddy, thank you so much for your excellent scientific

advice. I sincerely appreciate all of your help. Paul Dunbar, I have enjoyed all of our lab conversations, and am so glad that we had the chance to become friends. You will make a great scientist. Brianne Kallam, you are such a pleasant person, and I know you will go on to do great things. Robert Russo, you have always been so congenial, and thank you for the donuts! Tara Villinger, you are a very sweet person, and I have really enjoyed our "girl talk". Dawn Little, your smile could light up a room. You are one of the nicest people I know, and I'm so glad to have had the chance to become friends.

I am lucky enough to have many friends to thank as well. Through the years I have come to value the quality of my friends, rather than the quantity. In that regard, I am truly fortunate. To Mr. Ed Morgan, my friend and neighbor, thank you for all of your kindness and assistance. It means more to me than you know. To my running buddies, Dr. Kathryn Knoop, Dr. Erin West, and Dr. Krystal Hudson, I will always look back fondly on our conversations and all the laughter we shared. You guys are great friends. To my neighbors and friends, Katie and Chris Kitchen, thank you for your friendship, understanding, and support. I will miss our nights of cornhole and sitting out by the fire. And thanks for letting me back in my house when I get locked out! Dana Tucker, my friend and confidant, it has been so nice to have someone to relate to. I am so glad to have you for a friend. Shamika Danzy, I am going to thank you again, because you are that awesome. I love you. Dr. Noah Alberts-Grill, I cannot thank you enough for just being there. You have been a rock to me. You have become my life guru, and one of my closest friends. Dr. Justine Liepkalns, I have never met someone who can make me laugh half as much as you do. You are the other pea in my pod. You've been there through

thick and thin, and you are always there to catch me when I'm down, and I can't thank you enough.

To Colleen 'Donovan' Berube, my best friend in the world, I love you more than I can tell. You've been by my side since we were seven years old, and you've never faltered. You've been there through everything, and you've never given up on me. You are the most loyal, loving, thoughtful, and kind-hearted person I know. I don't know what I would do without you. A friend like you only comes around once in a lifetime, and I am so grateful for you. I love you Bean.

Yes, I am dedicating a section to my pets. Anyone who knows me should not be surprised. Todd, Mick, Bandit, and Cricket, thank you for all of your snuggles and kisses. You always make me smile when I walk in through the door at the end of the day.

To my family, you are amazing. I cannot believe how unbelievably lucky I am to belong to such an incredible group of people. To my grandfather, Robert Baker, I love you and the way you can always make me laugh. To my grandparents who have passed on, Grammy Baker, Grampy McLay, and Grammy McLay, I will always cherish my memories of you and all the hugs you gave me. To my nephews, Jacob and Cole, I love you to the ends of the earth, and I love your bear-hugs. Jacob, the "good luck" picture you sent me that I kept in my pocket while I took my qualifying exam is still on the fridge. To my sister-in-law, Susan McLay, thank you for your encouragement and support in everything I do. It means the world to me to know that you will always support me, in any decision. To my big brother, Jared McLay, thank you for always being there, whether I am stuck in a tree, or have fuses catching on fire in my house. You

are the best big brother anyone could hope for. To my little brother, Brian McLay, thank you for never being afraid to hug me in front of your friends. Also, thanks for putting up with me no matter how much I tease you. You always know how to make me smile, and you will always be my "schnookie bear".

Mom, you are incredible. I am so lucky to have you. You really are the best mother anyone could hope for. You are always there when I need to talk, and you always offer encouragement and a smile when times are tough. You have been my shoulder to cry on, and my partner in crime. I know I can always laugh and goof around with you. You always know when you are needed, without me having to say anything. If there's anyone I know I can always count on, it's you. Thank you for all of your hugs, they have never been in short supply.

Dad, I have looked up to you since I was little, and will continue to do so for the rest of my life (and this has nothing to do with the fact that you are taller than me). If there is anyone in this world that I strive to be more like, it is you. When I need advice, I know I can always turn to you. Thank you for supporting me in all of my decisions, it means more to me than you know. You have always pushed me to challenge myself, and for that I owe you thanks. But mostly I want to say thanks for just being my dad, you're the best.

"Friendship is the only cement that will ever hold the world together."

– President Woodrow T. Wilson

TABLE OF CONTENTS

LIST OF TABLES

(listed in order of appearance as they appear in the chapter)

CHAPTER 1

CHAPTER 2

LIST OF FIGURES

(listed in order of appearance as they appear in the chapter)

CHAPTER 1

CHAPTER 2

CHAPTER 3

CHAPTER 1: INTRODUCTION

CHAPTER 1.1:

Targeting virulence mechanisms for the prevention and therapy of arenaviral hemorrhagic fever [1]

Lisa McLay[1], Aftab Ansari[1], Yuying Liang[2] and Hinh Ly[1,2]

[1]Department of Pathology and Laboratory Medicine, Emory University, Atlanta, GA 30322, [2]Department of Veterinary and Biomedical Sciences, University of Minnesota, Twin Cities, MN 55108

Abstract:

A number of arenaviruses are pathogenic for humans, but they differ significantly in virulence. Lassa virus, found in West Africa, causes severe hemorrhagic fever (HF), while the other principal Old World arenavirus, lymphocytic choriomeningitis virus, causes mild illness in persons with normal immune function, and poses a threat only to immunocompromised individuals. The New World agents, including Junin, Machupo and Sabia virus, are highly pathogenic for humans. Arenaviral HF is characterized by high viremia and general immune suppression, the mechanism of which is unknown. Studies using viral reverse genetics, cell-based assays, animal models and human genome-wide association analysis have revealed potential mechanisms by which arenaviruses cause severe disease in humans. Each of the four viral gene products (GPC, L polymerase, NP, and Z matrix protein) and several host-cell factors (e.g., α-dystroglycan) are responsible for mediating viral entry, genome replication, and the inhibition of apoptosis, translation and interferon-beta (IFNβ) production. This review summarizes current knowledge of the role of each viral protein and host factor in the pathogenesis of arenaviral HF. Insights from recent studies are being exploited for the development of novel therapies.

Introduction: arenaviral diseases of humans

The *Arenaviridae* family consists of a large group of single-stranded ambisense RNA viruses that are separated phylogenetically, serologically, and geographically into Old World (OW) and New World (NW) viruses. Some viruses from both groups cause significant morbidity and mortality in humans. Lassa virus, found in West Africa, causes severe hemorrhagic fever (HF), while the other principal OW arenavirus, lymphocytic choriomeningitis virus (LCMV), produces only mild illness in immunocompetent humans. In contrast, Junin virus (JUNV) and the other NW arenaviruses found in South America, cause severe hemorrhagic fever (HF). There are currently limited prevention and treatment measures against these pathogenic arenaviruses. The only available vaccine (Candid #1) has been developed and used extensively to prevent Argentine hemorrhagic fever (AHF) caused by JUNV [2]. Ribavirin, the only licensed antiviral for the treatment of arenaviral hemorrhagic fevers, has had mixed success and significant toxicity in treating arenaviral HF [3].

A major question is why some arenaviruses cause severe disease in humans, while others do not. Many factors have been proposed to explain the differential degrees of pathogenicity, such as host genetic polymorphism, routes and doses of infection, and viral virulence factors. It has been postulated that virulent arenaviruses are able to replicate to high levels and can effectively suppress host immunity. Recent studies using viral reverse genetics, cell-based assays, animal models, and human genome wide association analyses have revealed potential mechanisms that arenaviruses utilize to cause virulent infections in the hosts. Understanding viral virulence mechanisms is expected to facilitate the development of appropriate preventive and therapeutic strategies

against these deadly viral hemorrhagic fevers. This paper summarizes current progress in understanding the roles of viral factors in mediating efficient viral entry, enhanced viral RNA synthesis, inhibition of cellular apoptosis, translation and host innate immunity, all of which contribute to the virulence of pathogenic arenaviruses for humans.

Old World arenaviruses

Lassa virus (LASV) causes Lassa fever, resulting in approximately 2 million infections and 5-10,000 deaths annually in endemic area of West Africa [4]. LASV infection results in heterogeneity in disease manifestation that ranges from non-symptomatic to multi-organ failure and death. Patients infected with LASV are often misdiagnosed because of the wide range of symptoms they may exhibit. These symptoms include fever, malaise, petechial hemorrhage, edema, nausea, vomiting and diarrhea [5]. Up to one third of patients experience sensorineural deafness which remains even after recovery from the illness [6]. Fatal cases may display respiratory distress, shock, encephalopathy, seizures, shock, coma, and mucosal bleeding [5].

Lujo virus (LUJV), the only other known hemorrhagic fever-causing OW arenavirus, was identified during an outbreak of the disease in Lusaka (Zambia) and Johannesburg (Republic of South Africa) in 2008 [7]. Symptoms noted for patients infected with Lujo virus include fever, edema, mild bleeding, elevated liver transaminases, and thrombocytopenia [8].

Lymphocytic choriomeningitis virus (LCMV), which is found worldwide, has also been identified as pathogenic for immunocompromised individuals [9-12]. The data

at hand suggests that approximately 5% of the human population show evidence of exposure to LCMV, however, most acquired infections are asymptomatic or mild (Table 1.1.1)[13, 14]. Because the natural host of LCMV, *Mus musculus*, has a worldwide distribution, this virus can likewise be found in most regions. While acquired LCMV infection does not pose a serious threat to the general population, congenital infection with LCMV can be quite serious. This infection can result in spontaneous abortion and fetal death, or leave the infant with brain dysfunction. The incidence of congenital LCMV infection is unknown, as only serious cases are investigated for the cause of infection and reported [15]. While 35% of reported cases of congenital LCMV infection are fatal [16], we do not know the incidence of mild or asymptomatic congenital LCMV infections, as infants are not tested for infection. In recent years, LCMV has proven to be an important pathogen for transplant recipients. Fourteen cases of LCMV infection in transplant recipients have been identified, eleven of which have proven fatal [10-12].

New World arenaviruses

Several NW American arenaviruses, such as JUNV, Machupo (MACV), Guanarito (GTOV), Chapare (CHPV) and Sabia (SABV), can cause HF with high mortality rates. The disease courses for NW arenavirus infections also show some differences (Table 1.1.2). While only one human infection has been noted each for SABV and CHPV [17, 18], JUNV, MACV and GTOV have caused many cases of human disease [19-25]. Many of the arenaviral hemorrhagic fevers (both NW and OW) display shared symptoms, with some variation in manifestation of disease caused by these related

pathogens. Frequently, individuals with severe arenaviral hemorrhagic fever develop fever, petechial hemorrhage, edema, respiratory distress, shock, thrombocytopenia, leukopenia, and mucosal bleeding. While hepatitis is common in severe cases of Lassa fever, hepatitis is unusual or mild in South American hemorrhagic fevers. Neurologic symptoms, hemorrhaging, leukopenia, and thrombocytopenia are much more common in JUNV, GTOV, or MACV infection than LASV infection [26].

Arenavirus genome structure and replication cycle

Genome structure

Arenaviruses are enveloped, ambisense RNA viruses with a single-stranded genome composed of two segments (Figure 1.1.1). The genomic L (large) segment encodes the Z matrix protein and the L polymerase protein, while the S (small) segment encodes the glycoprotein (GPC) and nucleoprotein (NP). The genes encoded within each segment are separated by an intergenic region (IGR) with secondary structure that is thought to be involved in viral mRNA transcriptional termination [27]. The genomic segments contain conserved 5' and 3' untranslated regions (UTR) that are complementary to each other and form a panhandle structure at the end of the viral genome [28].

Receptor binding

The life cycle of arenaviruses (Figure 1.1.2) begins with cellular entry that is mediated by different cellular receptors. OW arenaviruses, along with NW clade C viruses Oliveros and Latino, use cellular α-dystroglycan (αDG) as their receptor in order to gain entry into the cell [29-31]. Dystroglycan is post-translationally cleaved to the subunit αDG, which contains the binding site for arenaviruses, and βDG, which spans the cell membrane and binds dystrophin on the interior of the cell, thus linking the molecule to the cytoskeletal network. This cell surface molecule anchors the cell by binding to laminin, a component of the extracellular matrix (ECM). αDG is expressed on many cell types, which accounts for the pantropic nature of OW arenavirus infection. In mice, this receptor has been shown to be highly expressed on dendritic cells, which are early targets in arenavirus infections, allowing the virus to suppress the immune response [32] (see below for more details). On the contrary, very little αDG is expressed on CD4, CD8, and B cells, which arenaviruses fail to infect [32]. When the virus binds to αDG, it displaces laminin. This can result in destabilization of the membrane and potentially a loss of cellular signaling, which can contribute to pathogenesis [33].

In order for αDG to function properly as an ECM receptor, it must first be post-translationally modified. This receptor is composed of two globular domains, located at each terminus, separated by a mucin-like domain. The cellular like-acetylglucosaminyltransferase (LARGE) recognizes the o-mannosylated N terminal end of the mucin-like domain of αDG, and acts as a bifunctional glycosyltransferase, with both xylosyltransferase and glucuronyltransferase activities, which produces repeating units of [-3-xylose-α1,3-glucuronic acid-β1-] [34]. Without this modification, αDG

would no longer be capable of interacting with either the ECM or the arenaviral GP [35, 36].

While αDG has long been known to be the receptor for OW arenaviruses, recent studies have shown that additional receptor(s) may also be used by these viruses. While laminin was capable of blocking the binding of LASV GP to αDG, it could not block LASV GP mediated infection of Vero cells, indicating that the virus was able to use alternative receptor(s) [35]. In addition, mice lacking the LARGE gene were shown to be susceptible to LCMV infection at similar levels to wildtype mice, again implicating usage of alternative receptor(s) [37]. Recently, 4 cellular factors have been identified to be important for LASV cellular entry. Axl, Tyro3, DC-SIGN, & LSECtin were shown to be capable of functioning as receptors independently of αDG, although LASV entry via any of these proteins is less efficient [38]. These receptors may be used in cell types such as hepatocytes, which show high levels of viral titers, even though DG expression is undetectable in these cells [39-41]. Ebola virus also uses these four receptors [42-44] and shares a similar cellular tropism as LASV, targeting dendritic cells, macrophages, endothelial cells, and the liver.

While OW arenaviruses largely utilize αDG as the cellular receptor, Clade B New World arenaviruses exploit Transferrin Receptor 1 (TfR1) as the means by which they gain entry into host cells [45]. TfR1 is responsible for the endocytosis of iron-bound transferrin, which is then transported to an acidified vesicle within the cell. Subsequently, iron is released and is then transported across the membrane into the cytoplasm [46]. The New World arenaviruses that are responsible for causing hemorrhagic fever in humans (MACV, JUNV, GTOV, SABV, and CHPV) all utilize

human Transferrin Receptor 1 (hTfR1) for cellular entry [47]. The nonpathogenic viruses Amapari (AMPV) and Tacaribe (TCRV) use TfR1 orthologs, but are unable to gain cellular entry via hTfR1 [48].

Membrane fusion and entry

Upon binding to the cellular receptor arenaviruses are internalized by vesicles, and are then released into the cytoplasm through a pH-dependent membrane fusion step that is accomplished by the transmembrane portion of the viral glycoprotein, GP2 [49]. In a process unique to arenavirus entry, the Old World arenaviruses LCMV and LASV were found to subvert classical routes of endosomal trafficking. Instead of passing through the early endosomes, the viruses are delivered directly to the late endosomes. In bypassing the early compartments, these viruses have been proposed to evade detection by the host endosomal immune receptors, and therefore fail to initiate a robust innate immune signaling [50].

Genome replication and transcription

Arenaviral replication takes place in the cytoplasm. Due to the ambisense coding strategy of these viruses, the NP and L genes are transcribed directly from the viral genomic segments, but the GPC and Z mRNAs must be transcribed from the antigenomic strand (Figure 1.1.3) [3]. The minimal trans-acting requirements for arenavirus replication and transcription are the NP and L proteins [51]. Arenavirus NP encapsidates

the genome, and the L polymerase performs genome replication & viral mRNA transcription. The arenaviral polymerase is an extremely large protein (~250kD) which, based on sequence analysis, contains four conserved domains. The RNA dependent RNA polymerase (RdRP) activity is found in domain III, and can be identified as such based on its similarity to other viral RdRPs [52]. Additionally, mutational analysis has identified two residues within the putative palm-thumb domain of the RdRP that when mutated results in a reduction in mRNA transcriptional activity without affecting antigenome replication [53]. While domains II and IV are unique, resembling no other protein structures, domain I is located in the N terminus and contains endonuclease activity [54, 55].

Arenaviruses employ a cap-snatching mechanism to obtain cellular mRNA caps to serve as primers for mRNA synthesis [56]. This mechanism is also used by influenza virus, for which the mechanism is well defined [57]. The endonuclease domain found in the N terminus of arenavirus L is proposed to cleave mRNA caps from cellular transcripts for this purpose. This domain for LCMV has been crystallized, and the structure resembles the endonuclease domain found in the N terminus of influenza PA, which is also responsible for cleaving cellular caps for this purpose [55]. While the viral mRNA transcripts are capped, they are not polyadenylated [56]. The arenaviral polymerase is known to oligomerize, and this multimerization may be a requirement for transcription. Subunit analysis of the polymerase has shown that the polymerase is capable of interacting via head-to-head, tail-to-tail, and head-to-tail conformations [54]. In addition to oligomerizing, the TCRV polymerase has been shown to bind the Z matrix protein as

well [58]. Also, the L polymerases of MOPV, LASV, and LCMV have been shown to physically interact with the NP protein [59].

The TCRV Z protein has been shown to bind both the endonuclease and the RdRP domains of the L polymerase [58, 60]. Arenavirus Z has an inhibitory effect on viral genome replication [61, 62], and the interaction between TCRV Z and the polymerase appears to be essential for this transcriptional repression activity [60]. Z has been shown to lock the polymerase on the viral promoter in a catalytically inactive state, thus limiting viral replication [63].

Post-translational protein processing

During translation into the lumen of the ER, the SSP (stable signal peptide) of the GPC precursor protein is cleaved in this compartment by signal peptidase [64, 65]). The SSP remains associated with GPC, which oligomerizes into trimers in the ER before undergoing proteolytic processing by the cellular protease subtilisin kexin isozyme-1 (SKI-1)/site 1 protease (S1P) into GP1 (globular head) and GP2 (transmembrane domain) [66, 67]. This cleavage process takes place either in the ER or the Golgi [66, 68-70]. The GP1 domain of the viral glycoprotein is heavily N-glycosylated, and this glycosylation is important for GP expression, cleavage, and fusion [71, 72].The SSP has been shown to be important for efficient glycoprotein expression, cleavage, trafficking, formation of infectious particles, as well as membrane fusion [73, 74]. The SSP has also been shown to interact with the Z protein [75]. The viral Z matrix protein is required for virion budding [76, 77]. The myristoylation of the G2 residue of the arenavirus Z protein has

been shown to be necessary for Z self assembly and budding. This indicates that Z self association most likely occurs at the plasma membrane, where myristoylation would mediate membrane association [78].

Role of the Z protein in arenaviral replication

The Z protein has been shown to interact with all of the other viral proteins: NP, L, as well as GP [75, 78-83]. Recently, a review article detailing known arenaviral protein-protein interactions has been published [84]. The interaction with the viral ribonucleoprotein (vRNP) complex likely is responsible for genome packaging into virions, and Z has been suggested to play an important role in ensuring that the L polymerase is incorporated into virion particles [63]. The intergenic region (IGR) has been shown to be important for the incorporation of LCMV genomes into virion particles [27]. Reports on the involvement of NP in budding activity differ among arenaviruses. One study shows the necessary involvement of ALIX/AIP1 for recruitment of NP into virion particles for MOPV. In this case, both the MOPV NP and Z proteins were found to bind cellular AIP1 [85]. Meanwhile, the Z and NP proteins have been shown to have a direct interaction for LCMV and LASV [82]. The NP protein of TCRV has been shown to be required for efficient Z mediated budding activity [80], however, the similar observation was not detected for JUNV NP. The differences between budding mechanisms for different arenaviruses offer excellent opportunities for further studies. The Z protein also undergoes homo-oligomerization, which is likely important for its function in virion budding [86]. The fact that such a small protein can play so many

roles in viral replication highlights the importance of multifunctionality in the individual viral proteins in the *Arenaviridae* family of viruses.

The role of individual arenaviral proteins in HF pathogenesis

Role of the glycoprotein (GP) in pathogenesis

Viral entry is the first step for viral infection, and therefore is an important factor to consider in viral pathogenesis. Viral glycoproteins display different affinities for their cellular receptor, and increased affinity may contribute to disease pathogenesis. LCMV Clone 13 (Cl 13) strain, which causes a chronic infection, has a high affinity for αDG and is able to out-compete laminin for binding to the cellular receptor, while LCMV Armstrong (ARM) strain, which causes an acute and self-limiting infection in immunocompetent mice, is unable to displace laminin. Impressively, only a single residue at position 260 of the glycoprotein (GP) is responsible for the high binding affinity of Cl 13, and is essential for viral persistence [87]. The ability, or lack thereof, to displace laminin would therefore appear to determine tissue tropism and therefore the course of the disease for LCMV [30, 88].

Interestingly, OW arenavirus infection has been shown to result in the downregulation of αDG while expression of the precursor DG is unaffected. This downregulation is mediated by the viral GP, which targets the interaction between DG and LARGE in the Golgi, disrupting the glycosylation of αDG. This may play an important role in viral release, and may also further contribute to the destabilization of the membrane [36, 89]. Recently, analysis of over 3 million human polymorphisms

identified by the International HapMap Project revealed positive selection in a Nigerian population for allele variants of 2 genes, LARGE and dystrophin, a cytosolic adaptor protein that is required for the function of αDG. In this population, 21% of individuals show exposure to LASV, which may apply selective pressure on the allele frequencies in this region. These polymorphisms in LARGE and dystrophin may hinder binding and entry of LASV, affording an advantage to the immune system, and thereby protecting these individuals from severe LASV infection [90, 91].

Interestingly, a combination 4 specific amino acid changes in hTfR1 allow entry by AMPV, while only 1 change is required to permit entry by TCRV. While these mutations are located in the receptor, they imply that only small changes in the viral GP would be necessary to potentially convert a non-pathogenic arenavirus into a human pathogen [48].

While all the pathogenic NW arenaviruses are members of clade B, phylogenetic relatedness is not a good indicator of pathogenicity, as nonpathogenic members are also found in this clade. Additionally, the GP of the highly pathogenic MACV is more closely related to nonpathogenic TCRV than any of the pathogenic viruses. Similarly, GTOV GP is more closely related to AMPV GP [7, 92]. While the relatedness of these viral glycoproteins does not provide insight into the potential for disease, the usage of hTfR1 appears to be an important factor in determination of NW arenavirus hemorrhagic fever, as all clade B viruses that utilize hTfR1 cause hemorrhagic fever in humans [48]. Whitewater Arroyo virus (WWAV), a clade A/B virus, has been loosely associated with several cases of human disease in 1999-2000, but subsequent studies do not support the notion of this arenavirus being a human pathogen. Additionally, this virus is unable to

use hTfR1 as an entry receptor, and instead follows the *in vitro* tropism of nonpathogenic arenaviruses [48, 93]. This seems to suggest that this virus is not, in fact, a human pathogen.

Further evidence of the involvement in arenavirus GP as a determinant of pathogenicity can be seen in the guinea pig model of Pichinde virus (PICV) infection. While sharing high sequence identity, two strains of PICV result in vastly different disease outcomes in infected guinea pigs [94, 95]. Mutational analysis of these two strains of Pichinde, one virulent (P18) and the other avirulent (P2), has revealed that sequence differences between the GP of these two strains of PICV contribute to the vastly different disease phenotypes. While PICV GP is not wholly responsible for the virulence difference between P2 and P18, a single mutation at position 140 of GP is able to increase the survival rate of infected animals from 0% to 33% [96]. Similarly, mutational analysis of the attenuated Candid #1 strain of JUNV has revealed that residue 427 in the G2 domain of GPC is largely responsible for the attenuation of this vaccine strain [97]. Further analysis demonstrated that the residue change at this site results in increased fusion at neutral pH of the Candid #1 strain, and also increased dependence on hTfR1 for entry, contributing to attenuation [98].

Role of the nucleoprotein (NP) in pathogenesis

Arenaviral proteins have been shown to interfere with the host's innate immune response. The NP proteins of several arenaviruses have been shown to be capable of inhibiting type I IFN signaling in reporter assays. OW LCMV and LASV along with NW

JUNV, MACV, WWAV, PICV, and Latino virus (LATV) NPs were able to inhibit IFNβ production through inhibition of IRF3 translocation. In contrast, apathogenic TCRV NP was incapable of IFN inhibition and of IRF3 translocation [99], although these observations need to be confirmed by other laboratories. NP has been proposed to bind RIG-I, but separate studies have shown conflicting results [100, 101], and therefore this interaction also requires further investigation. Recently, arenavirus NP has been linked to inhibition of NFκB signaling and IKKε binding [100, 102]. We and other researchers have recently crystallized LASV NP and found that its C terminus contains a functional 3'-5' exoribonuclease domain that degrades dsRNA [103, 104]. This exonuclease function is directly involved in the IFN inhibition function as mutations of the catalytic residues significantly reduce its ability to inhibit IFNβ production in virally infected cells [103, 104]. The degradation of RNA by NP has been proposed to inhibit type I IFN by eliminating viral pattern-associated molecular pattern (PAMP) molecules that would otherwise be recognized by cellular pattern recognition receptors (PRRs). NP proteins with changes in residues that have been identified to be involved in RNA degradation function show loss of ability to suppress IFNβ production [103, 104]. Interestingly, these are the same residues identified in binding IKKε, suggesting that there may be some overlap in the domains responsible for these varying mechanisms of IFN inhibition, or alternatively, this could be the result of an allosteric effect [100]. The details of how IFN inhibition by arenavirus NP is accomplished remain to be resolved, but we can safely say that this protein is a potent inhibitor of type I IFN production, and therefore it provides an excellent new target for antiviral development.

Role of the polymerase (L) protein in pathogenesis

One consistent predictor of disease outcome in LASV infected patients is viral load. Those individuals who are able to progressively control the level of viremia are able to recover, while patients who demonstrate uncontrollable viral titers in the blood typically succumb to the disease [105]. Analysis of a reverse genetics system for LASV has shown a relationship between viral replication and virulence, as well as identifying a role for both the 5' and 3' noncoding regions of the S segment in both of these aspects of viral biology [106]. Reverse genetic techniques have also revealed that a single amino acid in the L polymerase of LCMV is responsible for the change from an acute to chronic infection between the ARM and Cl 13 strains [107]. This residue, L1079 of Cl 13, enhances the levels of intracellular viral replication, thereby increasing viral load, which accounts for the difference in rates of viral replication between the ARM and Cl 13 strains. The L1079 residue was shown to be responsible for generalized immune suppression as well, which is likely a result of T cell exhaustion due to the high viral loads. A single L1079 mutation was able to confer increased replication rate, increased intracellular viral RNA levels, as well as suppression of immune responses. The addition of the GPC mutation at residue 260 was able to enhance these phenotypes in the presence of the L1079 mutation, but had no effect in the absence of the L1079 mutation. It is clear that the enhanced replicative capacity of Cl 13 is the primary determinant for chronicity in LCMV infection [107]. Previous studies have shown that this same residue is also responsible for enhanced viral replication and tropism in macrophages [108]. This residue does not map to any of the known catalytic domains of the polymerase, and its exact contribution to increased replication is yet to be determined [107]. Likewise,

mutational analysis has revealed that the C terminal end of the PICV viral L polymerase might contribute to the virulence nature of the infection *in vivo* (our unpublished data).

Role of the Z protein in pathogenesis

Although it is a small protein, arenaviral Z has many binding partners, both viral and cellular. In addition to interacting with the other arenaviral proteins as discussed previously, the Z protein is known to interact with cellular promyelocytic leukemia protein (PML), which under normal conditions localizes to the nucleus. This transcription factor regulates the tumor suppressor p53 [109]. Upon arenaviral infection, however, this cellular protein is redistributed to the cytoplasm, and has been shown to inhibit cellular apoptosis. Additionally, the interaction of Z with cellular PML has been shown to inhibit translation through interaction with the eukaryotic translation initiation factor eIF4E by reducing the binding affinity of eIF4E for cellular mRNA cap structures [110, 111].

The Z protein of the NW arenaviruses have been shown to inhibit type I IFN inhibition. While the Z proteins of OW LCMV and LASV showed no effect, those from NW arenaviruses could inhibit IFNβ production, albeit the effect does not appear to be as potent as that of arenaviral NP. Furthermore, NW arenavirus Z was shown to bind RIG-I, and blocked complex formation between RIG-I and MAVS, providing a mechanism for the observed IFN inhibition by the Z protein [112].

Antiviral compounds targeting different steps of the arenaviral life cycle

As the mechanic of the arenaviral life cycle is better understood, several compounds have been tested experimentally and in the field (i.e., ribavirin) to block different steps of the virus life cycle (Figure 1.1.2), including entry, replication, and egress. A brief yet comprehensive review of some of these antiviral compounds is summarized below.

Compounds targeting viral entry

Many of the antivirals that are currently being developed for treatment of arenaviral HF prevent viral entry, thus preventing the establishment of infection. Amphipathic DNA polymers have been found to effectively inhibit the interaction between the glycoprotein of LCMV and αDG, thereby preventing viral entry. This interaction is independent of the sequence of the DNA polymer, but is related to its size and amphipathic nature [113]. Through the use of high throughput screening, small molecules have been identified that are able to specifically block arenavirus entry by preventing pH mediated fusion of the glycoprotein [114]. The small molecule ST-193, which is effective at blocking LASV, JUNV, MACV, and GTOV GP mediated entry, effectively blocks membrane fusion most likely through stabilization of the prefusion complex [115]. This molecule has also been tested in the guinea pig model of LASV, and was found to significantly reduce mortality in infected animals [116]. Similarly, ST-294 is also able to stabilize the prefusion complex by targeting the interaction with G2

and the SSP, and has been shown to be effective in blocking membrane fusion with GTOV, JUNV, TCRV, and MACV GPs [115].

Compounds targeting the viral RNA polymerase

Broad-spectrum inhibitors of RNA viruses (ribavirin and Favipivarir or T-705) have been used for the treatment of arenavirus infections in humans and/or experimental animals [117, 118]. The mechanism of action for T-705 appears to directly inhibit the viral polymerase [119]. Meanwhile, ribavirin (a nucleoside analog 1-β-D-ribofuranosyl-1,2,4-triazole-3-carboxamide) has been shown to be mutagenic for several RNA viruses including LCMV, indicating that lethal mutagenesis may be the mechanism by which ribavirin combats RNA virus infections [120]. Currently, the only treatment available for LASV infected patients is ribavirin. However, ribavirin is only effective if given early during the course of infection, and this treatment can lead to severe side effects [3]. Therefore, the discovery of new antiviral drugs for the treatment of arenaviral hemorrhagic fever is of utmost importance. Recently, peptide-conjugated phosphorodiamidate morpholino oligomers (PPMOs) have been shown to efficiently block arenavirus replication. These molecules are single stranded nucleic acid analogs designed to base pair with their target sequences and effectively block gene expression. PPMOs targeting the conserved 5' end of the arenavirus genome were found to reduce virus titers not only in tissue culture but also in LCMV infected mice [121]. Another compound, designated 3f, has also been found to block JUNV RNA synthesis, although its exact mechanism of action remains to be elucidated [122].

The endonuclease domain located in the N terminus of the L polymerase may also serve as another attractive target for drug development. This domain shares structural similarity with the endonuclease domains of orthomyxoviruses and bunyaviruses. Drugs are currently being developed against these viruses which target the endonuclease and cap snatching function in the polymerase, and these same drugs may have an application for arenaviruses as well, based on the structural and functional similarities [123].

Compounds targeting post-translational protein modification

The cellular protease subtilisin kexin isozyme-1 (SKI-1)/site-1 protease (S1P) is involved in the proteolytic processing of the arenaviral envelope glycoprotein precursor (GPC), a step strictly required for production of infectious particles. Recent studies have suggested that SKI-1/S1P-adapted serine protease inhibitors [124] and peptide-based small molecule suicide inhibitors of SKI-1/S1P [125] can efficiently inhibit productive arenavirus infection in *in vitro* but appear to have severe limitations as anti-viral drugs *in vivo*. A novel specific SKI-1/S1P inhibitor, the amino-pyrrolidine amide compound PF-429242, has recently been shown to efficiently block the biosynthesis of fusion-active mature GPC of the OW arenaviruses LCMV and LASV and has shown potent anti-viral activity against LCMV and LASV in acute infection in cell culture [126]. PF-429242 has recently been shown to also inhibit GPC processing and productive infection of New World arenaviruses [127], making PF-429242 a potential broadly active anti-arenaviral drug.

Compounds targeting the Z protein

Small molecules are being developed for use against arenaviral infection that target the viral Z protein. One such approach is through the use of siRNA against Z. The siRNAs were shown to be highly effective in reducing JUNV titer in cell culture [128]. Myristoylation of the N terminus of Z is essential for its role in budding at the cell membrane [129]. As such, myristic acid analogs have been shown to be efficacious against JUNV infection in cell culture, as well as in disrupting LASV Z protein subcellular localization [129, 130]. Other compounds target the zinc finger motif present in the Z protein structure. Several aromatic and thiuram disulfide compounds, which are known to interact with zinc finger motifs, have been shown to be effective against arenavirus infection *in vitro*, and most likely exert their effects through interaction with the Z protein [131]. Another aromatic disulfide compound, NSC20625, has been shown to induce unfolding and oligomerization of Z [132]. Additionally, this compound has been shown to disrupt the interaction of Z with cellular PML, thereby restoring formation of nuclear bodies which is normally disrupted by arenavirus Z [133].

Host immune suppression and inflammatory responses

In order to mount an effective immune response to viral infection, the pathogen must first be detected by antigen presenting cells (APCs). Dendritic cells and macrophages assume this responsibility, and once the virus has been detected by the PRRs found on these cells, they recruit other immune cells and initiate the adaptive response. One of the marked characteristics of pathogenic arenaviral infection is a

generalized immune suppression of the infected hosts. Macrophages and DCs are early targets of arenavirus infection. However, instead of signaling to other immune mediators, these cells fail to become activated [134] as evidenced by no increase in the production of inflammatory cytokines such as TNFα, IL-1β, IL-6, or IL-12 in response to LASV infection. These APCs also fail to show an increase in expression of costimulatory molecules CD80 and CD86, as well as CD40, CD54, and HLAs. The phagocytic activity of the DCs is unchanged upon infection, indicating that they fail to mature in response to LASV infection. This study also shows that DCs appear to be a more important target for arenavirus infection, as infected DCs produce larger amounts of virus than infected macrophages [134].

Similar results are seen in LCMV Cl 13 infected cells. While the parental LCMV ARM strain causes an acute infection in mice, the Cl 13 strain results in a chronic infection, which is immunosuppressive [135]. Many of the immunomodulatory effects noted in LASV infection *in vitro* are mirrored in LCMV Cl 13 infection. MHCI and MHCII as well as costimulatory molecules are downregulated, therefore preventing the APCs from presenting viral antigen [136]. Hence, they are unable to activate virus specific B cells and T cells. The lack of T cell and B cell responses is not due to malfunction in these cells, per se, but to the lack of activation from DCs, as the lymphocytes are functionally capable [135]. Additionally, as seen with LASV infected cells, DCs are unable to mature and they do not undergo the changes necessary to migrate to the lymph nodes, where antigen presentation would normally occur.

While inhibition of antigen presentation by APCs is an effective method of immune suppression, LCMV Cl 13 employs other mechanisms as well. As a result of Cl

13 infection, DCs are stimulated to produce IL-10, an immunosuppressive cytokine, which can render T cells unresponsive. Neutralization of IL-10 results in an acute infection and clearance of the virus, rather than the chronicity that is characteristic of LCMV Cl 13 infection [137]. Other evidence of immunosuppression during chronic infection with LCMV Cl 13 includes T cell exhaustion and upregulation of PD-1 (programmed cell death 1). During persistent exposure to antigen, PD-1 is able to attenuate T cell receptor (TCR) signaling, and therefore inhibit T cell activation. This molecule is not upregulated in acute LCMV ARM infection. Impressively, PD-1 blockade is able to restore function to exhausted T cells, allowing infected mice to clear the virus [138]. Recently, LAG-3, another inhibitory receptor, was found to be upregulated on T cells during LCMV Cl 13 infection. Combined blockade of PD-1 and LAG-3 resulted in more efficient rescue of function in exhausted T cells, as well as improved control of viral load [139]. These characteristics are not seen in acute infection with LCMV ARM.

Mopeia virus (MOPV) is another arenavirus which is closely related to LASV, but is not pathogenic in humans. In fact, MOPV has been shown to be protective against a lethal challenge with LASV infection in nonhuman primates [140]. Therefore, analysis of the interaction of MOPV with immune cells as compared to LASV cellular interaction can give important insight into the mechanisms of LASV pathogenesis. Like LASV, the primary targets of MOPV infection are DCs and macrophages. Similarly, DCs are not activated in response to MOPV infection as evidenced by the lack of upregulation of CD80, CD86, CD54, CD40, and HLA-abc. Also, transcription of IFNα, IFNβ, TNF, and IL-6 mRNA transcripts is not increased. Unlike LASV infection, macrophages did

become activated in response to MOPV infection, as demonstrated by an increase in the aforementioned molecules [141].

This strong induction of macrophages may be an important factor for the lack of pathogenicity observed for MOPV infection as compared to LASV infection. However, in a DC and T cell coculture model, MOPV-infected DCs did become activated, most probably through cross talk with T cells. In this model, MOPV-infected DCs were found to induce early and strong T cell responses, where LASV-infected DCs did not. These cells were able to differentiate into effector and memory T cell phenotypes in the case of MOPV infection, where LASV infection did not result in induction of effector cells, although a small number of memory cells were detected. This is likely a result of the differential responses of APCs to these two infection models [142]. Once again, these results underscore the importance of a lack of APC activation in arenaviral pathogenesis.

While fatal LASV infection is associated with immune suppression, Argentine AHF caused by JUNV is associated with increased levels of both inflammatory and anti-inflammatory cytokines. Patients with AHF display elevated levels of IFNα, TNFα, IL-6, & IL-10 [143-145]. Severe disease and mortality are strongly associated with elevated levels of IFNα and TNFα [143, 144]. However, like LASV infection, JUNV infection of macrophages does not increase cytokine production. JUNV-infected monocytes and macrophages show no increase in levels of IFNα, IFNβ, TNFα, IL-10, IL-12, and IL-6. Meanwhile, apathogenic TCRV infection results in increased amounts of IL-6, IL-10, and TNFα. Therefore, macrophages do not appear to contribute to the cytokine dysregulation observed in AHF. The contribution of DCs is yet to be determined.

As suggested for LASV infection, cytokine production could play an important role in controlling JUNV replication early during the course of infection, while delayed release could contribute to pathogenesis in the case of AHF [146]. Recently, pathogenic Romero JUNV was found to induce type I IFN production in A549 cells, although the level of induction was lower than the robust response induced by the attenuated Candid #1 vaccine strain. The ability of the pathogenic virus to inhibit the type I IFN response may be cell type specific, and may suggest an alternative source of the high levels of IFNα observed in AHF patients in the absence of any appreciable induction in APCs as seen in tissue culture [147]. Understanding the mechanisms of immune suppression and inflammation in response to arenaviral hemorrhagic fever infection will provide new opportunities for the development of therapeutic agents to modify the host response against these deadly human pathogens to limit the host disease process.

Conclusion

Although arenaviruses have a very limited number of gene products, these proteins play multiple roles in contributing to the pathogenesis of arenavirus HF. The glycoprotein plays an essential role in cellular tropism, and the binding affinity for the cellular receptor has also proven to be an important determinant for viral pathogenicity. Also, the ability of OW arenaviruses to subvert classical routes of endosomal trafficking may allow these viruses to go undetected by endosomal receptors. Viral replicative capacity is a major pathogenic determinant for arenavirus infection, and the L polymerase plays a critical role in this process. Mutations in the polymerase affect the rate of viral

replication, hence attenuating the disease pathogenesis. When interacting with cellular PML, the viral Z matrix protein can inhibit apoptosis as well as interfere with protein translation. In addition, the Z protein of NW arenaviruses can interact with components of the innate signaling pathway, and is able to inhibit type I IFN production albeit not to the levels observed with the viral NP protein. The effect of NP protein in inhibiting IFNβ production has been associated with the exoribonuclease function located in the C-terminal domain of the protein. This domain has also been implicated in binding to IKKε, thereby possibly inhibiting multiple signaling steps required for IFNβ production. Development of antivirals targeting various steps of the viral life cycle may allow for a multipronged approach for combating arenavirus infection, and provide an approach that will not only halt arenaviruses in the very beginning stages of infection but also help patients who suffer from more advanced disease.

Table 1
Human disease caused by Old World arenavirus infection.

	Syndrome produced in humans	Incidence of disease
LCMV (Worldwide)	*Acquired:* most cases are mild or asymptomatic. Symptoms include fever, cough, malaise, myalgia, headache, photophobia, nausea, vomiting, adenopathy, sore throat, thrombocytopenia, and leukopenia. Severe cases may develop meningitis or meningoencephalitis [1,2]	*Acquired:* >5% of humans show evidence of LCMV exposure <1% mortality [1]
	Congenital: spontaneous abortion and fetal death, vision impairment (via chorioretinitis), brain dysfunction (macrocephaly due to inflammation or microcephaly due to lack of growth and immune mediation destruction of brain tissue) [3]	*Congenital:* unknown, only severe cases are investigated and reported
	Transplant associated: severe disease – encephalopathy, coagulopathy, abdominal pain, thrombocytopenia, fever, leukocytosis, graft dysfunction	*Transplant:* 14 cases, 11 fatal [4–6]
Lassa virus (West Africa)	Fever, weakness, malaise, cough, severe headache, sore throat, nausea, vomiting, diarrhea, sensorineural deafness. Facial edema, pleural effusion, thrombocytopenia, and leukopenia are seen in more serious cases. Fatal cases may exhibit pulmonary edema, respiratory distress, shock, encephalopathy, seizures, coma, and bleeding from mucosal surfaces [7]	~2 million infections annually and 5000–10,000 deaths [8]
Lujo virus (South Africa)	Diarrhea, vomiting, fever, chest pain, sore throat, rash, myalgia, facial swelling, respiratory distress, cerebral edema, thrombocytopenia, elevated liver transaminases, fever, mild bleeding in 3 patients, leukopenia [9]	Cases, 4 fatal

[1] Peters (2006); [2] Rousseau et al. (1997); [3] Bonthius (2012); [4] Fischer et al. (2006); [5] MacNeil et al. (2012); [6] Centers for Disease Control and Prevention (2008); [7] Moraz and Kunz (2010); [8] McCormick (1999); [9] Paweska et al. (2009).

Table 2
Human disease caused by New World arenavirus infection.

	Syndrome produced in humans	Incidence of disease
Junín virus (Argentina)	Fever, myalgia, mild hypotension, conjunctivitis, petechiae in the axilla, soft palate, or gingival margin. Neurological symptoms such as irritability, lethargy, and hyporeflexia. Severe cases may exhibit hemorrhagic manifestations, leukopenia, thrombocytopenia, shock, and seizures [1]	*Before vaccine:* 300–1000 cases/year. *After vaccine:* 30–50 cases/year 15–30% mortality [1–3]
Machupo virus (Bolivia)	Fever, gingival hemorrhage, petechiae, nausea, gastrointestinal hemorrhage, thrombocytopenia, leukopenia, hematuria, tremor, asthenia, anorexia, and respiratory distress [4]	*1962–1964:* 1000 cases *1990s:* 19 cases 2007–2008: >200 cases ~ 20% mortality [4,5]
Sabiá virus (Brazil)	Fever, headache, myalgia, nausea, vomiting, weakness, leukopenia, elevated liver transaminases, hematemesis, mucosal bleeding, conjunctival petechiae, tremors, coma, shock, pulmonary edema, hepatic hemorrhage and necrosis, gastrointestinal hemorrhage [6]	1 naturally occurring case, fatal
Guanarito virus (Venezuela)	Fever, malaise, headache, arthraligia, sore throat, vomiting, abdominal pain, diarrhea, convulsions, leukopenia, thrombocytopenia, various hemorrhagic manifestations [7]	618 cases, 23% fatal [8]
Chapare virus (Bolivia)	Fever, arthralgia, myalgia, vomiting, hemorrhage [9]	1 confirmed case, fatal

[1] Harrison et al. (1999); [2] Enria et al. (2008); [3] Ambrosio et al. (2011); [4] Aguilar et al. (2009); [5] Charrel and Lamballerie (2003); [6] Lisieux et al. (1994); [7] Manzione et al. (1998); [8] Fulhorst et al. (2008); [9] Delgado et al. (2008).

Figure 1.1.1

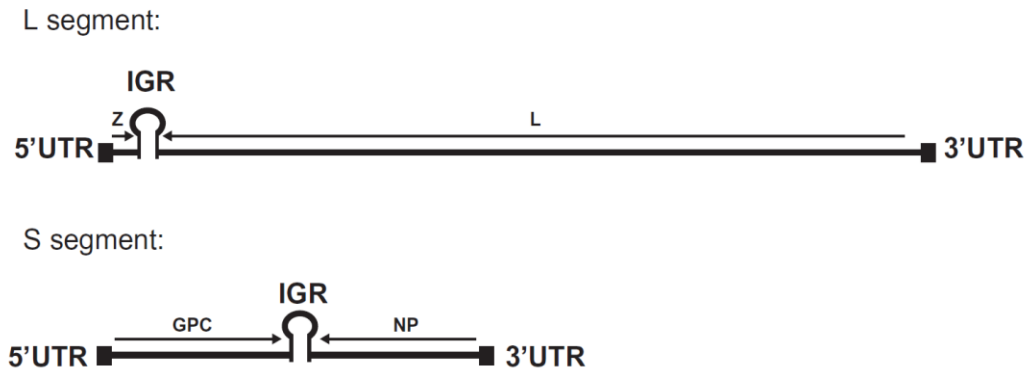

Figure 1.1.2

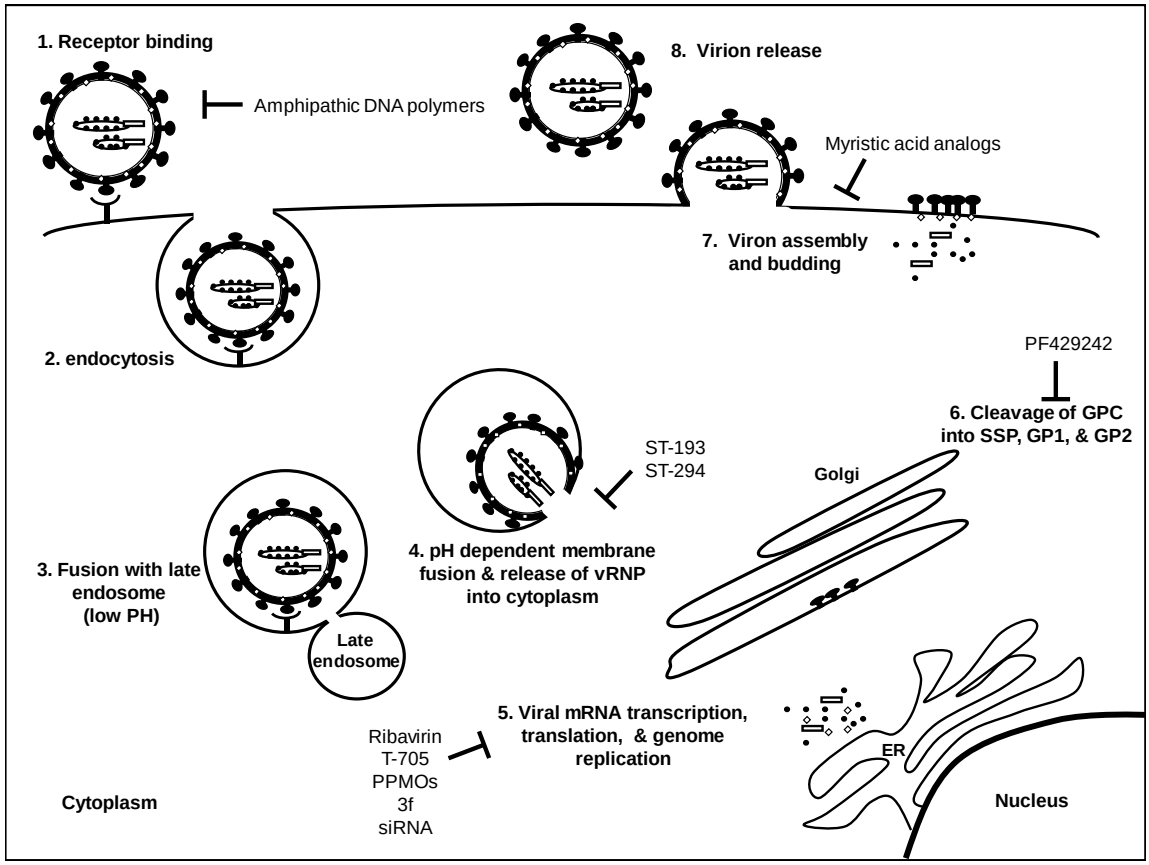
1. Receptor binding
Amphipathic DNA polymers
8. Virion release
Myristic acid analogs
7. Viron assembly and budding
2. endocytosis
PF429242
6. Cleavage of GPC into SSP, GP1, & GP2
ST-193
ST-294
Golgi
4. pH dependent membrane fusion & release of vRNP into cytoplasm
3. Fusion with late endosome (low PH)
Late endosome
5. Viral mRNA transcription, translation, & genome replication
Ribavirin
T-705
PPMOs
3f
siRNA
ER
Cytoplasm
Nucleus

Figure 1.1.3

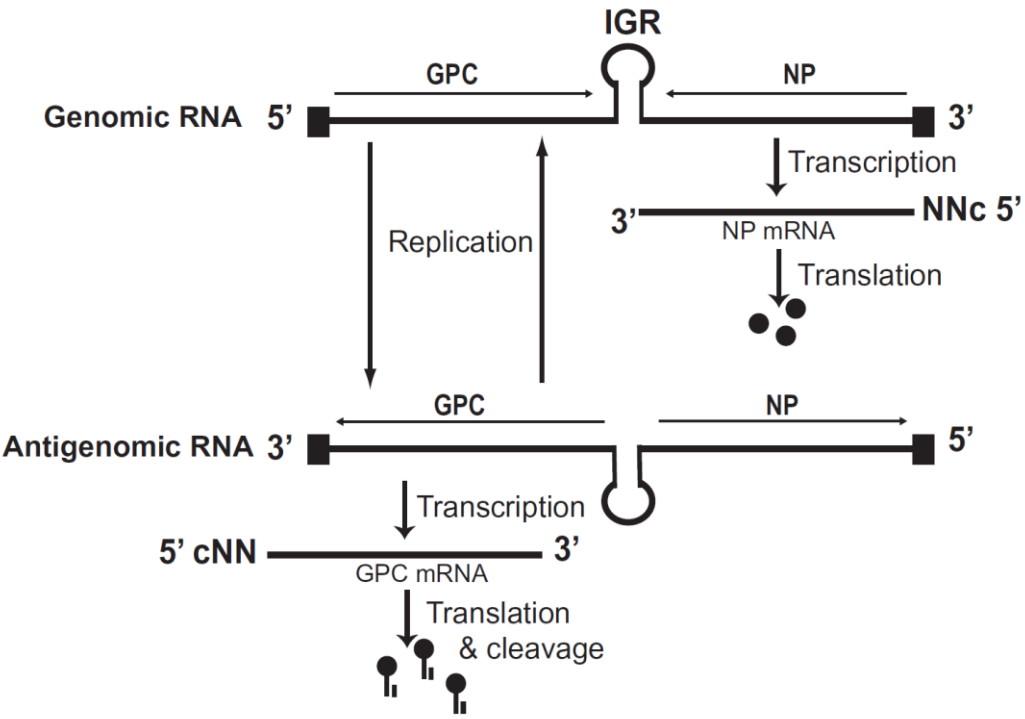
IGR
GPC
NP
Genomic RNA 5'
3'
Transcription
3'
NNc 5'
NP mRNA
Translation
Replication
GPC
NP
Antigenomic RNA 3'
5'
Transcription
5' cNN
3'
GPC mRNA
Translation
& cleavage

Figure Legends

Figure 1.1.1: Arenavirus Genome Structure. Arenaviruses are enveloped, ambisense RNA viruses with a single stranded genome composed of two segments: the genomic L (large) segment encodes the Z matrix protein and the L polymerase protein, and the S (small) segment encodes the glycoprotein (GPC) and nucleoprotein (NP). The genes encoded within each segment are separated by noncoding regions: the intergenic (IGR) region with strong secondary structures and the conserved 5' and 3' untranslated regions (UTR) at the termini of the genomic segments.

Figure 1.1.2: **Arenavirus Life Cycle and Compounds That Can Block Different Steps of the Virus Life Cycle.** 1. Cellular entry is mediated by different cellular receptors (αDG for OW and NW clade C arenaviruses, TfR1 for NW Clade B). 2. Virus uptake into cells is mediated by endocytosis (OW arenaviruses: clathrin independent, NW: clathrin dependent). 3. Virus fusion occurs with the late endosome (OW arenaviruses bypass the early endosome). 4. Viral RNP is released into the cytoplasm via a pH dependent membrane fusion mechanism (mediated by GP2 of the viral glycoprotein). 5. Viral genome replication, transcription, and protein expression occur in the cytoplasm (cap snatching is utilized for generation of viral mRNA). 6. Viral GPC precursor is cleaved into SSP, GP1 and GP2 proteins (SSP cleaved in ER by signal peptidase, GP1 & GP2 cleaved in either ER or Golgi by S1P/SKI-1). 7. Virion assembly and budding occur at the plasma membrane. 8. Progeny virion particle is released. As the mechanism of the arenaviral life cycle is better understood, several compounds have

been tested experimentally (e.g., T-705, amphipathic DNA polymers, ST-193, ST-294, PPMOs, 3f, siRNA, PF429241, and myristic acid analogs) and in the field (e.g., ribavirin) to block different steps of the virus life cycle.

Figure 1.1.3: **Ambisense Arenaviral Genome Replication Strategy and Protein Expressions.** Due to the ambisense coding strategy of the arenaviruses, the NP and L genes are transcribed directly from the viral genomic segments, but the GPC and Z mRNAs must be transcribed from the antigenomic strand after genome replication. The mRNAs are capped at the 5' ends via a cap-snatching mechanism, but are not polyadenylated at the 3' ends. The minimal trans-acting requirements for arenavirus replication and transcription are the NP and L proteins. During translation into the lumen of the ER, the viral glycoprotein (GPC) precursor is cleaved into the SSP (stable signal peptide), which remains associated with the transmembrane (GP2) subunit. The GP1 (globular head) subunit recognizes the cellular receptor and mediates cellular entry. (While only the S segment is depicted here, the L segment utilizes the same coding strategy.)

CHAPTER 1.2

A comparative analysis of the pathology and molecular mechanisms of New World and Old World Arenaviruses

Lisa McLay[1] and Hinh Ly[1,2]

[1]Department of Pathology and Laboratory Medicine, Emory University, Atlanta, GA 30322, [2]Department of Veterinary and Biomedical Sciences, University of Minnesota, Twin Cities, MN 55108

Abstract:

Both the New World (NW) and Old World (OW) groups of arenaviruses contain pathogens of significant human morbidity and mortality. While these two groups share many similarities, important differences with regards to pathogenicity and molecular mechanisms of virus replication exist as well. These closely related pathogens share many characteristics, including genome structure, viral assembly, natural host selection, and the ability to interfere with innate immune signaling. However, NW and OW arenaviruses use different receptors for cellular entry, and the mechanisms of virus internalization differ as well. General differences in disease symptoms and pathological lesions in patients infected with either the NW or OW arenaviruses are also noted and discussed herein. While both the OW Lassa virus (LASV) and the NW Junin (JUNV) can cause disruption of the vascular endothelium, an important pathological feature, the immune responses to these related pathogens seem to be quite distinct. LASV infection results in an overall generalized immune suppression, while patients infected with JUNV seem to develop a cytokine storm. Additionally, the type of immune response required for recovery and clearance of the virus is different between the NW and OW infections. These differences may be important to allow the viruses to evade host immune detection. Understanding these differences will aid the development of new vaccines and treatment methods against deadly hemorrhagic fever viral infections.

Introduction

Arenaviruses cause deadly hemorrhagic fever infections that are often neglected tropical diseases. Lassa virus (LASV) infection is responsible for up to 2 million infections and 5,000-10,000 deaths annually [4]. While most individuals exposed to LASV are able to mount an immune response that is capable of clearing the virus, those individuals who are unable to do so experience severe disease that often culminates in death. Currently, no vaccine is available for the prevention of Lassa hemorrhagic fever, and treatment options are extremely limited. Junin virus (JUNV), the causative agent of Argentine hemorrhagic fever (AHF), is also a pathogen of significant concern for humans. While a vaccine has been developed for the prevention of AHF, safety concerns exist, and development of better treatment methods are needed.

Arenaviruses are bi-segmented ambisense RNA viruses (Figure 1.2.1). The L (large) RNA segment encodes the L RNA-dependent RNA polymerase (RdRP) in a negative-sense orientation. The L polymerase is responsible for transcribing viral mRNAs as well as replicating the genome. This is an extremely large protein, at ~250kD, and contains four conserved domains. Domain I contains endonuclease activity, which is thought to be involved in cleaving 5' caps from cellular mRNAs in the process known as cap snatching for the purpose of priming viral mRNA transcription [55, 56]. Domain III of the L polymerase contains the RdRP domain [52]. To date, the function of the conserved domains II and IV are unknown [54]. The Z matrix protein is also encoded on the L genomic segment, but in a positive-sense orientation. The L and Z genes are separated by an intergenic region (IGR) that has secondary structure, and is thought to be involved in transcriptional termination of arenavirus mRNAs, which are not

polyadenylated [27]. The 5' and 3' untranslated regions (UTRs) are complementary to each other, and their base pairing allows the genome segment to circularize, thus forming a panhandle structure [28]. Likewise, the S (small) genomic segment encodes the nucleoprotein (NP) gene in negative sense and the glycoprotein (GPC) in positive sense, and separated by an IGR. The 5' and 3' UTRs of the S segment are also complementary to each other, and therefore form a panhandle structure. The GPC precursor protein must be proteolytically processed into 3 fragments: the stable signal peptide (SSP), globular head (GP1), and transmembrane domain (GP2). The SSP is cleaved in the endoplasmic reticulum (ER) by signal peptidase, while GP1 and GP2 are cleaved by the cellular protease subtilisin kexin isozyme-1(SKI-1)/ site 1 protease (S1P) [64-67]. The SSP remains associated with GP2, and these structures trimerize to form a functional glycoprotein [148].

While arenavirus infections in humans share many characteristics in terms of disease manifestation, pathology, and viral biology, many differences exist as well. Analysis of the different mechanisms of pathogenesis and viral molecular biology is important in an effort to develop new methods of treatment and vaccine for arenavirus infections. In the following sections, we aim to provide a comprehensive analysis of current knowledge about NW and OW arenavirus-induced hemorrhagic fever and to outline some of the significant differences between the major viruses (e.g., LASV and JUNV) that are responsible for severe hemorrhagic fever disease in humans.

Phylogenetic and epidemiological differences between NW and OW arenaviruses

The arenavirus family is separated into two groups: the New World (NW) and the Old World (OW) arenaviruses (Table 1.2.1). This distinction is based on geographic distribution, serological relatedness, as well as phylogeny. Here, we will focus on the arenaviruses that have pathogenic potential for humans. The Old World (OW) arenaviruses that have potential to cause human diseases include (LASV), Lymphocytic Choriomeningitis (LCMV), and Lujo (LUJV). The reservoir species for nearly all arenaviruses are various members of the rodent family (Table 1.2.1), and the natural hosts maintain high viral loads despite the lack of any inherent disease [149]. LASV is carried by *mastomys natalensis,* a multimammate rat common in West Africa where LASV infection is endemic. The host range for LCMV is much broader, as *mus musculus* (the common mouse) has a worldwide distribution, and thus LCMV does as well.

The South American arenaviruses that cause diseases in humans are (JUNV), Guanarito (GTOV), Machupo (MACV), Sabia (SABV), and Chapare (CHPV). These New World (NW) viruses are responsible for causing human hemorrhagic fever in Argentina, Venezuela, Bolivia, Brazil, and Bolivia, respectively. However, only one documented case each has been reported for SABV and CHPV infections. All of the NW arenaviruses that cause human diseases belong to NW Clade B. However, nonpathogenic viruses are also found in this clade, indicating that phylogenetic relatedness is not a good indicator of pathogenicity for arenaviruses. The reservoir species for the NW arenaviruses that cause human diseases are also rodents: JUNV is found in *Calomys musculinus* (Drylands vesper mouse) [150], GTOV has been shown to be carried by *Zygodontomys brevicauda* (common cane mouse)[151], and the natural reservoir for

MACV is *Calomys callosus* (large vesper mouse)[152]. The natural range of the host species for each respective virus is the determining factor for the endemnicity of human disease. Consumption of food contaminated with urine or feces from infected rodents is a common route of infection. Infection may also occur via inhalation of aerosolized particles or through contaminated medical equipment.

The incidence of disease varies for each of these arenaviruses. While LCMV has the largest worldwide distribution, and therefore the potential to infect larger numbers of people, the incidence of disease caused by this virus is low. Acquired LCMV infection is not a significant cause for concern in adult populations. While greater than 5% of humans show evidence of previous exposure to LCMV, the disease has a mortality rate of less than 1% [13]. Congenital LCMV infection can be quite serious, and may even result in spontaneous abortion or fetal death. However, the number of congenital infections is unknown, as only severe cases are reported. Therefore, we cannot objectively estimate the disease incidence for congenital LCMV infection [15]. Recently, LCMV has proven to be an important pathogen for immunocompromised individuals. Fourteen cases have been reported of LCMV infection resulting from organ transplant, and eleven of these cases proved fatal [10-12]. While LCMV infection is serious for immunocompromised individuals, this virus does not pose a significant threat to healthy adults. On the other hand, LASV infection can be quite serious. Each year there are approximately 2 million cases of Lassa hemorrhagic fever which result in approximately 5,000-10,000 deaths in the endemic region of West Africa [4]. Moreover, in some areas, as much as 55% of the population shows evidence of previous exposure to LASV infection, underscoring the importance of this pathogen as a risk to endemic populations [153]. LUJV infection,

which was recently discovered, has only been identified in 5 individuals to date. However, four of these cases proved fatal, highlighting the pathogenic potential for this newly discovered OW arenavirus [8].

While the number of NW arenavirus infections are not as impressive as the number of LASV infections that are seen annually, these viruses still cause significant human disease. Of these viruses, JUNV is responsible for the highest levels of morbidity and mortality, resulting in approximately 300-1000 infections per year before the development of the Candid #1 vaccine. Since the implementation of Candid #1 against this disease, the infection rate has decreased to 30-50 cases annually [20, 22, 24]. The mortality rate for untreated cases of JUNV infection is high, at 15-30%[24]. MACV infection is also a significant cause for concern. However, unlike JUNV infection that maintains a constant presence in endemic regions, MACV infections have surfaced sporadically in the form of outbreaks. From 1962 to 1964 there were 1000 reported cases. In the 1990s, 19 cases were reported. Again, from the years 2007-2008 over 200 cases of MACV infection were reported. While this virus only seems to emerge sporadically, the mortality rate is high, at 20%, and warrants the development of vaccines and therapies for those afflicted with disease [19, 21]. To date, 618 cases of GTOV infection have been reported, with 23% of these cases resulting in death [23]. Again, while GTOV infection is not common, the mortality rate is high, giving cause for concern. Only one case has been reported each for CHPV and SABV infections, but in both cases the disease resulted in death, underscoring the seriousness of disease caused by arenavirus induced hemorrhagic fevers [17, 18].

Similarities and differences in disease manifestations caused by NW and OW arenaviruses

Arenavirus hemorrhagic fevers vary widely in their disease manifestations (Table 1.2.2). Interestingly, even individuals infected with the same virus can show a wide variety of symptoms, which can make diagnosis difficult. This is very common with patients infected with LASV. Individuals infected with LASV are frequently misdiagnosed. Currently, the only treatment of Lassa hemorrhagic fever is the nucleoside analog ribavirin. However, this treatment is only effective if given early on during the course of infection. Therefore, misdiagnosis can have serious consequences. The symptoms of Lassa fever include fever, pharyngitis, retrosternal pain, proteinuria, sore throat, vomiting, mucosal bleeding, deafness, pleural effusion, pericardial effusion, malaise, headache, nausea, diarrhea, edema, thrombocytopenia, and leukopenia [5, 154]. Cases which typically result in death may also exhibit mucosal bleeding, pulmonary edema, respiratory distress, shock, encephalopathy, seizures, and coma [5]. Approximately 15% of patients also suffer from sensorineural deafness [6]. With such a wide range of symptoms which may range from asymptomatic to multiorgan failure and death, Lassa fever has proven difficult to diagnose, and is often mistaken for malaria, typhoid fever, influenza, among other febrile illnesses [155].

While LUJV has only recently been discovered, and only 5 cases identified, this virus elicits many shared symptoms as those displayed during LASV infection. Patients suffering from infection with LUJV were reported to experience diarrhea, vomiting, fever, chest pain, sore throat, rash, myalgia, facial swelling, respiratory distress, cerebral edema, thrombocytopenia, elevated liver transaminases, fever, and leukopenia. Mild

bleeding was observed in 3 of the 5 patients [8]. While only 5 cases have been identified, 4 of these resulted in death, underscoring the serious disease caused by this recently discovered arenavirus.

Among the NW arenaviruses, CHPV and SABV infection have only been identified as single incidents, while JUNV, MACV, and GTOV have infected many people. The disease manifestations caused by infection with these viruses display many of the same symptoms observed with OW arenavirus induced hemorrhagic fever. Symptoms produced by JUNV infection, the most serious of the NW arenaviruses in terms of human infection, include fever, myalgia, mild hypotension, conjunctivitis, and petechiae. Neurological symptoms such as irritability, lethargy, & hyporeflexia have also been observed. Severe cases may exhibit hemorrhagic manifestations, leukopenia, thrombocytopenia, shock, and seizures [24]. Similarly, patients infected with MACV may exhibit fever, gingival hemorrhage, petechiae, nausea, gastrointestinal hemorrhage, thrombocytopenia, leukopenia, hematuria, tremor, anorexia, and respiratory distress [19]. Symptoms reported for individuals infected with GTOV include fever, malaise, headache, sore throat, vomiting, abdominal pain, diarrhea, convulsions, leukopenia, thrombocytopenia, and various hemorrhagic manifestations [25]. While there is variation among the disease manifestations, many of these arenavirus infections display shared symptoms. It is important to note that while disease manifestation can vary based on the infecting virus, a wide range of symptoms may be exhibited by individuals infected with even the same arenavirus, in which some patients may experience very mild disease, whereas others present with severe hemorrhagic fever.

Pathological analyses of patients infected with JUNV (NW) or LASV (OW) arenavirus

While diagnosis of arenaviral hemorrhagic fever presents challenges because of the wide spectrum of symptoms displayed by infected patients, determination of the cause of death has also proven even more challenging. The cause of death from arenaviral hemorrhagic fever is not well understood. Recent studies are making progress in understanding the pathology of the disease. While similarities are seen between the pathologies of hemorrhagic fever induced by OW vs. NW viruses, many differences exist as well.

One consistent predictor of disease outcome in the case of LASV hemorrhagic fever is the level of viremia. Those individuals with high viral loads display more exacerbated disease and are given a poor prognosis [105]. Many of these cases result in fatal disease. In LASV infected patients, those individuals with viral loads higher than 8.5 log 10 PFU/mL typically succumb to the disease [156]. Meanwhile, infected individuals with lower initial viral loads typically are capable of clearing the infection, and survive [105]. While the LASV infects many vital organs and cell types, and replicates to high titers in various locations, the resulting histological damage is not severe enough to account for the cause of death in these patients. High viral titers can be found in the blood, liver, spleen, lung, and adrenal gland. The most consistent histopathological lesions are found in the liver, lung, and adrenal gland, with the most severe pathology being found in the liver. Hepatocellular necrosis, mononuclear phagocytic reaction, and focal hepatocellular cytoplasmic degeneration are the most common liver pathologies found, with little recruitment of inflammatory cells. However,

none of the pathological lesions found are severe enough to account for the cause of death [157].

While the level of viremia is a good indicator of disease prognosis for individuals infected with LASV, endogenous levels of IFNα are indicative of disease outcome in JUNV infected patients. During the second week of disease, the IFNα levels are extremely high in cases that result in fatality [144]. Hemorrhage, neurological changes, leukopenia, and thrombocytopenia are much more common in AHF patients than LASV infected patients [26]. While viral hepatitis is common in LASV infected patients, it is uncommon or mild in individuals infected with JUNV [26]. Renal papillary necrosis is also noted, and these necrotic sites coincided with the presence of viral antigen production [158, 159]. Myocarditis and secondary bacterial infection in the lungs were also observed in fatal cases [159]. Cases of GTOV and MACV infection resemble JUNV mediated pathology, which is not unexpected given the phylogenetic relatedness of these pathogens [25, 160-162] .

Differences in coagulopathies caused by JUNV (NW) and LASV (OW) infections

While arenaviruses can cause hemorrhagic fever in humans, the capacity for different arenaviruses to result in hemorrhage or coagulopathy differs between viruses. LASV is atypical, in the sense that hemorrhage is not common in infected individuals. Only a small percentage of patients develop hemorrhage, and this hemorrhage is limited primarily to mucosal surfaces [163]. Additionally, the amount of blood loss and pathological lesions are not sufficient to account for the terminal shock and death that

follows in lethal cases [40]. In the relatively few cases where bleeding does occur, it is typically associated with coagulopathy including thrombocytopenia and platelet dysfunction [164, 165]. The platelet malfunction has been attributed to a plasma inhibitor of platelet aggregation, which has yet to be identified [164].

LASV has a nonlytic cell cycle and does not cause any evident cellular damage in infected monocytes, macrophages, or endothelial cells [166]. The virus is able to efficiently infect the vascular endothelium, and infection of these cells yields high viral titers without causing cell death [166]. Infection of these cells is crucial to the pathology of the virus, as in both experimentally infected nonhuman primates as well as human patients, disruption of the function of the vascular endothelium is closely followed by shock and death [40]. Edema is closely associated with death in infected patients, and this is most likely due to increased vascular permeability. While autopsies on LASV infected patients and experimentally infected nonhuman primates failed to reveal vascular lesions, which correlates with the absence of cytopathic effect observed for this virus, vascular permeability is affected in the course of this disease. The mechanism by which the permeability of the vascular endothelium is increased has yet to be worked out, but most likely viral infection of this tissue is causing cellular changes allowing for the increased fluid flow, which results in the edema observed in severe disease. This, in combination with thrombocytopenia and platelet dysfunction, may be the cause of shock ultimately leading to death. In other viral hemorrhagic fevers, cytokine storm interferes with the integrity of the vascular endothelium. However, this does not appear to be the case for LASV infection [167]. Infected macrophages are not activated, and proinflammatory cytokines are not released [134, 168]. Increased levels of

proinflammatory cytokines are not detected in LASV infected patients, either [167]. Additionally, LASV infected human umbilical vein endothelial (HUVEC) cells have been shown to produce relatively low levels of IL-8, as opposed to those that have been infected with the apathogenic Mopeia arenavirus [166]. The relatively low levels of IL-8 are also observed in LASV infected patients [167]. While the release of inflammatory mediators does not appear to be the cause of increased vascular permeability, LASV infection may be influencing cellular integrity by some other mechanism.

While hemorrhage is not a common feature for LASV infected patients, for those suffering from AHF due to JUNV infection, hemorrhage is much more common. Even though an increase in the occurrence of hemorrhage is observed in JUNV infection, vascular damage is limited, as seen with LASV infection [169]. The receptor for JUNV, transferrin receptor 1 (TfR1), is highly expressed on vascular endothelial cells, and these cells support high levels of virus replication as observed *in vitro* [45, 170]. As this virus is not cytopathic, an absence of vascular lesions is observed *in vivo* [169, 171]. Experimentally infected endothelial cells show an increase in nitric oxide (NO) and prostaglandin PGI_2 production [171]. The release of these vasoactive mediators may be the cause of the increased vascular permeability upon JUNV infection of endothelial cells, and contribute to subsequent shock seen in patients. Experimentally infected cells also show an increase in the cellular adhesion molecules ICAM-1 and VCAM-1 [171]. Interestingly, while JUNV infected HUVEC cells show reduced levels of the coagulation von Willebrand factor (VWF), patients infected with JUNV display increased levels of VWF in serum samples [171, 172]. This discrepancy suggests that the VWF is originating from some other source rather than endothelial cells. In addition to alterations

in clotting factors, an as of yet unknown inhibitor of platelet aggregation exists in plasma, as is found with LASV infected patients [173]. Infected individuals also exhibit thrombocytopenia and reduced complement activity [174]. The coagulation activity of blood in infected patients is also low [175]. All of these factors may contribute to the coagulopathy and edema observed in AHF.

NW and OW arenaviruses trigger different immune responses

The outcome of arenavirus hemorrhagic fever is heavily dependent on an effective immune response. However, differences in immune responses are noted between NW and OW arenavirus infections that play a critical role in the clearance of the virus. In the case of LASV infection, an effective T cell mediated response appears to be critical for recovery from infection. In experimentally infected macaques, animals that survived infection exhibited circulation of activated T cells, while fatal infections displayed low and delayed T cell activation. The surviving animals were also able to control viral replication, while fatalities exhibited high viral loads [176]. In hospitalized patients, high IgG and IgM titers are not associated with outcome of the disease, while high viral titers were associated with a poor outcome, indicating the that the antibody response is not effective in controlling viral replication and resulting pathology [105].

In order to generate an adaptive response, the virus must first be recognized by antigen presenting cells (APCs), which will then initiate the production of an appropriate immune response. APCs, such as DCs and macrophages, are early targets of arenavirus infection. These cells are readily infected, but fail to become activated upon infection

[134]. No increase in the levels of TNFα, IL-1β, IL-6, or IL-12 is observed in response to LASV infection. Upon activation, APCs normally increase the levels of costimulatory molecules. However, in LASV infected APCs, there is no increase in the levels of CD80, CD86, CD40, CD54, or HLAs. Also, infected DCs fail to mature, as evidenced by the absence of increased levels of phagocytic activity. While both macrophages and DCs are targeted by LASV infection, DCs seem to be a more important target, as they produce much more virus than macrophages upon LASV infection [134]. The failure of these APCs to become activated is consistent with the generalized immune suppression that is one of the hallmarks of LASV infection. A closely related virus, Mopeia virus (MOPV), is apathogenic in humans and can actually provide protection against LASV infection in nonhuman primates [140]. Interestingly, MOPV infection also fails to activate DCs [141]. Similar to LASV infection, MOPV primarily targets DCs and macrophages. Upon infection with MOPV, DCs fail to upregulate CD80, CD86, CD54, CD40, and HLA-abc. Transcription of messages encoding proinflammatory cytokines is not increased, either. However, MOPV infection of macrophages does increase the transcription of messages encoding IFNα, IFNβ, TNF, and IL-6 [141]. Therefore, while MOPV fails to activate DCs, macrophages are capable of becoming activated when infected with this virus. However, in a DC and T cell coculture model, DCs were shown to be capable of activation in response to MOPV infection. This is speculated to be the effect of cross talk with T cells. These activated DCs were capable of inducing strong T cell responses, whereas DCs infected with LASV using the same coculture model remained inactive [142]. The activation of these APCs is critical for generating an

effective T cell response, which is needed for clearance of the virus and patient's recovery.

While the hallmark of LASV infection is a generalized immune suppression, JUNV infected patients display elevated cytokine levels. Infected patients show increases in levels of TNFα, IFNα, IL-6, and IL-10 [143-145]. Patients with exacerbated disease and fatal cases consistently show elevated levels of TNFα and IFNα [143, 144]. Although these increased levels of cytokines are observed in JUNV infected patients, *in vitro* infected macrophages show no increase in cytokine production, such as IFNα, IFNβ, TNFα, IL-10, IL-6, and IL-12 [146]. Therefore, the increased cytokine levels observed in patients must originate from another source, possibly DCs whose role in cytokine production upon JUNV infection has yet to be established. The exact role of cytokines in the pathogenesis of AHF has yet to be determined. A proposed theory is that cytokines may be important in controlling virus replication in the early stages of infection, while a delayed response could contribute to pathogenesis as seen in patients with severe disease and high levels of cytokines [146].

While the antibody response seems to be ineffective in controlling LASV infection, this is not true in the case of JUNV infection. When immune plasma from previously exposed individuals is administered to other JUNV-infected patients early during the course of infection, the mortality rate can be reduced from 16% to 1% [177]. However, this treatment is only effective when given within the first week of illness, emphasizing the importance of early diagnosis [178]. Plasma banks have been set up in endemic areas in order to collect serum from individuals who have survived Argentine HF. The efficacy of immune plasma treatment appears to be due the ability of the antibodies to

neutralize the virus, as viremia levels of patients are reduced after transfusion with immune plasma [179]. Although immune plasma therapy is highly effective, alternative therapies are needed. Potential complications associated with plasma transfusions, such as disease transmission, must also be taken into consideration. Additionally, a late neurologic syndrome has been observed in 10% of patients treated with immune plasma, which typically resolves, but underscores the need for alternative therapies [177]. Ribavirin has been tested in a small study at the eighth day after onset of illness. Treatment in this later stage of illness did lower viral titers and endogenous IFN levels while prolonging the time to death, but failed to reduce mortality [180]. Ribavirin treatment in LASV infected patients is only beneficial when given during the early stages of infection, and perhaps would be more effective for JUNV infected patients if administered earlier. However, the high efficacy rate of immune plasma in the treatment of Argentine HF demonstrates the importance of an effective antibody response for this disease. On the contrary, antibodies do not seem to play an important role in combating LASV infection. The reason for the disparity is unknown, but underscores the differences in hemorrhagic diseases caused by OW and NW arenaviruses.

Comparison of molecular strategies employed by OW and NW arenaviruses

Despite their classification into separate groups, the OW and NW arenaviruses share a large amount of similarity with regards to structural composition and viral biology. They share similar genome structure as well as molecular strategies for viral replication. They encode the same four proteins with functions that are largely shared

between the arenaviruses. Similarly, arenavirus infection produces many shared symptoms in infected patients. Both OW and NW arenaviruses target APCs early on during infection, followed by pantropic viral infection. Even though the OW and NW arenaviruses are closely related, on the molecular level these viruses do demonstrate differences in receptor usage, endosomal trafficking, and slight variations in the functions of the viral proteins.

Receptor Usage

OW arenaviruses LASV and LCMV, in addition to the pathogenic NW arenaviruses Oliveros and Latino, use cellular α-dystroglycan (αDG) in order to gain entry into host cells [30, 31]. This is a cell surface molecule that is used for attachment to the extracellular matrix (ECM), and as such is expressed fairly ubiquitously on cells, accounting for the ability of LASV to infect many cell types. Normally, αDG binds laminin, a component of the ECM, while the transmembrane portion of the receptor, βDG, anchors the receptor by binding dystrophin in the cytoplasm. When LASV infection occurs, laminin is displaced by binding of the virus to αDG, which causes the membrane to destabilize. The disturbance of the membrane could result in an interference with cellular signaling, which may also contribute to hemorrhagic fever disease pathogenesis [33]. Additionally, OW arenavirus infection results in the downregulation of αDG, which may further contribute to the destabilization of the membrane [89]. αDG has been shown to be highly expressed on macrophages and

dendritic cells in mice, which may explain why these cells are early targets of arenavirus infection [32].

Recent studies have shown that arenaviruses may use alternative receptors and do not rely solely on αDG for cellular entry. Addition of laminin was found to be capable of blocking binding of αDG to GP. However, laminin was not capable of blocking LASV GP mediated infection of Vero cells. This suggests that the virus was infecting the cells through the use of alternative receptors [35]. Recently, four cellular receptors were found to be capable of mediating LASV infection: Axl, Tyro3, LSECtin, and DC-SIGN. While entry through these receptors was less efficient, these molecules were found to be capable of mediating LASV infection independently of αDG [38]. These receptors may be important in infection of cell types such as hepatocytes, which display high viral titers despite the seeming lack of αDG expression on cell membranes [40, 41]. Interestingly, Ebola virus has also been shown to be capable of using these same receptors for entry into cells [42-44]. Ebola and LASV share the same cellular tropism, infecting macrophages, dendritic cells, endothelial cells, and the liver.

The New World arenaviruses that are responsible for human disease gain cellular entry through binding human transferrin receptor 1 (hTfR1) [45]. The normal function of this receptor is to mediate endocytosis of iron-bound transferrin, thereby transporting iron across the cell membrane and its subsequent release into the cytoplasm [46]. The specificity for the human homolog of TfR1 appears to be an important determinant of pathogenesis, as nonpathogenic NW arenaviruses AMPV and TCRV are capable of using TfR1 orthologs, but are incapable of binding the human receptor . Also, a single mutation in TCRV GP allows binding of hTfR1, while a combination of four mutations

in AMPV GP allows this interaction to occur. This suggests that modest mutations in the GP of these apathogenic arenaviruses would allow for infection of human cells [48].

Endosomal Trafficking

As OW and NW arenaviruses use different cellular receptors for entry into host cells, they also use different routes of intracellular trafficking as part of this entry process. OW arenaviruses that bind αDG enter the cell via internalization through smooth vesicles in a process that is cholesterol dependent but independent of both clathrin and caveolin [181-185]. Recent studies have found that binding of LASV to αDG causes phosphorylation of βDG by receptor tyrosine kinases. This phosphorylation is associated with the dissociation of βDG from the cytoskeletal adaptor protein utrophin, which may facilitate endocytosis [186]. The virus-receptor complex is then delivered via the multivesicular body (MVB) to the late endosome, and this process is dependent on microtubular transport [183, 185]. The virus-receptor complexes appear to be sorted by the ESCRT complex into intraluminal vesicles (ILV) in the MVB prior to being transported to the late endosome [50]. Through this route, the virus subverts classical routes of endosomal trafficking, and bypasses the early endosome. This compartment contains the toll-like receptors (TLRs) responsible for detection of RNA viruses, and by avoiding transport to the early endosome, OW arenaviruses can evade detection by innate immune receptors. This can partly explain the observed failure of the innate immune system to detect LASV infection, resulting in uncontrolled viral infection [163].

While OW arenavirus internalization is independent of clathrin, JUNV infection involves internalization via clathrin coated pits at the plasma membrane, which is not unexpected as TfR1 normally associates with clathrin coated pits [187]. Additionally, cholesterol sequestration has only a minor effect on JUNV infection, unlike LASV entry which is cholesterol dependent [187]. Upon binding, TfR1 is internalized and transported to the early endosome [188]. The early endosome has a pH of ~6.0, but JUNV GP requires a pH of <5.5 for optimal fusion activity. Thus, the virus must be transported to the late endosome, which is a more acidic compartment, and would allow for fusion to occur [188]. This is not a route normally taken in TfR1 trafficking, and may indicate that the virus can somehow reroute the normal pattern of TfR1 recycling. The trafficking of TfR1 seems to reply on the multimeric state of the receptor, as monomers are quickly recycled through early endosome while larger oligomers are retained in this compartment for an extended period of time [189]. Arenavirus binding may have some influence on the oligomeric state of TfR1, and may potentially influence the trafficking of the receptor by this method [190].

IFN inhibition by viral proteins

One of the hallmarks of severe LASV infection is generalized immune suppression. The innate response to viral infection is essential in the development of an effective adaptive immune response, which is needed to clear the infection. One mechanism employed by arenaviruses to interfere with the development of effective immune responses is the inhibition of type I IFN production. Pathologic arenavirus

infections, both by NW and OW arenaviruses, are characterized by the ability of viral proteins to inhibit type I IFN. A potent inhibitor of type I IFN is the viral nucleoprotein NP. The NP proteins of OW LASV and LCMV as well as NW JUNV, MACV, WWAV, TCRV, and LATV have all been shown to display this ability to inhibit type I IFN through the inhibition of IRF3 translocation. While it has been suggested that the NP protein of TCRV does not have the ability to suppress type I IFN [99], recent studies have shown that it is able to do so [191](our unpublished data). The same residues that are responsible for the IFN inhibitory function of NP have also been shown to be involved in the 3'-5' exonuclease activity of this protein, tying the two functions together. The proposed model is that the NP protein is able to degrade dsRNA, thereby preventing recognition of viral pathogen-associated molecular pattern (PAMP) RNAs by the innate pathogen recognition receptors (PRRs) (i.e., RIG-I and MDA5), thus preventing the signaling cascade that would lead to IFN production [103, 104]. Interestingly, these same residues have also been implicated in the binding of the NP protein to IKKε, thereby inhibiting the nuclear translocation and transcriptional activity of NFκB, which may indicate an overlap in functional domains of the protein or may be the result of allosteric effect [100, 102].

While the NP protein has been shown to be a potent inhibitor of IFN production, the Z protein appears to play a role as well. However, Z does not appear to be as potent as NP at performing this function. The NP proteins of NW arenaviruses JUNV, GTOV, MACV, and SABV were found to bind RIG-I, resulting in downregulation of the IFNβ response. Based on published data to date, this seems to be a function of NW arenaviral Z, while the Z proteins of LASV and LCMV do not have this capability. NW arenavirus

Z seems to inhibit the binding of MAVS to RIG-I, thus preventing the downstream signaling that would result in production of type I IFN [112].

Vaccine development for the NW (JUNV) and OW (LASV) viruses

Currently, no licensed vaccines are available for the prevention of Lassa fever. An attempt to generate a whole virus vaccine via inactivation of LASV by gamma irradiation generated good humoral responses in nonhuman primates, but this response failed to protect animals against lethal challenge with LASV [192], therefore suggesting that T cell responses rather than humoral responses are important for protection against LASV infection. Studies in humanized mice confirm the need for cell mediated immune defense against LASV. Control of LASV infection in humanized mice has been shown to be T cell dependent. Interestingly, these mice could be protected from disease through T cell depletion, indicating a role for T cells in LASV pathogenesis as well as defense. This contradiction could be reconciled by the hypothesis that T cells are necessary for rapid clearance of the virus, but if the host response proves incapable of doing so, the disease becomes mediated by the same cells which would otherwise protect against it [193].

Multiple attempts have been made to generate an effective LASV vaccine. MOPV infection has shown to be capable of providing protective immunity to LASV infection in nonhuman primates [140]. Additionally, the recombinant ML29 vaccine that expresses the L segment of MOPV and the S segment of LASV has been shown to protect marmosets against LASV infection by inducing sterilizing cell mediated

responses [194]. However, there are obvious safety concerns for these as vaccine candidates, as the genome of this recombinant virus contains the S segment from LASV, a BSL-4 virus, and the L segment from MOPV, which is currently classified as a BSL-3 virus. Also, in regions endemic for LASV, a large portion of the population also suffers from HIV infection. Therefore, the efficacy and safety of such a vaccine when applied to immune compromised individuals must also be addressed. A recombinant vaccinia virus vaccine has also been developed expressing combinations of LASV NP, GP1 & GP2 proteins. Recombinants expressing all 3 proteins, or the combination of GP1 and GP2 were able to protect macaques from fatal infection but not viremia. Again, this vaccine would not be applicable for use in immune compromised individuals. Also, preexisting immunity from the smallpox vaccine would potentially be problematic [140]. A recombinant VSV vaccine expressing LASV GPC was also found to be protective in nonhuman primates. Although the animals were protected, LASV viremia was detected in the animals at day 7 post challenge [195]. A similar approach was taken using the Yellow Fever vaccine, YF17D, as a vector for LASV GP. One construct contained both glycoproteins from YFV and LASV, and was capable of protecting strain 13 guinea pigs from LASV challenge. However, it replicated poorly and was not stable upon sequential passages in tissue culture [196, 197]. Another construct expressing only LASV GP also protected strain 13 animals from death, but did not prevent disease or viremia and was poorly immunogenic [197].

While development of a protective vaccine for LASV infection has proven challenging, development of a vaccine against JUNV infection has been more fruitful. The Candid #1 strain of JUNV has shown itself to be a highly successful vaccine against

AHF. This strain was generated by passaging the virus twice in guinea pigs, followed by sequential passaging in suckling mice and tissue cultures [198]. Unfortunately, it is not an appealing vaccine candidate for commercial production because of its small target population. However, the Argentine government has taken up production, and Candid #1 is now used in Argentina as an effective vaccine against JUNV infection. This vaccine has not been approved by the FDA due to a lack of proper FDA compliant documentation, the lack of detailed genetic composition of the vaccine strain, and the association of foot & mouth disease in several regions of Argentina. More importantly, the molecular basis for the attenuated phenotype of Candid #1 remains unresolved. Recently, a reverse genetics system has been developed for Candid #1. This system has the potential to address all of these concerns, and hopefully provide a safe and effective vaccine which would meet FDA approval criteria [199]. In addition, while humoral responses seem to be unimportant in LASV infection, serum treatment has shown to be efficacious in the treatment of Argentine HF [177]. While infection with JUNV can be prevented with Candid #1 or treated with patient serum, measures against LASV infection remain lacking.

Summary

Arenaviruses are pathogens of significant human morbidity and mortality, and their status as neglected tropical pathogens warrants further investigation into the mechanisms of pathogenesis, immune response, and viral biology of these important viral pathogens. While arenaviruses share many characteristics, such as genome structure,

viral assembly, natural host reservoirs, and interference with immune responses, many differences do exist between the viruses. Receptor usage and the mechanisms of viral entry differ between NW and OW viruses. While individuals infected with different arenaviruses may share some symptoms, differences do exist. Compounding these differences is the fact that even individuals infected with the same arenavirus species show varied disease manifestations, and some individuals may recover from the illness while others display severe and fatal diseases. The same can be said for the differences in pathological lesions observed in patients. However, certain symptoms may be more common for one pathogen than another. An example is the late neurological syndrome that may occur in some JUNV infected patients, which is not observed in LASV infected individuals. Alternatively, sensorineural deafness is often found in patients suffering from Lassa fever, while this is not noted in Argentine HF patients. While hemorrhage is much more common in the case of JUNV infection than for LASV infection, the disruption of the vascular endothelium is an important hallmark for both viral infections in terms of exacerbated disease. Likewise, the type of immune response generated for arenavirus hemorrhagic fevers is critical for clearance of the virus. While an effective T cell mediated response is critical for the clearance of LASV, the antibody response seems to be important for recovery from JUNV infection, as evidenced by the efficacy of treatment with immune plasma. The interaction with the immune system also demonstrates critical differences between OW and NW arenavirus infections. While severe LASV infection is characterized by a generalized immune suppression, JUNV infection seems to result in cytokine storm. Interestingly, while both NW and OW NP proteins are capable of inhibiting production of type I IFN, NW arenaviruses take an

extra precaution through the use of Z mediated inhibition of IFN through the disruption of RIG-I signaling. Taken together, while these viruses share many similarities in molecular mechanisms as well as characteristics of disease manifestation, understanding the differences between these related viruses will be beneficial in the development of new vaccines and treatment methods against these deadly viral pathogens.

Table 1.2.1:

Arenavirus distribution, host species, and disease incidence

		Geographic location	Natural host species	Incidence of disease
Old World	LCMV	Worldwide	*Mus musculus* (common mouse)	Over 5% of people show evidence of previous exposure, <1% mortality
	Lassa virus	West Africa	*Mastomys natalensis* (multimammate rat)	Approximately 2 million infections annually and between 5,000-10,000 deaths
	Lujo virus	South Africa	Unknown	5 identified cases, 4 fatal
New World	Junín virus	Argentina	*Calomys musculinus* (drylands vesper mouse)	300-1000 cases/year before vaccine, 30-50 cases/year after introduction of vaccine, 15-30% mortality
	Machupo virus	Bolivia	*Calomys callosus* (large vesper mouse)	1962-1964: 1000 cases; 1990s: 19 cases; 2007-2008: >200 cases; ~ 20% mortality
	Sabiá virus	Brazil	Unknown	1 naturally occurring case, fatal
	Guanarito virus	Venezuela	*Zygodontomys brevicauda* (common cane mouse)	618 cases, 23% fatal
	Chapare virus	Bolivia	Unknown	1 confirmed case, fatal

(Aguilar et al., 2009); (Ambrosio et al., 2011); Charella and Lamballerie, 2003); (Delgado et al., 2008); (Enria et al., 2008); (Fulhorst et al., 2008); (Harrisson et al., 1999); (Lisieux et al., 1994); (McCormick, 1999); (Paweska et al., 2009).

Table 1.2.2:

Disease symptoms of arenavirus hemorrhagic fevers:

	Old World		New World				
	Lassa	**Lujo**	**Junin**	**Machupo**	**Guanarito**	**Sabia**	**Chapare**
Hemorrhage	Mild	Yes	infrequent	infrequent	Yes	Yes	Yes
Fever	Yes	Yes	Yes	Yes	Yes	Yes	Yes
Leukopenia	Yes	Yes	Yes	Yes	Yes	Yes	--
Thrombocytopenia	infrequent	Yes	Yes	Yes	Yes	--	--
Edema	Yes	Yes	Yes	Yes	Yes	Yes	--
Shock	Yes	--	Yes	Yes	Yes	Yes	--
Petechiae	Yes	Yes	Yes	Yes	Yes	Yes	--
Elevated AST/ALT	Yes	Yes	Yes	Yes	Yes	Yes	--
Late neurologic syndrome	No	--	Yes	--	--	--	--
Seizure	Yes	--	Yes	Yes	Yes	Yes	--
Respiratory distress	Yes	Yes	--	--	--	--	--
Myalgia	Yes	Yes	Yes	Yes	Yes	Yes	Yes
Vomiting	Yes	Yes	Yes	Yes	Yes	Yes	Yes
Arthralgia	Yes	--	Yes	Yes	Yes	--	Yes
Sensorineural deafness	Yes	--	No	No	No	--	--
Hypotension	Yes	--	Yes	Yes	--	--	--
Vascular lesions	No	--	No	No	--	--	--
Elevated cytokines	No	--	Yes	Yes	--	--	--

(Aguilar et al., 2009); (Delgado et al., 2008); (Enria et al., 2008); (Harrison et al., 1999); (Kilgore et al., 1997); (Lisieux et al., 1994); (Maiztegui et al., 1979); (Manzione et al., 1998); (Moraz and Kunz, 2010); (Paweska et al., 2009); (Salas et al., 1991); (Vainrub and Salas, 1994).

Figure 1.2.1:

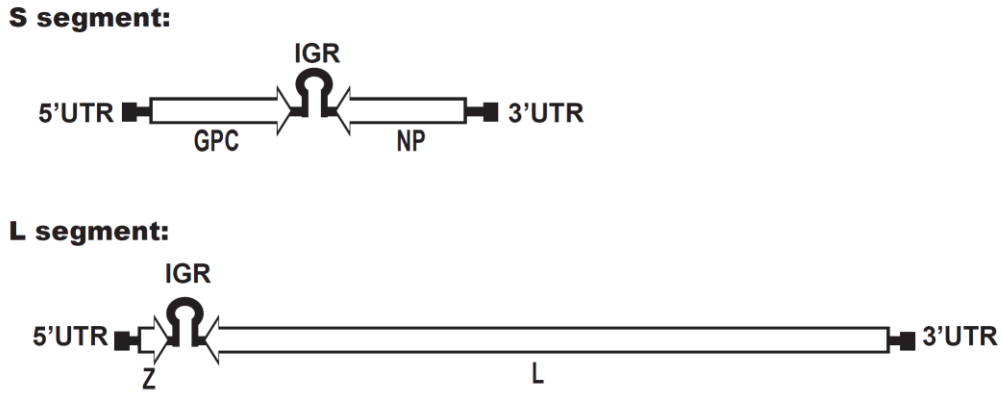

Figure Legends:

Figure 1.2.1: Arenavirus genome structure. Arenaviruses are bisegmented, ambisense RNA viruses. The L segment (or large segment) encodes the Z matrix protein in positive sense and the L polymerase in negative sense. The two genes are separated by an intergenic region (IGR) with secondary structure. The S segment (or small segment) contains the glycoprotein (GPC) gene in positive orientation and the nucleoprotein (NP) gene in negative orientation. Both segments have 5' and 3' untranslated regions (UTRs) with complementarity, allowing the genome segments to circularize into a panhandle structure.

CHAPTER 2.1

Genome comparison of virulent and avirulent strains of the Pichinde Arenavirus [200]

Shuiyun Lan[1], Lisa McLay[1], Judy Aronson[2], Hinh Ly[1], and Yuying Liang[1]

[1]Department of Pathology and Laboratory Medicine, Emory University, Atlanta, GA USA, [2]Department of Pathology and Center for Tropical Diseases, University of Texas Medical Branch, Galveston, TX, USA

Abstract

A virulent (P18) strain of the Pichinde arenavirus produces a disease in guinea pigs that somewhat mimics human Lassa fever, whereas an avirulent (P2) strain of this virus is attenuated in infected animals. It has been speculated that the composition of viral genomes may confer the degree of virulence in an infected host; the complete sequence of the viral genomes, however, is not known. Here, we provide for the first time genomic sequences of the S and L segments for both the P2 and P18 strains. Sequence comparisons identify three mutations in the GP1 subunit of the viral glycoprotein, one in the nucleoprotein NP, and five in the viral RNA polymerase L protein. These mutations, alone or in combination, may contribute to the acquired virulence of Pichinde virus infection in animals. The three amino acid changes in the variable region of the GP1 glycoprotein subunit may affect viral entry by altering its receptor-binding activity. While NP has previously been shown to modulate host immune responses to viral infection, we found that the R374 K change in this protein does not affect the NP function of suppressing interferon-b expression. Four out of the five amino acid changes in the L protein occur in a small region of the protein that may contribute to viral virulence by enhancing its function in viral genomic RNA synthesis.

Introduction

Arenaviruses are bi-segmented ambisense single-stranded RNA viruses [149]. Five of the viruses (i.e., Lassa, Junin, Machupo, Guanarito, and Sabia viruses) can cause severe viral hemorrhagic fevers (VHFs) in humans [3]. Lassa fever is endemic in certain regions of West Africa [201]. Currently, there are few effective vaccines and treatment options for VHFs. As a result, highly pathogenic arenaviruses are included in the Category A Pathogen List of the Center for Disease Control and Prevention (CDC). Efforts to understand the basic biology and pathogenesis of these pathogenic arenaviruses in order to develop effective antiviral strategies are hampered by the hazardous nature of these infectious agents and the necessary requirement to work with them in a BSL-4 laboratory.

Pichinde virus (PICV) is a nonpathogenic arenavirus that acquires virulence in guinea pigs upon long-term passaging in the animals in a conventional BSL-2 laboratory [95]. The high-passage, virulent (P18) strain of PICV causes a disease in guinea pigs that mimics human Lassa fever in some aspects, including the correlation between viremia and outcome [94, 105], terminal vascular leakage syndrome [202], and identical distribution of viral antigens within infected hosts [203].

PICV shares a similar genomic organization with all other arenaviruses [149]. Its genome consists of two RNA segments, the large segment (L) of approximately 7.2 kb and the small (S) fragment of ~3.4 kb. The L RNA segment encodes the viral polymerase L protein and a small multi-functional Z protein. The S RNA segment encodes the nucleoprotein (N or NP) and the envelope glycoprotein precursor GPC that is post-

translationally processed into GP1 and GP2 subunits. The genes are encoded in an ambisense orientation [149], such that the NP and L genes are encoded in the conventional negative sense, whereas the GPC and Z genes are encoded in the positive sense. At both ends of the RNA segments, the terminal 19 nucleotides, conserved among all arenaviruses, are complementary to each other and are predicted to form panhandle structures that are the cis-acting signals required for viral RNA transcription and replication [28, 204]. A unique feature among the arenavirus genomic RNAs is the noncoding intergenic regions (IGRs) located between the two ORFs on each of the segments [149]. The IGRs, ranging from 59 to 217 nts in length, are predicted to form one to three energetically stable stem-loop structures in both the genomic and antigenomic RNAs [205] and are proposed to contribute to transcriptional termination [27, 206-208]. Both the L and NP proteins are essential for viral transcription and replication [209]. The viral glycoprotein GPC is expressed as a single polypeptide with an extended signal peptide and is posttranslational processed by the cellular SKI-1/S1P subtilase into GP1 and GP2 [66, 69]. GP1 is a peripheral membrane protein, and GP2 a transmembrane protein. The Z protein carries short proline-rich sequences called the L domains, which are known to promote virus particle budding by interacting with cellular proteins, such as Tsg101 and Nedd4 [210]. It has been shown that Lassa fever Z protein alone is sufficient for the formation of virus-like particles [77].

The molecular determinants of Pichinde virus virulence in guinea pigs have not been characterized due in part to the lack of sequence information of both of the viral genomic segments and a molecular clone for the virus. Published sequences of the S segment have identified several sequence variations between the P2 and P18 strains

within the GPC and NP genes, suggesting that viral genomic sequence variations may dictate the differential behaviors of different strains of the virus in an infected host [211]. Reassortment experiments have further suggested that genes encoded on both the S and L segments may contribute to the acquired virulence [212]. To our knowledge, the full-length sequences of the L segment for the P2 and P18 viruses are not yet available. Here, we report for the first time the complete sequences of both L and S segments of P2 and P18 viruses. Our data have confirmed the previously identified sequence variations in coding sequences of the S segments and revealed novel sequence changes in the L segments that may help define the molecular determinants of PICV virulence in an infected animal.

Materials and methods

Viruses and cells

Both P2 and P18 viruses are derived from the Pichinde Munchique strain CoAn4763 (the 2 and 18 indicate passage numbers). The Pichinde CoAn4763 virus was passaged once in guinea pigs in Dr. Peter Jahrling's laboratory (USAMRID). This strain was subsequently passaged once more in a guinea pig in order to produce the P2 strain. Virulent, high-guinea-pig-passage Pichinde virus, derived from Jahrling's original passage-adapted CoAn4763 adPIC virus, was obtained from Dr. Dorian Coppenhaver (UTMB) as spleen stock of the 15th guinea pig passage and was successively passaged further in inbred guinea pigs in order to obtain the P18 strain [95]. Both BHK-21 and

Vero cells were maintained in modified Eagle's medium (MEM) supplemented with 10% fetal bovine serum and 50 µg/ml of penicillin and streptomycin.

Viral RNA isolation

The P2 and P18 viruses were amplified once in BHK-21 cells at low multiplicity of infection (MOI = 0.1). At 4 days post-infection (dpi), viral RNA was extracted from viral particles using the Qiagen viral RNA extraction kit (Qiagen).

cDNA synthesis and PCR amplification of viral sequences

Viral RNA samples extracted from virus supernatants were cleared of possible DNA contamination by DNase I treatment for 30 min at 37°C and then at 85°C for 15 min. Reverse transcription was conducted using specific primers for PICV S and L segments (5' CGCACCGGGGATCCTAGG 3', 5' CGCACCGAGGATCCTAGGC 3', and 5' CGCACAGTGGATCCTAGGC 3') according to the protocol outlined in the SuperScript III first-strand synthesis kit (Invitrogen).

PCR amplification of the L or S segment was conducted using the Phusion Hot Start High-Fidelity DNA Polymerase in GC-rich buffer (New England BioLabs) with paired primers, 5' CGCACCGGGGATCCTAGG 3' and 5' CGCACCGAGGATCCTAGGC 3' for the L segment, 5' CGCACCGGGGATCCTAGG 3' and 5' CGCACAGTGGATCCTAGGC 3' for the S segment. The PCR reaction conditions were 30 cycles of 98°C for 30 s, 59°C for 20 s, and 72°C for 3.5 min (L

segment) or 1.5 min (S segment). The PCR reaction was performed using Pfu Turbo Taq polymerase (Stratagene) with paired primers targeting the flanking sequences of the IGR to amplify either a 360-bp IGR of the S segment or a 455-bp IGR of the L segment. The PCR reaction conditions were 30 cycles of 98°C for 30 s, 56°C for 30 s, and 72°C for 30s.

Cloning and sequencing

A minimum of five plasmids for each of the PCR products were sequenced in order to obtain a consensus sequence. All sequence analyses were conducted using either the Vector NTI Advance 10.0 software from InforMax (Invitrogen) or the MacVector 7.2.3 software (MacVector Inc.). GenBank accession numbers for the reported sequences are: P2 S segment, EF529744; P2 L segment, EF529745; P18 S segment, EF529746; P18 L segment, EF529747.

Interferon-β reporter assay

293T cells were cotransfected using calcium phosphate with 0.5 μg of a vector that expresses the firefly luciferase (Fluc) reporter gene from a known functional promoter of the IFN-β gene (pIFNβ-LUC) and 2 μg of the individual protein expression plasmid pCAGGS (‘empty’ control vector), pCAGGS-P2NP (expressing the P2 NP protein), pCAGGS-P18NP (expressing the P18 NP), or pcDNA3.1-NS1 (expressing the influenza A virus NS1 protein, which is known to inhibit IFN expression [213]). A β-gal-

expressing plasmid was included in each of the transfection reactions for normalization. Six hours post-transfection, cells were washed with phosphate-buffered saline and supplemented with fresh DMEM medium. At 24 h posttransfection, cells were infected with Sendai virus (at moi = 1) in order to induce IFN-β expression. At 24 hpi, cell lysates were prepared for luciferase and β-gal assays using the appropriate kits, which were purchased from Promega. Fluc activities obtained from the transfection reactions were normalized to the β-gal values and compared.

Results and discussion

Cloning and sequence analysis of the S segments of the P2 and P18 viruses

PICV P2 and P18 viruses were amplified once in BHK-21 cells in order to extract enough viral RNAs for further manipulations. A previous study [212] has shown that limited passages of viruses on cultured cells required for plaque purification did not change viral pathogenicity *in vivo*. We therefore believe that a single round of virus amplification should not greatly alter the native genomic sequences of the P2 and P18 viruses. Viral RNAs were reverse transcribed using primers specific for the PICV viral terminal sequences that were deposited in GenBank. The S segment was amplified using a high-fidelity enzyme and cloned into the pCR-XL-TOPO vector using the TA cloning technique. Consensus sequences of most of the S segments, except for the IGRs, were assembled from multiple sequences of the respective P2 and P18 strains. We chose to subclone the PCR products prior to sequencing because sequence data obtained by direct sequencing of the PCR products were usually suboptimal in quality and hard to interpret,

especially around the GC-rich IGR region. In order to obtain accurate IGR consensus sequences for P2 and P18, we amplified short sequences spanning only the IGRs of the respective strains and cloned them into pGEM-T-Easy Vector. Multiple independent clones reveal identical sequences of the IGR for P2 and P18, as have previously been reported [211]. All in all, we believe that we have successfully assembled the consensus sequence for the full-length S segments of P2 and P18 strains, which only show minor sequence variations from those that have been published previously [211]. The P2 S segments differ at 17 positions (81, 135, 187, 405, 471, 567, 699, 1014, 1158, 1206, 1242, 1365, 2466, 2712, 3222, 3374, 3398), whereas the P18 S segments differ at 5 positions (1336, 1713, 1860, 3236, 3387) from the published sequences [211]. The differences in sequence variations of the S segments obtained from the current study and the previous one might result from the different sequencing methods employed. Nevertheless, both studies revealed the same set of amino acid changes in the S segment, except for one in the NP protein.

A published report compared sequences of the S segments between the different guinea-pig-passaged PICVs and found a total of 43 nt changes [211]. However, only 19 nt changes between the avirulent strains P1 and P2 and the virulent strains P17 and P18 appeared to be associated with the degree of viral virulence. Interestingly, these nucleotide substitutions are located within the GPC and NP protein coding regions, and most of them are silent mutations. Five substitution mutations (G407C, A469G, A541G, C2218T, and C3236T) result in three nonsynonymous amino acid changes (S119T, K140E, and I164 V) in the GP1 subunit of the viral glycoprotein and two residue changes (R374 K and A35T) in the NP protein. In the current study, a total of 33 nt differences,

all of which are located within protein coding regions, were found between the P2 and P18 viruses (Table 1). Consistent with the published data, most of these changes produced silent mutations. We have not formally ruled out the possibility that any of these nucleotide substitutions can alter the synthesis and/or stability of the viral S RNA segment. Four of the nt changes in the S segment (G407C, A469G, A541G, and C2218T) result in 3 amino acid substitutions in the GP1 subunit of the viral glycoprotein (S119T, K140E, and I164 V) and a residue change in the NP protein (R374 K). Unlike the published report, however, we did not observe the A35T change at position 3236 of the NP gene [211]. Taken together, our study has mostly confirmed data reported previously and suggests that sequences of the avirulent PICVs differ from the virulent ones at positions 119, 140, and 164 of the GPC gene and at position 374 of the NP gene (Table 2.1.1).

The arenaviral GPC precursor protein contains a long conserved 58-aa signal peptide (SP) and is cleaved into GP-1 and GP-2 by the host SKI-1/S1P subtilase [66, 69]. Sequence alignment of all known arenaviral GPC proteins suggests that GP-1 is highly variable among the arenaviruses, with only a few short stretches of conserved sequences (Fig. 2.1.1a, gray boxes), whereas the sequences of GP-2 and the signal peptide (SP) are highly conserved. Sequence variations in GP1 may correlate with its functions: GP-1 forms the receptor-binding site and is recognized by host neutralizing antibodies, which may drive the evolution of this viral glycoprotein subunit. GP-2, on the other hand, is a transmembrane-anchored subunit of the glycoprotein, which is usually not exposed to neutralizing antibodies and therefore can maintain its conserved sequence and structure. Accordingly, the three mutations (S119T, K140E, and I164 V) identified in our study are

located within the highly variable regions of the GP-1 subunit (Fig. 2.1.1a). These residue changes may affect virus-receptor binding specificity and may contribute to pathogenesis in an infected host. Many viral surface glycoproteins play a major role in determining viral tropism and pathogenic processes. For example, influenza virus hemagglutinin (HA) is one of the virulence determinants of the H5N1 viruses in mammals. Sequence changes in the viral HA glycoprotein have been shown to alter its receptor binding specificity, allowing the virus to ‘‘jump’’ host species [214-216]. The Ebola GP glycoprotein is another example of a major determinant of viral tropism and virulence [217-219].

The NP protein is indispensable for viral RNA replication and transcription as it intimately interacts with viral genomic RNA. Its primary sequence is, therefore, generally highly conserved among the arenaviruses (Fig. 2.1.1b). A single residue change identified between P2 and P18 viruses turns out to be a conserved amino acid substitution (i.e., R374 K). Although this amino acid residue is located within one of the conserved domains of the protein (Fig. 2.1.1b), the residue itself is not conserved among the arenaviruses. Recently, a novel function for the NP protein of the LCMV virus in down-regulating interferon expression of the infected cells has been revealed [220]. This implicates NP as a potential virulence factor. We have therefore undertaken a study to determine whether the R374 K substitution can inhibit IFN-β production. To do this, 293T cells were cotransfected using calcium phosphate with 0.5 μg of a vector that expresses the firefly luciferase (Fluc) reporter gene from a known functional promoter of the IFN-β gene and 2 μg of the individual protein-expression plasmid pCAGGS (‘empty’ control vector), pCAGGS-P2NP (expressing the P2 NP protein), pCAGGS-P18NP (expressing the P18 NP), or pcDNA3.1- NS1 (expressing the flu-A NS1 protein, which

has been shown to strongly inhibit the IFN-β gene). A β-galexpressing plasmid (0.1 μg) was included in each of the transfection reactions for normalization. Six hours posttransfection, cells were washed with phosphate-buffered saline and supplemented with fresh DMEM medium. At 24 h post-transfection, cells were infected with Sendai virus (at moi = 1) in order to induce IFN-β expression. At 24 hpi, cell lysates were prepared for luciferase and β-gal assays using the appropriate kits and protocols supplied byPromega. Fluc activities obtained from the transfection reactions were normalized using the β-gal values and compared. Our data show that both the P2 NP and P18 NP inhibited IFN-β expression, as judged by the decreased levels of Fluc reporter expression, to a similar extent (Fig. 2.1.2), suggesting that the single conservative amino acid differences in the NP gene between the P2 and P18 virus does not affect its role in IFN-β inhibition. This is consistent with recent findings that NP proteins from Pichinde virus and a variety of other arenaviruses, except for Tacaribe virus, inhibit activation of the promoters of IFN-β and interferon regulatory factor 3 (IRF3) as well as the nuclear translocation of the IRF3 factor [99].

Cloning and sequence analysis of the L segments of the P2 and P18 viruses

To clone the L segment, we first attempted to amplify the entire segment in a single PCR reaction using primers that annealed to the conserved ends. We successfully amplified a 7-kb PCR product, which is the approximate size of the full-length L segment, but failed to clone it into a vector. Since no published sequences of the L segment for P2 or P18 viruses were available, we could not design PCR primers to

amplify shorter fragments for subcloning purposes. Instead, we decided to digest the 7-kb PCR product with BamH I and Bgl II restriction enzymes and subcloned a 1.4-kb DNA fragment representing the middle region of the L segments into the pBluescript vector. Using the consensus sequences of this fragment, we designed primers to amplify the rest of the viral L segments from viral genomic RNA. At least five independent clones for each of the fragments, representing the 5', middle, and 3' regions of the L segments, were sequenced in order to obtain the consensus sequences. The IGR sequence of the L segment was obtained in a way similar to that described above for the S segment.

The full-length sequences of the L segment of the P2 and P18 viruses have a length of 7,057 nt and carry 16 nucleotide differences between these two virus strains. The sequence of the Z protein is absolutely conserved between P2 and P18 viruses, suggesting that no differences in its known multiple activities, such as virus assembly and budding [76, 77, 221, 222] and regulation of viral RNA replication [58, 61, 62, 223, 224], are expected between the viruses. All changes on the L segments are localized to the L polymerase protein-coding region, five of which cause amino acid changes (N355D, A1808T, V1839L, D1889 N, and D1906 N) (Table 2). These changes are predicted to affect the function of the L polymerase protein and thus to potentially alter the viral replicative potential *in vivo*. The rest of the sequence changes (at nts #473, 860, 1178, 1529, 2972, 3173, 3485, 3611, 6149, and 6812) produce silent mutations (Table 2.1.2). Again, we have not determined whether these silent mutations can alter the synthesis and/or stability of the L RNA segment.

The L polymerase is a large protein of more than 2,100 residues that functions as an RNA-dependent RNA polymerase. Due to its enormous size, no structural information

is currently available for this protein. However, sequence alignments of all known arenaviral L proteins have provided some insights into the possible functional domains of this protein. The L protein contains, in the central region, the four conserved motifs (A, B, C, and D) identified in all RNA-dependent polymerases, which constitute the ‘‘polymerase module’’ implicated in template recognition and polymerizing activity [225] (Figs. 2.1.3, 2.1.4a). In particular, the highly conserved SDD sequence in the motif C of the protein (Fig. 2.1.4a) is predicted to play a central role in the enzyme’s polymerizing activity. Alignment of all available sequences of arenaviral L proteins also reveals multiple conserved domains across this protein (Fig. 2.1.3, gray boxes), suggesting that the mechanism for the L protein to recognize, replicate, and transcribe the ambisense segmented RNA genome is conserved among the arenaviruses. Among the 5 identified residue changes in the L protein between the P2 and P18 viruses, four (N355D, A1808T, D1889 N, and D1906 N) are localized in the variable regions, whereas the V1839L change is located within a region conserved among the New World arenaviruses (Fig. 2.1.3). This residue always encodes a valine among the New World arenaviruses (Fig. 2.1.4b) but nevertheless is variable among the Old World arenaviruses (data not shown). We have yet to determine whether the V1839L substitution has an effect on L polymerase functions.

Mutagenesis of the LCMV L gene has produced various mutations that affect plaque morphology [226], induce lethality in infected guinea pigs [227], or suppress the cytotoxic T-cell response in order to initiate persistent viral infection [228]. It is, therefore, reasonable to suggest that any of the five amino acid substitutions in the L gene identified in our study, either individually or in combination (Fig. 2.1.3), may specify

determinants of viral virulence of the PICV P18 virus in an infected animal. Although we do not know how these mutations affect the function of L polymerase in viral RNA synthesis, we speculate that some of these changes are significant as they represent amino acid substitutions that can potentially alter the overall folding of the protein. Interestingly, four of the mutations (A1808T, V1839L, D1889N, and D1906N) are localized within a small region of 99 amino acid residues, implying that this domain may affect the efficiency of viral RNA synthesis and/or replication. It is not uncommon that the molecular determinant of viral virulence is localized in the polymerase enzyme. A single amino acid substitution in one subunit of the influenza viral polymerase (e.g., PB2 E627K) has been shown to enhance the degree of virulence of the H5N1 virus in mice [229], which might explain the high lethality observed with the 1918 pandemic flu virus. It has also been documented that a single amino acid change(K1079Q) in the L gene of the LCMV virus increases virus production and infection of macrophages, which may possibly be responsible for viral persistence and immune suppressive effect in an infected animal [108].

In summary, our sequence analyses of both the S and L segments of the P2 and P18 viruses have uncovered three amino acid changes in the GPC protein, one in the NP protein, and five in the L protein that may be responsible for their observed phenotypic differences in infected animals. We hypothesize that these mutations, either acting alone or in combination, are potential determinants of viral virulence in the animals. Previous studies have suggested that aberrant cytokine production and suppressed immune signaling are the underlying mechanisms for the high virulence of P18 virus in guinea pigs [230-233]. These observations are consistent with those made for other hemorrhagic

fever-causing viruses. For example, Lassa fever virus does not activate macrophages following infection [134, 166]. The immuno-regulatory function of dendritic cell are known to be inhibited by Ebola or Lassa virus infection [168]. How natural mutations in the GPC, NP, and/or L proteins contribute to altered production of proinflammatory cytokines and a suppressed immune signaling mechanism are not understood. Several mechanisms to explain the phenomenon are proposed: (1) mutation of the GPC protein may change the receptor specificity and thus allow for a more efficient spread of the virus within an infected host, which can lead to increased proinflammatory cytokine production; (2) mutations in the GPC protein may enable the virus to more efficiently infect host immune cells and impair their functions, leading to the observed suppressed immune response; (3) mutations in the NP and/ or L proteins may enhance viral replication *in vivo* and thus overwhelm the normal host immune responses to viral infection; and (4) mutations in any of the viral proteins identified in this study may modulate their interactions with host cell signaling proteins, leading to the differential responses to viral infection. Development of a reverse genetics system for PICV will help to unravel the molecular mechanisms leading to acquired virulence of viral infection in guinea pigs and the roles of the individual viral proteins in viral replication and pathogenesis. These efforts will undoubtedly provide important insights into the pathogenesis of hemorrhagic fever caused by the different arenaviruses.

Acknowledgments

This research was supported by the Emory University Research Committee (URC) and the Southeast Regional Center of Excellence for Emerging Infections and Biodefense (SERCEB) to HL and YL, the Emory Digestive Diseases Research and Development Center P/F fund (DK64399) and the Center for AIDS Research (CFAR P30 AI050409) to HL, and the pilot project component of Dr. Ahmed's U19 grant (RFA-AI-02-042) to YL.

Table 2.1.1

Table 1 Sequence comparison of the S segment of different Pichinde virus strains (sequences are reported by Zhang et al. and in this paper)

nt #	Avirulent P1 (Zhang et al.)	Avirulent P2 (Zhang et al.)	Virulent P17 (Zhang et al.)	Virulent P18 (Zhang et al.)	Avirulent P2 (this paper)	Virulent P18 (this paper)	Codon
81	C (Ser)	C (Ser)	T (Ser)	T (Ser)	T (Ser)	T (Ser)	
99	A (Gln)	A (Gln)	G (Gln)	G (Gln)	A (Gln)	G (Gln)	
135	C (Thr)	C (Thr)	C (Thr)	C (Thr)	T (Thr)	C (Thr)	
136	C (Leu)	T (Leu)	C (Leu)	C (Leu)	T (Leu)	C (Leu)	
187	C (Leu)	**T (Phe)**	C (Leu)	C (Leu)	C (Leu)	C (Leu)	
225	C (Asp)	T (Asp)	T (Asp)	T (Asp)	T (Asp)	T (Asp)	
226	A (Ser)	G (Gly)	G (Gly)	G (Gly)	G (Gly)	G (Gly)	
243	A (Arg)	A (Arg)	G (Arg)	G (Arg)	A (Arg)	G (Arg)	
405	T (Thr)	T (Thr)	T (Thr)	T (Thr)	C (Thr)	T (Thr)	
407	**G (Ser)**	**G (Ser)**	C (Thr)	C (Thr)	**G (Ser)**	C (Thr)	**GPC (S119T)**
469	**A (Lys)**	**A (Lys)**	G (Glu)	G (Glu)	**A (Lys)**	G (Glu)	**GPC (K140E)**
471	A (Lys)	G (Lys)	A (Lys)	A (Lys)	A (Lys)	A (Lys)	
541	**A (Ile)**	**A (Ile)**	G (Val)	G (Val)	**A (Ile)**	G (Val)	**GPC (I164V)**
567	A (Glu)	A (Glu)	G (Glu)	G (Glu)	G (Glu)	G (Glu)	
699	C (Asn)	T (Asn)	T (Asn)	T (Asn)	C (Asn)	T (Asn)	
897	C (Asp)	C (Asp)	T (Asp)	C (Asp)	C (Asp)	C (Asp)	
1014	G (Glu)	A (Glu)	A (Glu)	A (Glu)	G (Glu)	A (Glu)	
1053	A (Gln)	G (Gln)	G (Gln)	G (Gln)	G (Gln)	G (Gln)	
1158	C (Leu)	C (Leu)	C (Leu)	C (Leu)	T (Leu)	C (Leu)	
1206	C (Tyr)	C (Tyr)	C (Tyr)	C (Tyr)	T (Tyr)	C (Tyr)	
1242	A (Pro)	G (Pro)	G (Pro)	G (Pro)	A (Pro)	G (Pro)	
1336	C (Leu)	C (Leu)	C (Leu)	**G (Val)**	C (Leu)	C (Leu)	
1365	C (Gly)	T (Gly)	T (Gly)	T (Gly)	C (Gly)	T (Gly)	
1625	C	T	T	T	T	T	IGR
1698	G (Pro)	G (Pro)	A (Pro)	A (Pro)	G (Pro)	A (Pro)	
1703	G (Leu)	G (Leu)	A (Leu)	A (Leu)	G (Leu)	A (Leu)	
1713	T (Pro)	T (Pro)	G (Pro)	T (Pro)	T (Pro)	C (Pro)	
1716	C (Lys)	C (Lys)	T (Lys)	C (Lys)	C (Lys)	C (Lys)	
1728	G (Val)	G (Val)	A (Val)	A (Val)	G (Val)	A (Val)	
1860	A (Tyr)	A (Tyr)	A (Tyr)	A (Tyr)	A (Tyr)	G (Tyr)	
2067	G (Leu)	G (Leu)	A (Leu)	A (Leu)	G (Leu)	A (Leu)	
2218	**C (Arg)**	**C (Arg)**	T (Lys)	T (Lys)	**C (Arg)**	T (Lys)	**NP (R374K)**
2300	C (Asp)	T (Asn)	T (Asn)	T (Asn)	T (Asn)	T (Asn)	
2328	C (Lys)	T (Lys)	C (Lys)	C (Lys)	T (Lys)	C (Lys)	
2343	C (Val)	T (Val)	C (Val)	T (Val)	T (Val)	T (Val)	
2355	G (Asp)	A (Asp)	G (Asp)	A (Asp)	A (Asp)	A (Asp)	
2435	G (Leu)	G (Leu)	A (Leu)	A (Leu)	G (Leu)	A (Leu)	
2466	A (Thr)	A (Thr)	A (Thr)	A (Thr)	G (Thr)	A (Thr)	
2712	G (Phe)	G (Phe)	G (Phe)	G (Phe)	A (Phe)	G (Phe)	
2757	G (Val)	G (Val)	A (Val)	A (Val)	G (Val)	A (Val)	
2805	C (Leu)	C (Leu)	T (Leu)	T (Leu)	C (Leu)	T (Leu)	
2844	G (Asn)	G (Asn)	A (Asn)	A (Asn)	G (Asn)	A (Asn)	
2945	G (Leu)	G (Leu)	A (Leu)	A (Leu)	G (Leu)	A (Leu)	
2946	T (Gln)	T (Gln)	C (Gln)	C (Gln)	T (Gln)	C (Gln)	
3078	A (Leu)	G (Leu)	A (Leu)	A (Leu)	G (Leu)	A (Leu)	
3213	G (Phe)	G (Phe)	A (Phe)	A (Phe)	G (Phe)	A (Phe)	
3222	A (Ala)	A (Ala)	A (Ala)	A (Ala)	G (Ala)	A (Ala)	
3236	**C (Ala)**	**C (Ala)**	T (Thr)	T (Thr)	**C (Ala)**	**C (Ala)**	

Table 2.1.1 continued:

Table 1 continued

nt #	Avirulent P1 (Zhang et al.)	Avirulent P2 (Zhang et al.)	Virulent P17 (Zhang et al.)	Virulent P18 (Zhang et al.)	Avirulent P2 (this paper)	Virulent P18 (this paper)	Codon
3374	G	A	G	G	G	G	3′UTR
3387	A	A	A	G	A	A	
3398	G	A	G	G	G	G	

Bold values indicate the sequence changes between the virulent and avirulent strains

Table 2.1.2:

Table 2 Sequence comparison of the L segment from avirulent P2 and virulent P18 Pichinde viruses

nt #	Avirulent P2	Virulent P18	Codon
473	G (Phe)	A (Phe)	
860	T (Val)	A (Val)	
1178	C (Lys)	T (Lys)	
1312	C (Asp)	T (Asn)	**L (D1906N)**
1363	C (Asp)	T (Asn)	**L (D1889N)**
1513	C (Val)	G (Leu)	**L (V1839L)**
1529	G (Tyr)	A (Tyr)	
1606	C (Ala)	T (Thr)	**L (A1808T)**
2972	T (Gly)	C (Gly)	
3173	G (Asn)	A (Asn)	
3485	C (Leu)	T (Leu)	
3611	A (Asn)	G (Thr)	
5965	T (Asn)	C (Asp)	**L (N355D)**
6149	A (Cys)	G (Cys)	
6812	G (Leu)	A (Leu)	

Bold values indicate the sequence changes between the virulent and avirulent strains

Figure 2.1.1:

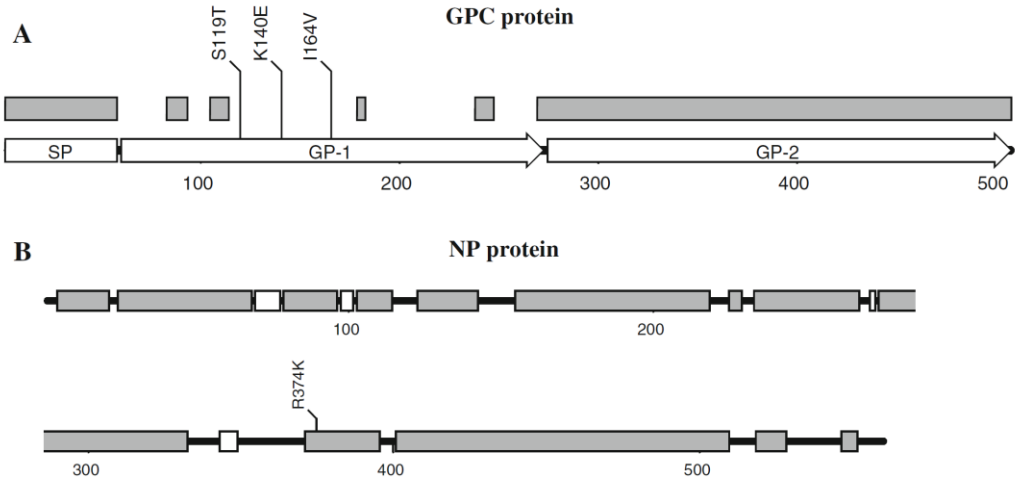
A
GPC protein
S119T
K140E
I164V
SP
GP-1
GP-2
100
200
300
400
500
B
NP protein
100
200
R374K
300
400
500

Figure 2.1.2:

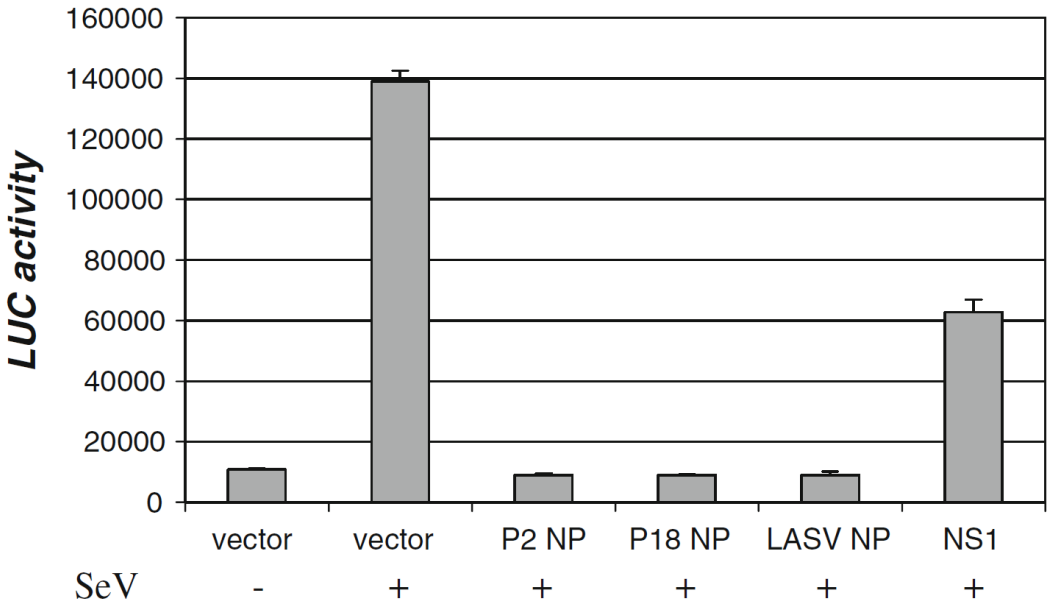
LUC activity
160000
140000
120000
100000
80000
60000
40000
20000
0
vector
vector
P2 NP
P18 NP
LASV NP
NS1
SeV
-
+
+
+
+
+

Figure 2.1.3:

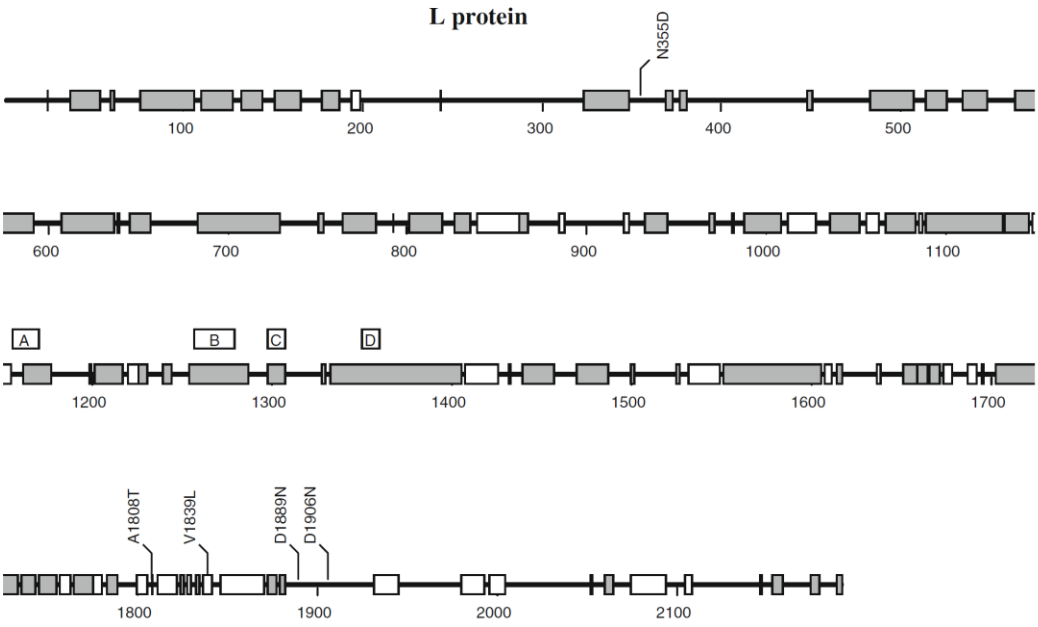
L protein
N355D
100
200
300
400
500
600
700
800
900
1000
1100
A
B
C
D
1200
1300
1400
1500
1600
1700
A1808T
V1839L
D1889N
D1906N
1800
1900
2000
2100

Figure 2.1.4:

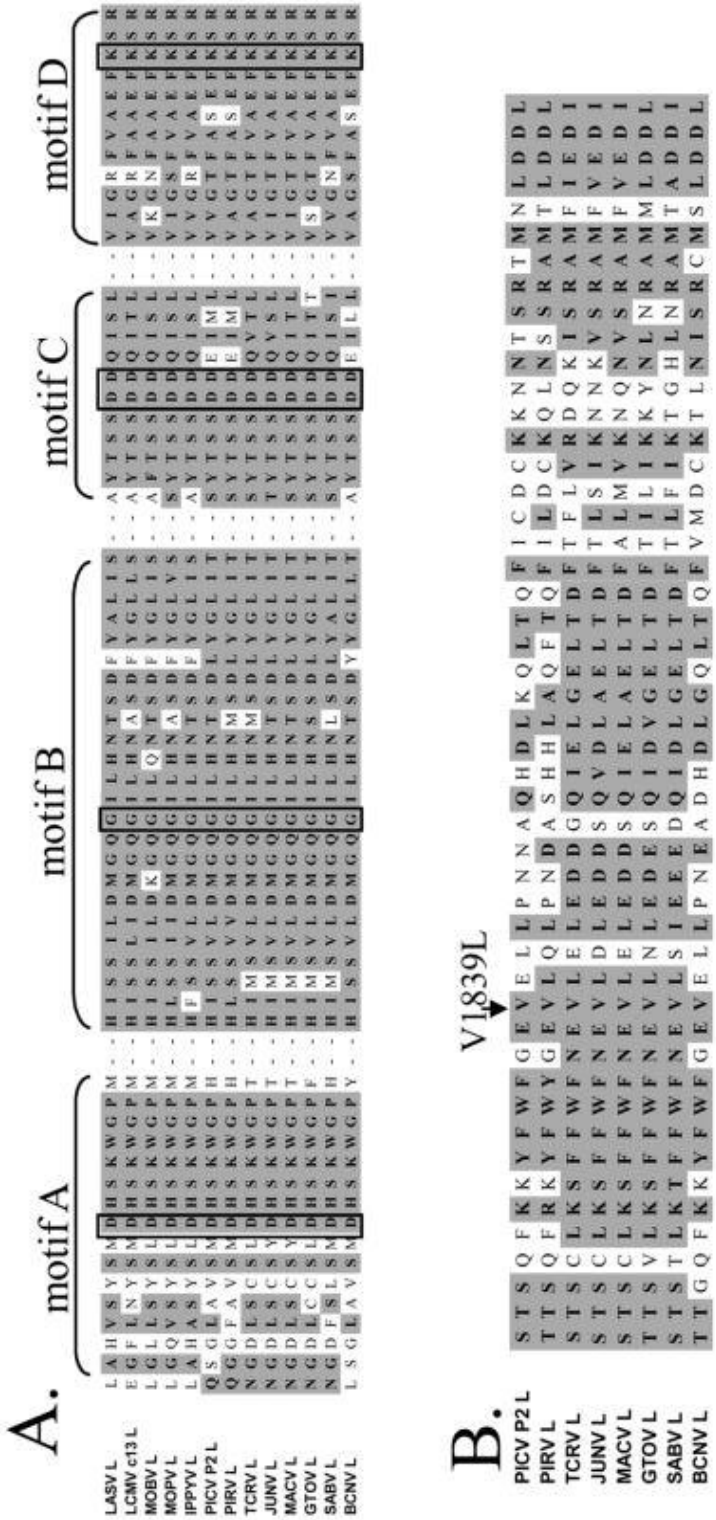
A.
motif A
motif B
motif C
motif D
LASV L
LCMV c13 L
MOBV L
MOPV L
IPPYV L
PICV P2 L
PIRV L
TCRV L
JUNV L
MACV L
GTOV L
SABV L
BCNV L
B.
V1839L
PICV P2 L
PIRV L
TCRV L
JUNV L
MACV L
GTOV L
SABV L
BCNV L

Figure Legends

Figure 2.1.1: Location of various natural mutations in viral GPC and NP proteins. **A)** A schematic representation of the GPC protein, which consists of a long signal peptide (SP), GP-1, and GP-2. The conserved regions among GPC proteins of arenaviruses are shown as gray boxes. The three natural mutations identified between the P2 and P18 viral variants are also shown. **B**) A schematic representation of the NP protein. The conserved domains among all arenaviruses are shown as gray bars, while the regions conserved only among the New World arenaviruses are shown as white bars. The single R374K mutation identified between the P2 and P18 viral variants is also shown.

Figure 2.1.2: Both P2 and P18 NP proteins inhibit IFN-b expression. 293T cells were transfected with an IFNb-LUC reporter plasmid together with either empty vector or vector expressing P2 NP, P18 NP, Lassa virus NP, or influenza A virus NS1. A b-gal expression plasmid was included in each reaction for normalization purposes. Cells were infected with or without Sendai virus to induce IFN-b expression. Luciferase activity was measured at 24 hpi and normalized against b-gal activity.

Figure 2.1.3: A schematic representation of the viral polymerase L protein. The domains of this protein that are conserved among arenaviruses are shown as gray bars, whereas the regions conserved only among the New World arenaviruses are shown as white bars. The

four domains (A, B, C, D) conserved among all RNA-dependent polymerases are indicated [225]. The six mutations identified between P2 and P18 viral variants are also shown.

Figure 2.1.4: A) Sequence alignment of the four domains in the arenavirus L proteins (A, B, C, and D) that are conserved in RNA-dependent polymerases [225], with the invariant D, G, DD, and K residues in each domain boxed. **B**) Sequence alignment of a conserved region among the New World arenavirus near the V1839L mutation.

CHAPTER 2.2

Development of infectious clones for virulent and avirulent Pichinde viruses: a model virus to study arenavirus-induced hemorrhagic fevers [234]

Shuiyun Lan, Lisa McLay Schelde, Jialong Wang, Naveen Kumar, Hinh Ly, and Yuying Liang

Department of Pathology and Laboratory Medicine, Emory University, Atlanta, GA USA

Abstract

Several arenaviruses can cause hemorrhagic fever diseases (VHFs) in humans, the pathogenic mechanism of which is poorly understood due to their virulent nature and the lack of molecular clones. A safe, convenient, and economical small animal model of arenavirus hemorrhagic fever is based on guinea pigs infected by the arenavirus Pichinde (PICV). PICV does not cause disease in humans, but an adapted strain of PICV (P18) causes a disease in guinea pigs that mimic arenavirus hemorrhagic fever in humans in many aspects, while a low-passaged strain (P2) remains avirulent in infected animals. In order to identify the virulence determinants within the PICV genome, we developed the molecular clones for both the avirulent P2 and virulent P18 viruses. Recombinant viruses were generated by transfecting plasmids that contain the antigenomic L and S RNA segments of PICV under the T7 promoter into BSRT7-5 cells, which constitutively express T7 RNA polymerase. By analyzing viral growth kinetics *in vitro* and virulence *in vivo*, we show that the recombinant viruses accurately recapitulate the replication and virulence natures of their respective parental viruses. Both parental and recombinant virulent viruses led to high levels of viremia and titers in different organs of the infected animals, whereas the avirulent viruses were effectively controlled and cleared by the hosts. These novel infectious clones for the PICV viruses provide essential tools to identify the virulence factors that are responsible for the severe VHF-like disease in infected animals.

Introduction

Arenaviruses are enveloped RNA viruses with single-stranded ambisense RNA genome [149]. The genome of these viruses consists of two RNA segments, the large segment (L) of ~ 7.2 kb and the small (S) segment of ~ 3.4 kb [149]. The L RNA segment encodes the viral polymerase L gene in a negative orientation and a small multi-functional Z protein in a positive sense. The S RNA segment encodes the nucleoprotein NP in a negative orientation and the envelope glycoprotein precursor GPC in a positive sense [149]. The terminal 19 nucleotides from both ends of the segments are imperfectly complementary to each other and are predicted to form the panhandle structures that serve as the cis-acting elements required for viral RNA transcription and replication [28, 204, 222, 235]. A unique feature of the arenavirus genomic RNAs is the noncoding intergenic regions (IGRs) located between the two open-reading frames (ORFs) [149]. They range from 59 to 217 nts in length and are predicted to form one to three energetically stable stem-loop structures [149, 205] that are proposed to contribute to transcriptional termination. Currently the only available molecular clone of arenavirus was developed for the prototype lymphocytic choriomeningitis virus (LCMV)[236, 237]. This system has served as an invaluable tool to study the biological functions of arenavirus proteins and RNA elements.

Several arenaviruses have been known to cause deadly hemorrhagic fever diseases (VHFs) in humans, including Lassa fever that is endemic in West Africa [238, 239]. The disease is caused by infection of Lassa fever virus, an Old World arenavirus that is usually found in the rodent *Mastomys natalensis* [201]. The consequences of human Lassa fever infection may range from asymptomatic to severe multi-system

disease that is clinically indistinguishable from other febrile illnesses such as Ebola and Dengue [154]. Besides Lassa, several other arenaviruses (i.e., Junin, Machupo, Guanarito, Sabia, and Chapare) are known to cause VHFs in humans [3, 17]. Currently, there are no effective vaccines, except for Junin virus, and limited treatment options for these pathogenic arenaviruses. Therefore, these highly pathogenic arenaviruses must be handled in Biosafety Level-4 (BSL-4) facilities.

The pathogenesis of arenavirus-induced VHFs is poorly understood. Despite the presence of high virus titers in a wide range of tissues and organs, the pathological lesions are generally not severe enough to explain the cause of death [157]. Nevertheless, high viremia level is closely associated with poor prognosis [105]. Several animal models for Lassa fever have been developed in rodents and non-human primates, which have provided invaluable information on disease pathogenesis and have been used as important tools to evaluate efficacy of vaccines and antiviral treatments [196, 240-247]. Experiments done on these animals, especially on non-human primates, are expensive and restricted to BSL-4 laboratories. A safe, convenient, and economical small animal model for Lassa fever has been developed by Jahrling and colleagues, which is based on guinea pigs infected by a non-pathogenic arenavirus – the Pichinde virus (PICV) [94, 95]. PICV is a BSL-2 agent that does not cause disease in humans. Guinea pigs infected with a long-term spleenpassaged PICV strain developed a severe disease mimicking Lassa fever in many respects [95, 248, 249]. Both types of infection resulted in a fulminating disease course with terminal vascular leak syndrome [202]. Viral distribution in infected tissues appears to be identical in both Lassa and PICV infections [95, 157]. The viremia level is closely associated with the disease outcome [94, 105]. Like those found in fatal

Lassa infections, histopathological findings in lethally infected animals by PICV generally could not explain the main cause of death of the animals [95, 157, 203, 249, 250]. Generalized immune suppression is also seen in both types of infection [230, 231, 233].

In contrast to the highly virulent strain P18 of PICV that has been passaged in guinea pig spleens for 18 times, a low spleen-passage strain P2 causes a limited febrile illness in the infected animals [95, 211]. We have recently reported the complete genomic sequences of both the P2 and P18 strains, which differ in 48 nucleotides and 9 amino acids that are localized to the GPC, NP, and L genes [200]. In order to determine the molecular determinants of virulent PICV infection, we have decided to build reverse genetics systems for both the P2 and P18 strains. These novel molecular clones have allowed for generation of recombinant rP2 and rP18 viruses that can recapitulate the parental viruses in terms of viral growth kinetics *in vitro* and virulence *in vivo*. The availability of these systems allows for an opportunity to characterize viral virulence determinants *in vivo* in order to understand the molecular mechanisms involved in VHF pathogenesis.

Materials and Methods

Cells, viruses, and antibodies

BSRT7-5 cells, which stably express the T7 RNA polymerase, were obtained from Dr. Conzelmann (Ludwig-Maximilians-Universität, Germany) and cultured in MEM media supplemented with 10% fetal bovine serum (FBS), 1 mg geneticin per ml,

and 50 mg penicillin and streptomycin per ml. We obtained the avirulent P2 and virulent P18 PICV viruses from Dr. Aronson (UTMB, USA) [211]. Both the P2 and P18 viruses originated from the Pichinde Munchique strain CoAn4763 with different passage numbers. The P2 strain was the spleen stock of CoAn4763 after passaging twice in guinea pigs. The P18 strain was derived from Dr. Jahrling's original passage-adapted CoAn4763 adPIC virus with a total of 18 successive passages in inbred guinea pigs [95].

Construction of the T7 promoter-directed RNA expression vector.

The T7 promoter-directed RNA expression vector was based on the pUC19 vector. First, we amplified and cloned the sequences of hepatitis delta virus ribozyme (HDR) followed by the T7 terminator into the pUC19 vector between the BamH I and Hind III sites to generate the pUC19-HDVT7t vector. Next, we inserted into the pUC19-HDVT7t vector, in between the EcoR I and Sma I sites, a pair of oligos (AATTCtaatacgactcactatagCGCACAGTGGATCCCCGGTGCG) that contains the T7 promoter (in lower case) followed by the antigenomic strand of the terminal 3' UTR sequences (underlined) linked to the terminal 5' UTR sequences (underlined) of the S segment by BamH I site, which exists in UTR sequences of both the S and L segments. This vector, pUC19-T7-Sag, was used for cloning and expression of the full-length S segment in antigenomic orientation from the T7 promoter. Similarly, we inserted into the pUC19-HDVT7 vector, in between the EcoR I and Sma I sites, an oligo pair (AATTCtaatacgactcactatagCGCACCGAGGATCCCCGGTGCG**C**) that contains the T7 promoter (in lower case), the antigenomic strand of the terminal 3' UTR sequences

(underlined) linked to the terminal 5' UTR sequences (underlined) of the L segment by BamH I site, and an extra cytosine (in bold), which has been shown to increase the HDR-mediated RNA processing without affecting viral RNA replication activity (35, 42). This vector pUC19-T7-LagC was used to express the full-length L segment in an antigenomic orientation from the T7 promoter.

Assembly of the full-length S segment in the T7 promoter-driven vector.

The primers used for cloning the full-length P2 and P18 viral RNA segments will be provided upon request. The viral S segment of P2 or P18 origin was amplified as a single PCR product of 3.4 kb and cloned into the pGEM-T easy vector (Promega) by TA cloning strategy. After sequencing multiple clones, we found that one clone from each of the P2 and P18 S segments contained all the consensus sequences except at the IGR region. These are clone 8 for the P2 S segment and clone 19 for the P18 S segment. A silent Nco I restriction enzyme site was introduced into both clones 8 and 19 at nt 807 within the GPC gene by PCR-mediated mutagenesis. Due to its high GC-rich content and stable secondary structures, the IGR region was obtained separately (24). We specifically amplified and cloned a 363-nt fragment spanning the IGR of the P2 and the P18 S segments, respectively, into the pGEM vector by TA cloning. Sequencing multiple clones revealed the same consensus sequences for both the P2 and P18 IGR sequences. The IGR sequences were subcloned into the S segment in the pGEM vector by using the convenient restriction enzyme sites Sac I and Psi I (Fig. 1A). We then used the BamH I sites that exist in both terminal UTR sequences to subclone the entire S segment in the

antigenomic sense (Sag) into the pUC19-T7-Sag vector (Fig. 1A). The respective clones for the P2 and P18 S segments in the T7 promoter-directed expression vector were named pT7- P2Sag and T7-P18Sag, respectively.

Assembly of the full-length L segment in the T7 promoter-driven vector.

The L segments of the P2 and P18 viruses were individually cloned into the pTOPO vector (Invitrogen) as two overlapping PCR products, fragment A of nt 1 to 4501 and fragment B of nt 4428 to 7057. After sequencing multiple clones, we chose one clone from each of the fragments A and B that contains the consensus sequences for subsequent cloning purpose. To obtain accurate IGR sequences for the L segments, we amplified a 455-nt PCR product spanning this region in the P2 and P18 viruses and cloned it into the TA vector. Sequencing multiple clones revealed that the IGR sequences were identical to those existing in the cloned fragment A of both the P2 and P18 strains. To assemble the full-length L segment in the expression vector pUC19-LagC, we first subcloned fragment A into the pUC19-LagC vector using BamH I site (Fig. 1B). The subsequent insertion of fragment B unfortunately failed to give proper DNA product. We therefore decided to include additional subcloning steps (Fig. 1B). We first subcloned the EcoRI-KpnI fragment, which consists of the T7 promoter, the terminal 3' UTR sequences of nt 7057 - 7044 that is linked by the BamH I site to those of nt 4467- 3268, from the pUC19-LagC-fragA vector into the pcDNA 3 vector. We then inserted the BamH I fragment, containing nt 7044-4467, from fragment B in correct orientation. This led to the generation of the pcDNA 3-fragC vector that contains sequences from the 3' end of the L segment ranging

from nt 7057 to 3268. Lastly, we used the 3.8-kb EcoRI-Kpn I fragment from the pcDNA3-fragC vector to replace the 1.2-kb EcoRI-KpnI fragment in the original pUC19-LagCfragA vector in order to assemble the full-length L segment in antigenomic orientation (Fig. 1B). The vectors that contained the P2 and P18 L segments were named pT7-P2Lag and pT7-P18Lag, respectively.

Generation of infectious PICV viruses from plasmid transfection.

Using Lipofectamine 2000 reagent (Invitrogen), BSRT7-5 cells seeded in 6-well plates were transfected with plasmids encoding the L and S RNA segments. The supernatant was replaced with fresh media at 4 h post-transfection, harvested at different time points post-transfection, and used for plaque assaying on Vero cells.

PICV plaque assay.

Vero cells were seeded into 6-well plates at 90-100% confluency and infected with 0.5 ml of serial 10-fold dilutions of viruses in MEM medium for 1 h at 37 °C. After removing the medium, cells were incubated in fresh MEM supplemented with 0.5% agar and 10% FBS, and cultured for 4 days at 37°C. Plaques were stained overnight with diluted neutral red solution (1:50) in 0.5%agar/MEM/10%FBS.

Growth curve analysis.

Cells were seeded in 6-well plates at 90-100% confluency and infected (in triplicates) with viruses at moi of 0.01 for 1 h at 37 °C. After washing with PBS, a fresh aliquot of media was added into the culture. At different times post infection, aliquots of the supernatant were harvested for plaque assaying on Vero cells.

Isolation and culture of primary guinea pig peritoneal macrophages.

All animal experiments were conducted according to the guidelines and approved protocol from the Emory University Institutional Animal Care and Use Committee (IACUC). Healthy outbred Hartley guinea pig was injected with 3 ml of mineral oil (Sigma) one week prior to peritoneal macrophage isolation. After euthanization, macrophages were obtained from intraperitoneal lavage in a buffer that contains 5% FBS and 1% penicillin/streptomycin. After resuspended in RPMI1640 medium containing 10% FBS and 1% penicillin/streptomycin, macrophages were allowed to settle into culture dish overnight. After removing suspended cells, the attached cell population was determined to be >90% macrophages by flow cytometric analysis using a macrophage-specific antibody MCA518S (Serotec).

Guinea pig experiments.

We followed the experimental procedures described originally by Dr. Aronson and colleagues [212, 237]. Briefly, healthy 350 - 400 g male outbred Hartley guinea pigs

were housed for 5 to 7 days for acclimatization, after which they were randomly divided into different groups and injected intraperitoneally (i.p.) with 10,000 PFU of each of the virus strains, or PBS as a mock infection. Rectal temperature and body weight were measured daily for 18 days. Blood was drawn from the saphenous vein at different days post-infection and used for virus titer determination by plaque assay. Guinea pigs were declared moribund and euthanized when body weight decreased by 25% and rectal temperature fell below 39.8 ºC.

Results and Discussion

The avirulent P2 and virulent P18 strains of the Pichinde virus (PICV), a nonpathogenic member of the Arenaviridae family, cause distinct disease phenomena in guinea pigs, the molecular mechanism of which is not understood. We report here the development of two separate reverse genetics systems for P2 and P18 PICV strains, as the first step to identify the viral virulence factors.

We have previously provided the complete genomic sequences for both P2 and P18 strains [200]. In the current work, we assembled the full-length cDNA sequences of the L and S segments of both viruses into expression vectors (Fig. 2.2.1). Briefly, the full-length viral RNA segments, in an antigenomic orientation, are individually placed immediately downstream of the T7 promoter. The T7 promoter produces viral RNA transcripts with the correct viral 5’ termini that includes a non-templated G residue as has previously been shown to exist in arenaviral genomic and antigenomic RNAs [237]. The hepatitis delta virus ribozyme (HDR) sequence was engineered into the 3’ end of the

primary RNA transcript in order to mediate a self-cleavage reaction to generate the authentic arenaviral 3’ ends. A non-viral cytosine nucleotide was added immediately upstream of the HDR sequence, as this has previously been shown to enhance the self cleavage of LCMV RNA without affecting viral RNA replication activity [76, 237]. Additionally, the unique Nco I restriction enzyme site was introduced into the GPC gene (at nt position 807) without changing its coding sequence in order to distinguish the recombinant viral S segment from the parental one.

To generate recombinant viruses, BSRT7-5 cells, a stable cell line that constitutively expresses the T7 RNA polymerase, were transfected with plasmids containing the T7 promoter-driven antigenomic RNA strands of the L and S segments. Virus in the supernatant was collected at 48 h post transfection and used in plaque assay on Vero cells. Infectious viruses were recovered from both the P2 and P18 molecular clones, as evidenced by plaque formation on Vero cells (Fig. 2.2.2A). To distinguish the recombinant viruses from the original stock viruses, we amplified a fragment of the S segment that contains the engineered silent Nco I site, and showed that this restriction enzyme site was present only in the recombinant viruses (designated as rP2 and rP18) (Fig. 2.2.2B). Taken together, these data suggest that we have successfully generated high-titer infectious PICV viruses purely from plasmids transfection, highlighting the functionality of the novel reverse genetics systems for both the virulent P18 and avirulent P2 strains.

The rP18 viruses appeared to grow faster than rP2 in Vero cells, as judged by the differences in plaque size generated from these viruses (Fig. 2.2.2A). In order to validate this observation, we conducted a growth curve analysis of the recombinant rP2 and rP18

viruses, and of the parental P2 and P18 viruses, in Vero cells using moi of 0.01. As shown in Fig. 2.2.3A, similar growth kinetics were observed between the virulent viruses P18 and rP18, and between the avirulent viruses P2 and rP2, suggesting that the recombinant viruses can accurately recapitulate the growth capacity of their respective parental viruses in cell cultures. As predicted, the virulent P18 and rP18 viruses grew to higher titers than the avirulent P2 and rP2 by ~ 0.5 - 1 log at 48 hpi. The avirulent viruses peaked at 72 hpi while the virulent viruses at 48 hpi (Fig. 2.2.3A). These results were replicated in a variety of established cell lines, including the guinea pig cell lines JH4 (data not shown). In addition, we compared virus growth kinetics in primary guinea pig cells. As it has been shown that monocytes/macrophages are the early target cells of Lassa fever virus and PICV infections *in vivo* [203, 251], we infected primary peritoneal macrophages isolated from healthy guinea pigs with P2, P18, rP2, and rP18 viruses at an moi of 0.01. Consistent with results obtained from established cell lines, the virulent P18 and rP18 viruses grew to higher titers than the avirulent P2 and rP2 viruses by ~1 log (Fig. 2.2.3B). Taken together, our data strongly suggest that the virulent P18 and rP18 viruses appear to exhibit an inherent g`rowth advantage, which may contribute to a higher degree of virulence caused by these viruses in infected animals.

To determine the degree of virulence generated by the recombinant viruses, we injected guinea pigs intraperitoneally (i.p.) with 10,000 pfu of P2, rP2, P18, rP18 virus, or PBS as a control. The degree of virulence was determined by mortality rate, febrile reaction, duration of fever, and body weight loss. The mortality rate in animals infected with rP18 virus was 100% (6 out of 6 animals died) and with P18 virus was ~ 90% (5 out of 6 animals died), whereas no animals died due to either P2 or rP2 virus infection or

PBS injection. The P18 and rP18 viruses led to an early onset of disease (as early as 4 dpi) and prolonged fever (an average of 8 days), whereas P2 and rP2 viruses caused a late-onset and brief (1 - 2 days) fever (Fig. 2.2.4A and B). Accordingly, guinea pigs infected with the P18 or rP18 virus suffered from greater body weight loss than those infected with the P2 or rP2 virus (Fig. 2.2.4C). Euthanization of some moribund animals at day 13 resulted in a slight increase in the average rectal temperature and body weight for the groups of animals infected with virulent viruses (Fig. 2.2.4A and C). Similarly, the seemingly higher average body weight for the virulent P18-infected animals from days 15 to 18 post infection is due to the recovery of one of the animals in this cohort at around day 15 (Fig. 2.2.4C). Regardless, our data demonstrate that P18 and rP18 viruses are distinctly more virulent than P2 and rP2 viruses in outbred guinea pigs, and that the recombinant viruses can accurately recapitulate phenotypes generated by their respective parental viruses *in vivo*.

We next quantified viremia level in infected animals at every 3 dpi. Fig. 2.2.5 shows viremia levels in animals infected by rP18 (two animals), P18 (three animals), P2 (three animals) and rP2 (three animals). Viremia levels differ drastically in animals infected with either the virulent or avirulent viruses over the course of the infection. In P18- or rP18-infected animals, viremia levels rose above the detection threshold (200 pfu/ml) at 6 dpi and quickly increased over $3x10^4$ pfu/ml by 12 dpi, after which 4 out of 5 virulent virus-infected animals approached terminal point (Fig. 2.2.5A). In contrast, viremia levels were below detection level (i.e., <200 pfu/ml) in those animals infected with the avirulent P2 or rP2 viruses throughout the course of the infection. Taken together, these results reiterate the close association between viremia levels and disease

severity, which is an important feature of arenavirus-induced hemorrhagic fevers in humans.

Similar to postmortem findings on fatal human Lassa infections in which viruses were pantropical [157], the rP18 virulent viruses were found at high levels in almost all organs at terminal points, ranging from $3.1x10^6$ pfu/g in the lymph nodes to $3.2x10^8$ pfu/g in the adrenal glands (Table 2.2.1). The highest levels of virus were found in the livers, lungs, stomachs, and adrenal glands, and lowest levels were in the brains (8.8×10^4 pfu/g). In contrast, the levels of avirulent rP2 viruses in the infected animals, which were sacrificed at the same time post infection as the rP18- infected animals, were below the limit of detection by plaque assaying method. Since we failed to detect any viruses in the blood or in different organs of animals infected by the avirulent viruses (P2 or rP2) (Fig. 2.2.5A and data not shown), we ask whether these viruses can indeed replicate *in vivo* or they were effectively cleared by the host. To address these issues, we collected spleens from animals infected with rP2 or rP18 viruses at early stages of infection (0, 4, 6, and 8 dpi), and quantified virus titers by plaque assay. As shown in Fig. 2.2.5B, rP2 and rP18 levels in the spleen increased sharply from 0 to 6 dpi. The virulent rP18 virus reached a titer of $\sim 1\times10^7$ pfu/g at 4 dpi, peaked at 6 dpi with a level of 5×10^7 pfu/g, and remained high thereafter (Fig. 2.2.5B). In contrast, the avirulent rP2 virus replicated to a level of $\sim 1\times10^6$ pfu/g at 4 to 6 dpi, after which the virus titer decreased sharply to below detection level at day 18. These data strongly suggest that rP2 avirulent viruses are indeed replication competent *in vivo*, but they are effectively cleared by host immune responses. In contrast, host immune responses failed to control rP18 virulent viruses, which eventually resulted in fatality of the infected animals.

In summary, we have successfully developed two novel infectious cDNA clones for the avirulent P2 and virulent P18 PICV strains, and have shown that these recombinant viruses can recapitulate the parental viruses in terms of virus growth *in vitro* and virulence *in vivo*. The infectious cDNA clones for PICV and LCMV [236, 237] provide convenient systems to study the basic mechanism of arenavirus replication. Furthermore, the ability to generate both recombinant virulent and avirulent PICV viruses from plasmid DNAs will allow us characterize the molecular determinants of virulent PICV infection in guinea pigs, which could potentially shed important light on human infection by other deadly arenaviruses [3]. For example, why only a few arenaviruses causes VHF upon human infection and what determines the degrees of heterogeneity in clinical manifestations in Lassa fever infection [239] remain unresolved. One hypothesis is that molecular changes in the pathogenic arenaviruses lead to the acquired virulence in infected hosts. Indeed, there is a significant sequence heterogeneity in circulating Lassa fever virus strains in the endemic area of West Africa with some being more lethal in animal models than others [252, 253]. However, there are no systematic studies to link Lassa fever virus variants to degrees of disease severity. Using an established small animal model of arenaviral VHF – guinea pigs infected by PICV - we and other investigators have shown in the current work and elsewhere [200, 211, 212] that the genetic differences between two PICV strains (P2 and P18) can partly account for the distinct degrees of virulence in infected animals. Our newly developed reverse genetics systems for both of these PICV strains provide a unique opportunity to directly test the hypothesis that molecular determinants existed in the genome of these viruses can contribute to the acquired virulence in infected animals by altering the efficiency of virus

replication and/or by modulating the host immune responses to viral infection. These studies are currently underway in our laboratory and will be discussed in future reports.

Acknowledgements

We thank Dr. Aronson (University of Texas Medical Branch) for providing the stock P2 and P18 viruses, Dr. Conzelmann (Ludwig-Maximilians-Universität, Germany) for the BSRT7-5 cells, and Drs. Tristram G. Parslow and Aftab A. Ansari (Emory University) for advice and technical consultations. This research was supported in part by the University Research Committee of Emory University, the pilot project component of U19 grant RFA-AI-02-042, the new directions award from SERCEB (Southeast Regional Center of Excellence for Emerging Infections and Biodefense) (3U54AI057157-06S10032), and the Emory DDRDC pilot grant (DK064399).

Table 2.2.1:

TABLE 1. Virus titers in different organs of rP18-infected animals[a]

Organ	rP18 virus titer (PFU/g)
Heart	6.5E+06
Lung	6.7E+07
Liver	1.9E+08
Spleen	3.0E+07
Stomach	5.6E+08
Pancreas	6.5E+06
Intestine	1.4E+07
Adrenal gland	3.2E+08
Kidney	3.9E+06
Lymph node	3.1E+06
Brain	8.8E+04

[a] Organs were collected at terminal points of infected animals. Organs were weighed and homogenized in PBS. Virus titers in organ homogenates were determined by plaque assay on Vero cells and shown as PFU per g. Results shown are the averages of the results from three independent experiments.

Figure 2.2.1:

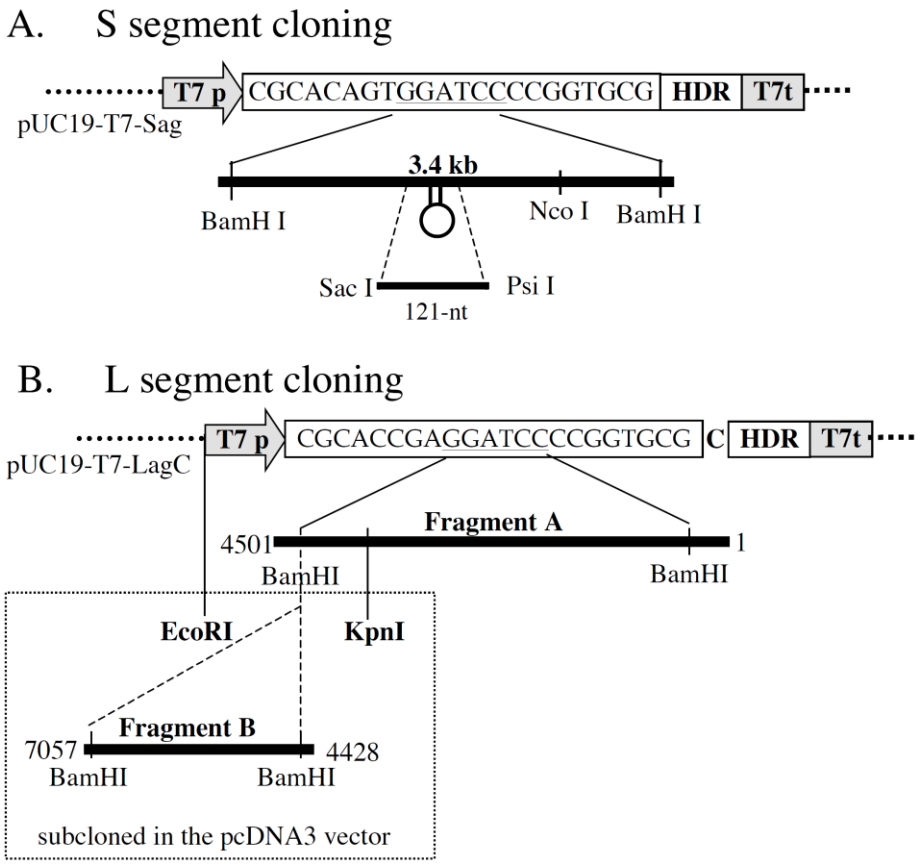
A. S segment cloning
T7 p
CGCACAGTGGATCCCCGGTGCG
HDR
T7t
pUC19-T7-Sag
3.4 kb
BamH I
Nco I
BamH I
Sac I
Psi I
121-nt
B. L segment cloning
T7 p
CGCACCGAGGATCCCCGGTGCG
C
HDR
T7t
pUC19-T7-LagC
Fragment A
4501
1
BamHI
BamHI
EcoRI
KpnI
Fragment B
7057
4428
BamHI
BamHI
subcloned in the pcDNA3 vector

Figure 2.2.2:

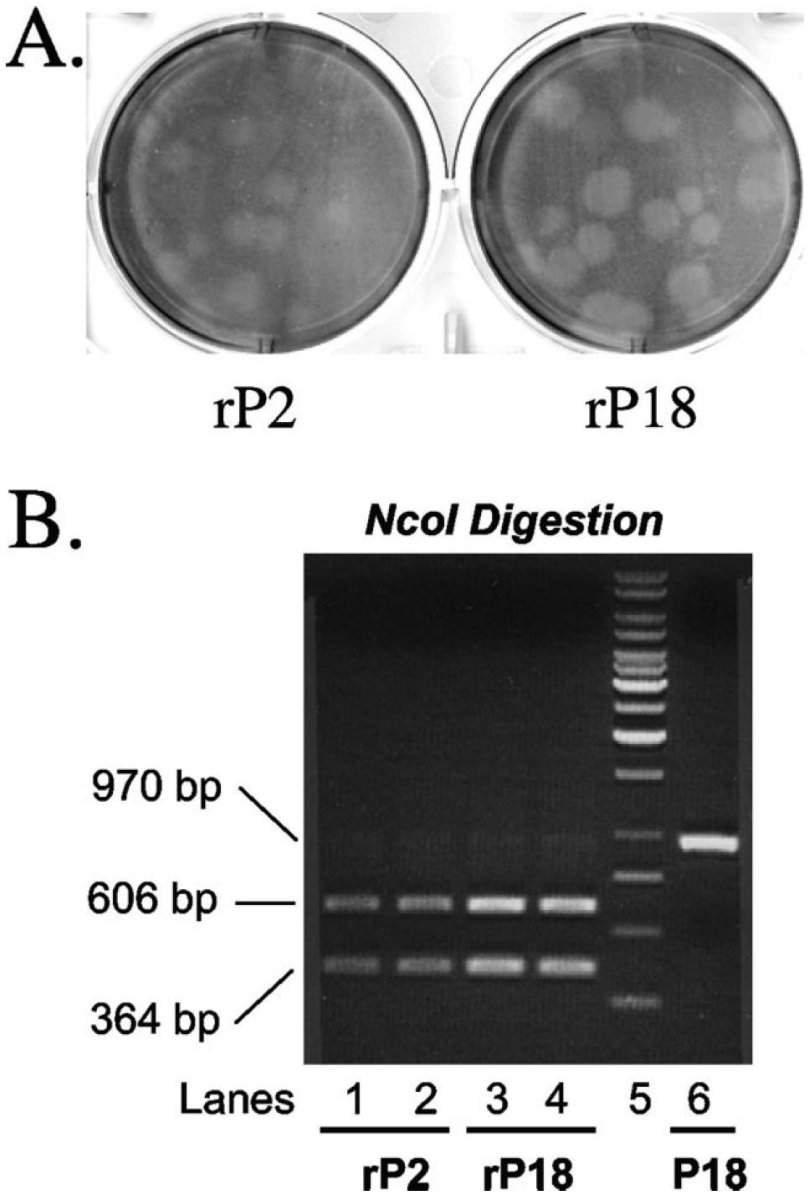
A.
rP2
rP18
B.
NcoI Digestion
970 bp
606 bp
364 bp
Lanes 1 2 3 4 5 6
rP2
rP18
P18

Figure 2.2.3:

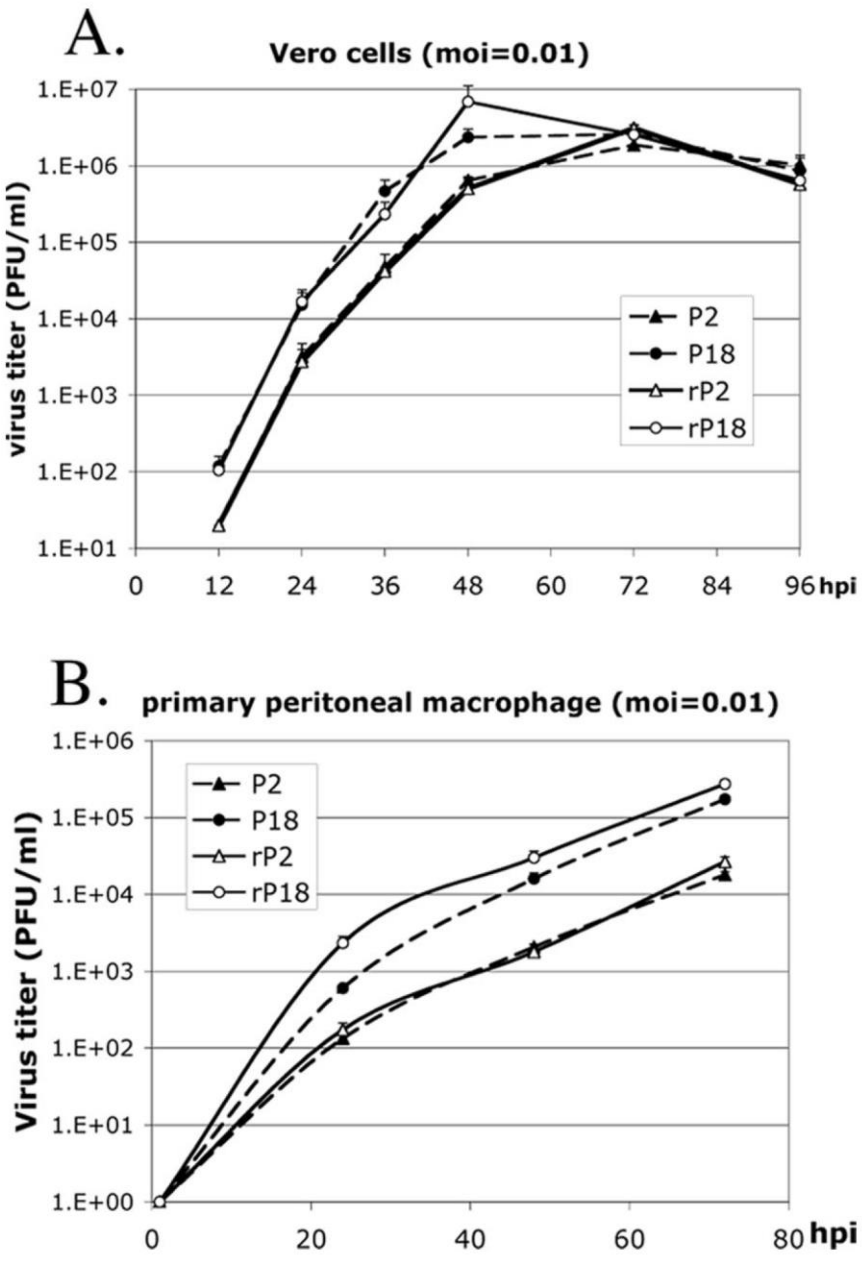
A.
Vero cells (moi=0.01)
virus titer (PFU/ml)
1.E+07
1.E+06
1.E+05
1.E+04
1.E+03
1.E+02
1.E+01
0
12
24
36
48
60
72
84
96
hpi
P2
P18
rP2
rP18
B.
primary peritoneal macrophage (moi=0.01)
Virus titer (PFU/ml)
1.E+06
1.E+05
1.E+04
1.E+03
1.E+02
1.E+01
1.E+00
0
20
40
60
80
hpi
P2
P18
rP2
rP18

Figure 2.2.4:

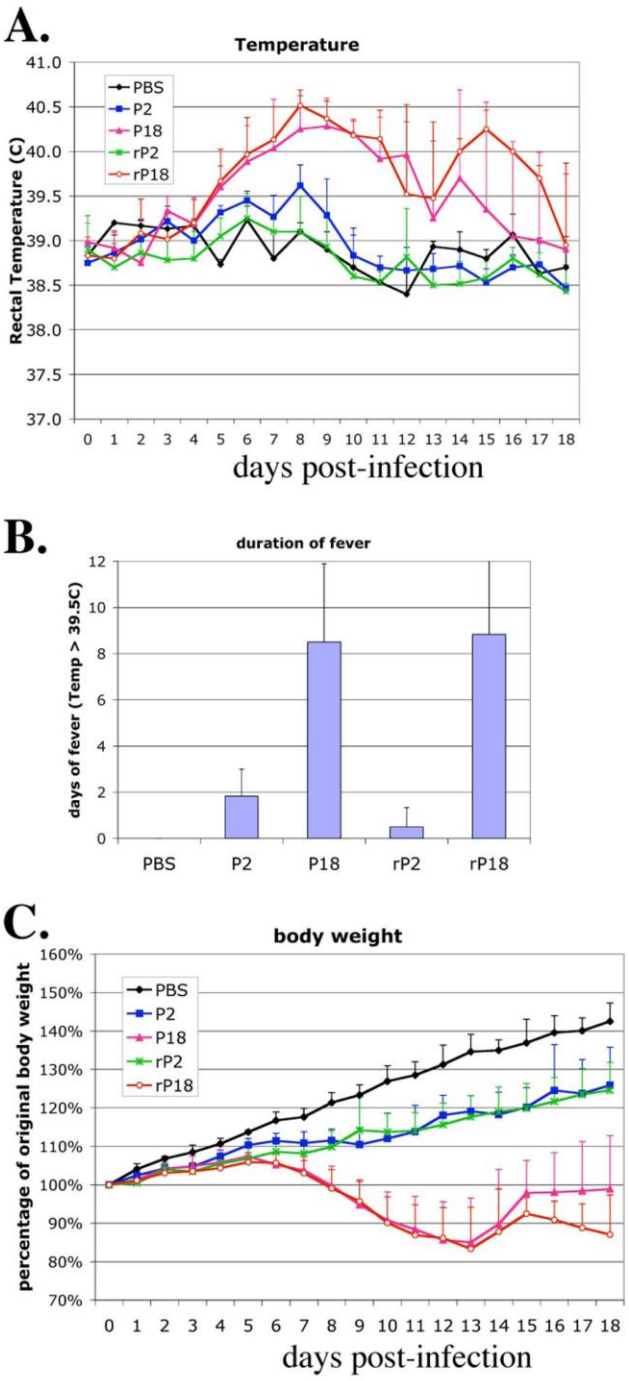
A.
Temperature
Rectal Temperature (C)
41.0
40.5
40.0
39.5
39.0
38.5
38.0
37.5
37.0
PBS
P2
P18
rP2
rP18
0 1 2 3 4 5 6 7 8 9 10 11 12 13 14 15 16 17 18
days post-infection
B.
duration of fever
days of fever (Temp > 39.5C)
12
10
8
6
4
2
0
PBS
P2
P18
rP2
rP18
C.
body weight
percentage of original body weight
160%
150%
140%
130%
120%
110%
100%
90%
80%
70%
PBS
P2
P18
rP2
rP18
0 1 2 3 4 5 6 7 8 9 10 11 12 13 14 15 16 17 18
days post-infection

Figure 2.2.5

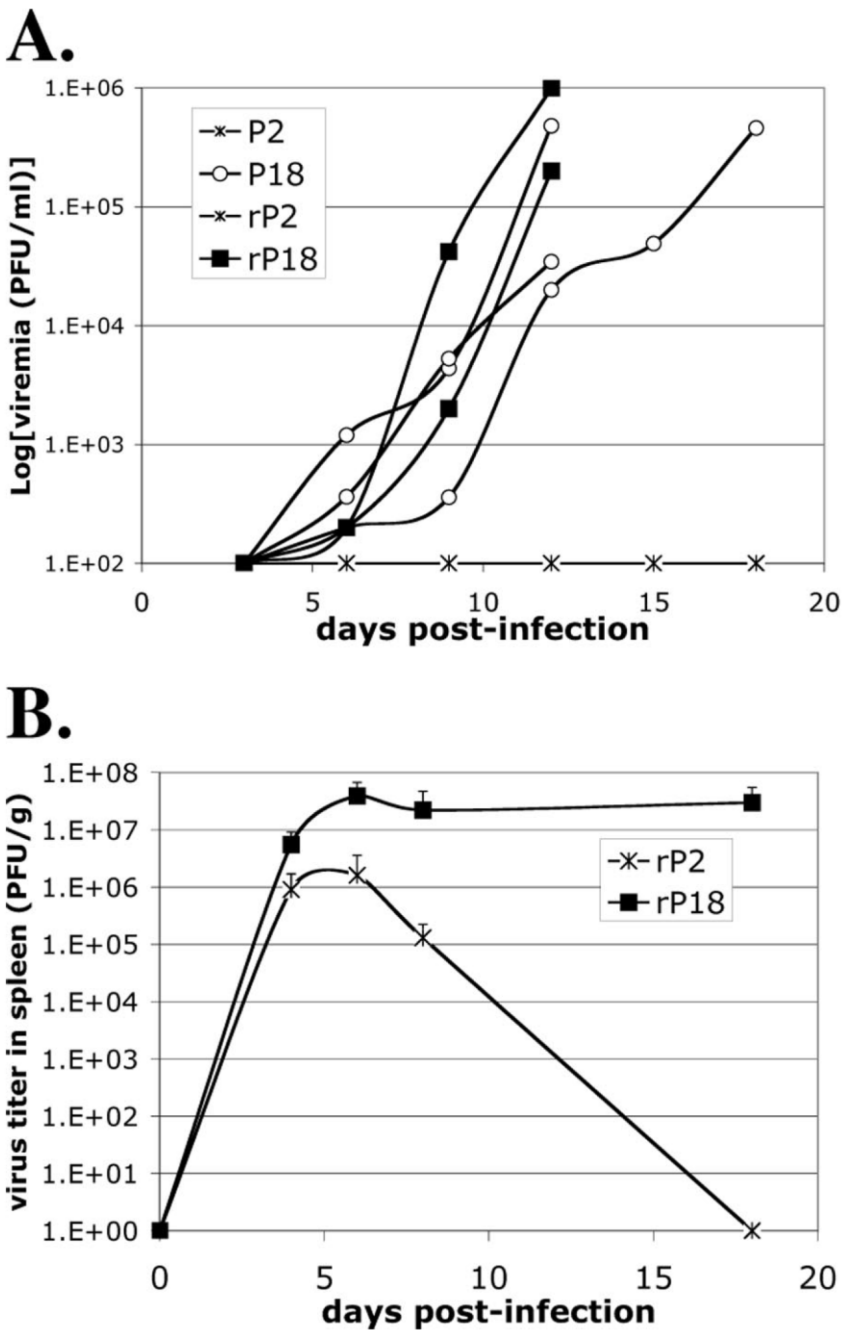
A.
1.E+06
1.E+05
1.E+04
1.E+03
1.E+02
Log[viremia (PFU/ml)]
P2
P18
rP2
rP18
0
5
10
15
20
days post-infection
B.
1.E+08
1.E+07
1.E+06
1.E+05
1.E+04
1.E+03
1.E+02
1.E+01
1.E+00
virus titer in spleen (PFU/g)
rP2
rP18
0
5
10
15
20
days post-infection

Figure Legends

Figure 2.2.1: Schematic illustration of the cloning strategies for expressing the S (A) and L (B) segments in the T7 promoter-driven RNA expression vectors. The various steps involved in this cloning process were described in Materials and Methods. T7 p, the T7 promoter; HDR, hepatitis delta ribozyme sequence; T7t, the T7 terminator.

Figure 2.2.2: Generation of the recombinant viruses by plasmid transfection. The BSRT7-5 cells were transfected with two plasmids bearing the antigenomic strands of the L and S segments under the control of the T7 promoter, as described in Materials and Methods. (A) Plaques formed on Vero cells by the recombinant viruses rP2 or rP18, which were collected from the supernatants of the transfected BSRT7-5 cells. (B) The engineered genetic marker NcoI site was present in the genomes of the recombinant viruses rP2 (lanes 1 to 2) and rP18 (lanes 3 to 4) but was absent in that of the parental virus P18 (lane 6). Lane 5, DNA molecular size markers.

Figure 2.2.3: Comparison of the growth kinetics between the parental viruses (P2 and P18) and recombinant viruses (rP2 and rP18) in Vero cells (A) and in the primary peritoneal macrophages of guinea pigs (B).

Figure 2.2.4: Comparison of the degrees of virulence in animals infected with either the parental viruses (P2 and P18) or recombinant viruses (rP2 and rP18). (A) Daily rectal temperature of animals injected with different PICV strains or with PBS as a control. (B) Average duration of fever (temperature of _39.5°C). (C) Daily body weight as a percentage of the original body weight at day 0.

Figure 2.2.5: (A) Comparison of viremia levels (PFU/ml) in animals infected with P18 (○), rP18 (■), or P2 and rP2 (X) throughout the course of the infections. (B) Comparison of the virus titers in the spleens of animals infected with rP2 (X) and rP18 (■) throughout the course of the infections.

CHAPTER 2.3

Identification of virulence determinants within the L genomic segment of the Pichinde arenavirus

Lisa McLay[1], Shuiyun Lan[1], Aftab Ansari[1], Yuying Liang[2*] and Hinh Ly[1,2*]

[1]Department of Pathology and Laboratory Medicine, Emory University, Atlanta, GA 30322, [2]Department of Veterinary and Biomedical Sciences, University of Minnesota, Twin Cities, MN 55108

Abstract

Several arenaviruses are responsible for causing viral hemorrhagic fevers (VHF) in humans. Lassa fever virus (LASV), the causative agent of Lassa fever, is a BSL-4 level pathogen that requires handling in BSL4 facilities. In contrast, the Pichinde arenavirus (PICV) is a BSL-2 pathogen that can cause hemorrhagic fever-like symptoms in guinea pigs that resemble those observed in human Lassa fever. Comparative sequence analysis of the avirulent P2 strain of PICV and the virulent P18 strain shows a high degree of sequence homology in the bi-segmented genome between the two strains despite the polarized clinical outcomes noted in the infected animals. Using reverse genetics systems that we have recently developed, we have mapped the sequence changes in the large (L) segment of the PICV genome that are responsible for the heightened virulence phenotype of the P18 strain. By monitoring the degree of disease severity and lethality caused by the different mutant viruses, we have identified specific residues located within the viral L polymerase gene encoded on the L segment essential for mediating disease pathogenesis. Through quantitative RT-PCR analysis, we have confirmed that the same set of residues is responsible for the increased viral replicative potential of the P18 strain and its heightened disease severity *in vivo*. Our laboratory findings serve to reinforce field observation that a high level of viremia often correlates with severe disease outcomes in LASV-infected patients.

Introduction

Arenaviruses are enveloped, ambisense RNA viruses that have a single-stranded genome which is composed of a large (L) segment of ~7.2 kb and a small (S) segment of ~3.4 kb [149]. The S segment encodes the glycoprotein (GPC) in the positive sense and nucleoprotein (NP) in the negative sense, whereas the L segment encodes the Z matrix protein in positive and the L polymerase in negative orientations [149]. Each segment contains highly structured intergenic regions (IGRs) located between the two open reading frames. These are thought to be involved in transcriptional termination [149, 205]. Additionally, the distal 19 nucleotides of the viral genomic segments are imperfectly complimentary to each other, and are presumed to form panhandle structures, thereby circularizing the genome [28, 204, 235]. These panhandles are also thought to form an attachment point for the L polymerase, which together with NP mediates both viral genome replication and mRNA transcription [51, 62, 204, 254]. NP has also been shown to mediate type-I IFN suppression in response to viral infection [99, 104, 220, 255].

Several arenaviruses are responsible for causing viral hemorrhagic fever (VHF) in humans in South America (Junin, Guanarito, Sabia, Machupo, and Chapare viruses), West Africa (Lassa virus), and South Africa (Lujo virus). Of these viruses, Lassa infection results in the highest levels of morbidity and mortality. Each year, there are up to 300,000 Lassa infections that result in approximately 5,000 deaths in endemic areas of West Africa [3, 201]. While a majority of infected individuals recover, approximately 20% of the infected individuals will develop a severe form of the disease affecting multiple organs. Although the virus infects many tissues, the resulting pathology is not

severe enough to account for the cause of death [157]. One consistent indicator of clinical prognosis is viral load [105]. Those individuals with viremia levels of 8.5 log 10 PFU/mL will usually succumb to the disease [156]. Only one experimental vaccine exists for arenaviral VHF infection (Junin Candid #1 for Argentine hemorrhagic fever), and limited treatment options are available. Currently, ribavirin is the only therapeutic drug used in the treatment of Lassa fever, and has proven efficacious, but only if administered early on during the course of infection [256]. Unfortunately, Lassa fever is often misdiagnosed and therefore the window of opportunity for effective ribavirin usage can be missed [154, 256]. Therefore, a better understanding of the pathogenesis of arenavirus infection may allow for the development of novel targeted therapeutics.

Because of the severity of the diseases they cause and the lack of effective vaccines and therapeutics, the arenaviruses that cause VHF in humans are classified as BSL-4 agents, which restricts research to those who have access to such specialized facilities. Pichinde virus (PICV) is a related arenavirus that does not cause disease in humans, but infection of guinea pigs with a strain that has been passaged 18 times (P18) through the spleens of guinea pigs (P18) (Materials and Methods) produces a disease whose characteristics are similar to LASV infection of humans [94, 95]. These characteristics include the correlation between the level of viremia with the severity of the disease, a similarity in the host tissue distribution of the virus, the development of a vascular leak syndrome which is often observed during terminal illness, the generalized immune suppression, and finally the fact that the histopathological findings are not severe enough to explain the cause of death [94, 95, 105, 157, 202, 203, 230, 231, 233, 248-

250]. This model thus provides a safe, economical, and informative alternative for studying VHF in a BSL-2 setting.

An earlier passaged strain of PICV (P2) also causes disease in guinea pigs. However, the disease is mild and is characterized by a brief febrile period and slight weight loss from which the animals quickly recover. This is in stark contrast to the disease course of the P18 infection, in which the animals develop high fever and demonstrate dramatic weight loss until they reach a terminal point when the animals must be euthanized [95, 211, 234]. This viral infection model provides us with the opportunity to examine what viral components are responsible for the phenotypic differences between these two strains, and should help to elucidate which viral factors are involved in the pathogenesis of arenaviral VHF. It is remarkable that while the difference in phenotype between these two viral strains is dramatic, the viral sequences show limited diversity. In the L segment, the sequences encoding the Z proteins are completely identical while the sequence for the L polymerase contains 5 amino acid differences between the two strains. In addition to the changes resulting in amino acid differences, there are also 11 silent mutations. There are 14 nucleotide changes in the GPC gene, 11 of which are silent and 3 of which are responsible for the amino acid differences between the two strains. Lastly, while there are a total of 19 nucleotide changes in the NP gene, only one of these results in an amino acid change between the viruses [200].

Our laboratory has previously described a reverse genetics system for both the P2 and P18 strains of PICV [234]. For both strains, the L and S segments are expressed on separate plasmids, allowing for genetic manipulation of the viruses and generation of reassortant and recombinant mutant viruses. We present data herein that localize the L

protein residues of the P18 strain that contribute to rapid virus replication in cell culture and *in vivo* and the enhanced disease pathogenesis in infected animals.

Materials & Methods

Viruses

The P2 and P18 PICV strains were adapted from the Pichinde Munchique strain CoAn4763. This strain was passaged once in guinea pigs in Dr. Peter Jahrling's laboratory (USAMRIID). Subsequently, the virus was passaged again through the spleen of guinea pigs in Dr. Judy Aronson's laboratory (UTMB) in order to produce the avirulent P2 strain. A virulent passaged 15 virus, originating from Dr. Jahrling's original passage-adapted CoAn4763 adPIC virus, was obtained from Dr. Dorian Copenhaver (UTMB) and subsequently passaged 3 more times in inbred guinea pigs in Dr. Judy Aronson's laboratory (UTMB) to generate the virulent P18 virus [95].

Plasmids

L segment P2/P18 fragment swapping mutants were generated by using convenient restriction enzyme sites to cut and ligate fragments of P2 sequence from a plasmid expressing the P2 L segment into the corresponding location on a plasmid expressing the P18 L segment (previously described) [234]. Point mutants were introduced to the P18L segment plasmid [234] via site directed mutagenesis using the Quikchange mutagenesis kit (Stratagene). Mutagenesis was verified through DNA sequencing, and the point mutations were subcloned into the original P18 L segment plasmid.

Generation of recombinant viruses

BSRT7 cells constitutively expressing the T7 RNA polymerase were transfected in 6 well plates via Lipofectamine 2000 reagent (Invitrogen) with plasmids expressing the L & S genomic segments from the T7 promoter and terminator sequences. The media was replaced at 4 hours post transfection and supernatants were collected at 48 & 72 hours. Viruses recovered in supernatants were plaque purified via plaque assay in Vero cells as previously described [234]. Viruses from plaques were amplified by infection of BHK-21 cells cultured in 60 mm plates and supernatants were collected at 72 hours post infection.

Plaque assay

Vero cells at near confluency were infected with 0.5 mL of serial dilutions of virus samples for 45 min at 37˚C. After infection, viral samples were aspirated, and the cells were overlaid with fresh MEM medium with 10% FBS and 0.5% agar. The cells were incubated for 4 days at 37°C. At day 4 post infection, the cells were overlaid with MEM containing 10% FBS, 0.5% agar, and 0.02% neutral red dye. Plaques were enumerated on day 5 post infection.

Animal experiments

Outbred male, 350-400g, 4-5 week old Dunkin Hartley guinea pigs were purchased from Charles River laboratories and acclimatized for 5-7 days before initiation of the experimental studies. Animals were infected intraperitoneally (i.p.) with 10,000

PFU of virus. Body weights and rectal temperatures were monitored daily for 18 days. Beginning on day 7 post infection, animals were supplemented with 40 mL/kg of lactated ringer's solution plus 100 mg ascorbic acid administered subcutaneously. Mortality was defined as animals having reached terminal points either when their body weight decreased by >30% as compared to a nomogram or if the rectal temperature fell below 38°C in addition to body weight loss. According to our approved IACUC protocol, animals were allowed to be monitored for a maximum of 18 days post viral infection at which time all surviving animals must be euthanized. This is based on a comprehensive analysis of the disease course established in a large number of animals infected with P2 and P18 viruses [[212, 234] and our unpublished data].

In the current study, 19 animals were used to determine the attenuation levels of the fragment swapping mutants. Three animals were infected with the rS18L18(C2) viruses, and two separate groups of 8 animals each were infected with the rS18L18(D2) or rS18L18(A2) viruses. Groups of 6 animals each were used to test the single- and multiple-point mutant viruses. Statistical analyses of the survival curves were performed using the Log-rank (Mantel-Cox) χ^2 Test using GraphPad prism 5 software. The statistical significance of the viral titers in the serum of the infected animals was analyzed using the student "t" test.

Histopathology

Liver samples collected from animals infected with recombinant PICV were fixed using 4% formaldehyde, embedded in paraffin, sectioned, and stained with

hematoxylin and eosin. The tissue slides were examined microscopically for histopathological changes by expert pathologists.

Viral growth curve analysis

Vero cells were seeded in 6 well plates at approximately 90% confluency. Cells were infected at MOI = 0.01 for 45 min at 37°C. After infection, cells were washed with PBS before being supplemented with 2 mL fresh media. Supernatants were collected at various time points post infection and assayed by plaque assay on Vero cells as previously described [234].

Real Time RT-PCR

Vero cells were infected with WT or mutant viruses at MOI=1. At 10 hpi, total cellular mRNA was collected using the Purelink RNA Mini kit (Ambion). On column DNase digestion was performed using Purelink DNase according to the manufacturer's instructions (Ambion). Reverse transcription for generation of cDNAs was performed using the Superscript III kit (Invitrogen). Primer 5'CGCACAGTGGATCCTAGGC3', which aligns to the 3' UTR of the S segment, was used to generate cDNAs of the viral genomic segment, while oligo d(T) was used to generate GAPDH cDNA for normalization purposes. Real time PCR was performed using SYBR green (Applied Bioscience) and primers 5'CAGGCTGAGACAAACTCTCAGTTC3' and 5'GGACACAAGAGCACTGTTATCTGC3' each at 0.2 μM were used for S segment detection while primers 5'GAAGGTGAAGGTCGGAGTC3' and 5'CAAGCTTCCCGTTCTCAGCC3' each at 0.4 μM were used to detect GAPDH. The

cycling conditions included an initial incubation at 95°C for 10 min, followed by 40 cycles of 95°C for 15 seconds and 60°C for 1 min. Melting curve analysis was performed from 60°C to 95°C at a rate of 0.3°C/s.

Results

Generation of fragment swapping mutants between the P2 and P18 strains of the Pichinde virus L segment.

In order to determine which segment(s) of the Pichinde virus might contain the virulence factor(s), we previously generated and characterized a reassortant virus that expresses the L segment of the virulent P18 strain and the S segment of the avirulent P2 (S2L18) as well as the reverse reassortant virus that contains the L segment of P2 and the S segment of P18 (S18L2) [257]. Both reassortant viruses were highly attenuated in infected guinea pigs, indicating that the virulence determinants were likely located on both segments of the viral genome. Analysis of these viruses indicated that the L segment was responsible for the faster rate of replication observed for the rP18 virus in tissue cultures, as the S2L18 reassortant virus showed a similar growth rate as the wildtype rP18 virus, whereas the S18L2 virus showed a similar growth curve as the rP2 virus [257]. In Lassa fever infected patients, high levels of viremia usually correlate with poor prognosis [105, 156]. This implies that the rate of viral replication is an important factor in determining the degree of virulence, and that amino acid substitutions are present in the L protein sequence that may be responsible for this phenotype.

In order to map the specific residue(s) that contribute to virulence within the L segment, we generated various fragment swapping mutants, effectively substituting

different L fragments of the P2 sequence into the P18 genome (Figure 2.3.1A). We reasoned that recombinant viruses with the substituted regions that contain virulence determinants would produce a loss-of-virulence phenotype in the infected animals.

The L segment contains 5 amino acid differences between the P2 and P18 strains: 4 aa substitutions are located in the C terminus and another amino acid substitution is located in the N terminus of the L gene. Multiple silent mutations are also found in this region of the viral genome, whereas the sequences encoding the Z protein are completely identical between the two strains of the virus [200]. Based on unique restriction enzyme sites available along the L segment, we divided it into 4 fragments: D, C, B, & A. Since the B fragment is identical between the P2 & P18 strains, no fragment swapping mutant was generated for this region. With the other 3 fragments (D, C, and A), we introduced each fragment containing P2 sequence into the rP18 L segment. Specifically, the L18(A2) mutant contains the A fragment of P2 with an amino acid substitution at L protein sequence position 355 as well as 2 silent mutations, whereas the L18(C2) contains the C fragment of P2 with 5 silent mutations, and the L18(D2) mutant contains the D fragment of P2 with 4 amino acid differences at L protein sequence positions 1808, 1839, 1889, and 1906 as well as 3 silent mutations.

Virulence determinants of PICV P18 are localized to the C terminus of the L polymerase.

In order to determine which fragment(s) of the L segment contain virulence determinants, we infected animals with the fragment swapping mutants (Figure 2.3.1A), and monitored them for a loss of virulence. To do this, guinea pigs were infected intraperitoneally with 10,000 PFU of each recombinant virus, and body weight and

temperature were monitored for 18 days. Three animals were infected with the rS18L18(C2) viruses, and two separate groups of 8 animals each were infected with the rS18L18(D2) or rS18L18(A2) viruses. Terminal points were defined as the point at which an animal either reached >30% weight loss as compared to a nomogram or rectal temperature dropped below 38°C in combination with continuing weight loss. While the survival rate for rP18 infected animals was very low, all animals infected with rP2 virus survived. Results obtained with the recombinant viruses showed that both groups of guinea pigs that were infected with rS18L18(A2) or with the rS18L18(C2) showed 100% mortality (Figure 2.3.1B). However, the group of animals infected with rS18L18(D2) showed a much higher (75%) percentage of survival at day 18. The levels of viremia of the infected animals at terminal or experimental end points were determined by plaque assays. While sick animals maintained high viremia at time of death, the recovered animals had undetectable levels of virus (Figure 2.3.1C).

Several point mutations in the C terminus of the L polymerase are involved in virus attenuation.

Data from the fragment swapping experiment indicate that the D fragment of the L segment contains virulence determinants (Figure 2.3.1). This fragment contains 4 amino acid substitutions at positions 1808, 1839, 1889, and 1906 as well as 3 silent mutations. We next wished to narrow down which of these sequence changes were responsible for the varying phenotypes between the two strains of the virus. As the amino acid changes are the most likely candidates for disease attenuation, we decided to create point mutations at these residues by substituting the corresponding residue of the

P2 sequence at each of these individual sites into the rP18 virus backbone. As such, the recombinant viruses N1906D, N1889D, L1839V, and T1808A were generated and used to infect guinea pigs. Six animals per group were infected intraperitoneally with 10,000 PFU of each of the recombinant viruses and monitored for 18 days for fever and body weight loss. While the L1839V virus seemed to be somewhat attenuated, the N1906D and N1889D viruses do not show any appreciable levels of attenuation (Figure 2.3.2A). Notably, all animals infected with the T1808A recombinant virus died. Although the 1839V recombinant virus was somewhat attenuated, this virus did not reflect the dramatic loss of virulence that was noted in the fragment swapping mutant virus rS18L18(D2) (Figure 2.3.1B).

As no single point mutation at the C terminus of the L polymerase could mirror the effect of introducing P2 sequence into the entire fragment D of the L segment, we reasoned that it is likely that a combination of the amino acid substitutions are required for the increased virulence of the P18 strain. We therefore generated several recombinant viruses carrying various combinations of these point mutations: N1906D/N1889D, N1906D/L1839V, N1906D/N1889D/L1839V, and N1906D/N1889D/L1839V/T1808A. While N1906D/L1839V was somewhat attenuated (Figure 2.3.2B) in infected animals (n=6), neither of the double mutants showed the dramatic attenuation noted with the fragment swapping mutant rS18L18(D2) (Figure 2.3.1B). However, when all four residues were mutated to the corresponding residues of P2, the recombinant virus showed levels of attenuation that mirrored those of S18L18(D2) virus (Figure 2.3.2B). Moreover, the triple mutant virus (N1906D/N1889D/L1839V) showed similar levels of attenuation as the quadruple mutant virus (N1906D/N1889D/L1839V/T1808A) and the fragment-

swapped virus S18L18(D2), suggesting that residues N1889, L1839, and possibly N1906 located in the C terminal domain of the viral polymerase work in concert with each other. In addition, 5 of the 6 animals infected with either the triple or quadruple mutant viruses had extremely low or undetectable levels of viremia, while most of the animals infected with the single point mutant viruses or double mutant viruses retained high viral titers at terminal points (Figure 2.3.2C). The degree of pathogenicity noted upon necropsy of infected animals reflected the mortality data (Table 2.3.1). Organs (liver, lung, small intestine, large intestine, and stomach) were visually inspected, and moderate gross pathology was defined as discoloration covering 50% of the individual organ, while severe pathology was determined by discoloration covering 75% of the organ or with signs of internal hemorrhaging. The most severe gross pathologies were noted in the liver and lungs. One animal in the N1906D/L1839V infected group suffered rectal prolapse and was classified as having severe pathology. We therefore believe that certain residues in the L gene of the P18 strain are responsible for the intrinsic difference noted in the gross pathological changes in the organs of the infected animals.

H&E staining of liver tissue samples demonstrate that animals infected with the combination-point mutant virus show reduced histopathology.

In order to confirm visual inspection of the pathological differences between animal organs, H&E staining was performed on representative liver tissue samples from animals infected with the rP2, rP18, N1906D/N1889D, or N1906D/N1889D/ L1839V/T1808A mutant virus. While the rP2 infected liver tissue sample looked relatively normal, the rP18 infected liver tissue showed severe pathology (Figure 2.3.3).

Large zones of necrosis were observed throughout the sample. Severe fatty change was noted throughout the tissue of the rP18 infected animals along with acidophil bodies and ballooning degeneration. The pathology in the N1906D/N1889D liver sample was less severe, but still showed ballooning degeneration and individual hepatocytes that appeared to be dying. While not as severe as the rP18 sample, fatty changes were still noted. The histopathology from the liver sample of the N1906D/N1889D/ L1839V/T1808A infected animals showed hepatocytes that were largely healthy in appearance, while the presence of inflammatory cells within the portal veins was noted. Taken together, these histopathological results reflect the degrees of attenuation of some of the recombinant viruses noted in the mortality data shown in Figure 2.3.2.

The increased virulence of PICV P18 is likely due in part to an increase in the rate of virus replication and efficiency of viral genomic RNA replication.

As we have noted previously [234], the rP18 virus shows a faster rate of replication than its less pathogenic rP2 counterpart in cell culture. We therefore proceeded to analyze the growth curves of the recombinant mutant viruses used in the current study. To do this, Vero cells were infected with the different recombinant viruses at MOI=0.01 and virus supernatants were collected at 6, 12, 24, 36, 48, 60, 72 & 84 hours post infection. The single T1808A mutant virus appeared to replicate at a similar rate as that of the P18 virus (Figure 2.3.4). The two recombinant double mutant viruses N1906D/N1889D and N1906D/L1839D showed replication rates that are faster than those of the triple and quadruple recombinant viruses (N1906D/N1889D/L1839V and N1906D/N1889D/L1839V/T1808A), which remarkably almost overlapped with the

growth curve produced by the rP2 virus (Figure 2.3.4). These data suggest that the faster replication rates of some of these recombinant viruses may partly explain their more virulent nature in the infected animals.

In order to confirm that the slower growth rate of the recombinant virus exhibiting the combination of point mutations correlated with the lower rate of virus genome replication, we performed real-time RT-PCR to measure the amount of RNA genome replication occurring in the infected cells. To do this, Vero cells were infected with rP2, rP18, or the combination point-mutant virus at MOI=1. RNA samples were collected at 10 hpi, and assayed by real time RT-PCR. The primer used for reverse transcription amplified only the viral genomic S segment, thus allowing for determination of the rate of virus genome replication. While the difference was not dramatic, the rP18 virus showed significantly higher levels of genome replication than rP2 (Figure 2.3.5), which was reflected by the growth curves of these recombinant viruses in cell cultures (Figure 2.3.4). Most notably, the quadruple mutant showed replicative levels similar to that of the rP2 virus, suggestive of its attenuation level noted in the *in vivo* experiments (Figure 2.3.2). Taken together, these data suggest that a modest increase in replicative efficiency of the P18 polymerase can partly contribute to the heightened degree of virulence in infected animals, and that the three amino acid residues located at positions 1906, 1839, and 1889 of the L protein are critical for this phenotypic difference between the two PICV strains.

Discussion

The mechanism by which arenaviruses cause severe hemorrhagic fever has long been speculated, but remains poorly understood. Here, we have systematically analyzed natural sequence changes in the L segment of a virulent PICV arenavirus (P18) in order to elucidate which changes are responsible for the severe disease phenotype.

In LASV infected patients, a strong correlation is observed between the levels of viral titer in the blood and clinical prognosis. Patients who recover from the illness are able to progressively reduce the levels of viremia, while fatally infected patients demonstrate uncontrolled viremia, eventually succumbing to the disease [105]. Similarly, guinea pigs infected with virulent rP18 PICV virus maintain high viral titers in the blood until the animals reach terminal points, and must be euthanized. Meanwhile, animals infected with the avirulent rP2 virus demonstrate undetectable levels of virus in the blood (Figure 2.3.1C). However, rP2 viral replication is evidenced in the spleen, which is quickly eliminated [234]. When the L polymerase mutant viruses were tested, they showed a similar trend, i.e., those animals with severe disease maintained high levels of viremia at the terminal points whereas animals that were able to recover quickly controlled virus replication (Figure 2.3.2C). Recently, a determinant of viral chronicity was mapped to position 1079 of the polymerase of LCMV. The Clone 13 strain is able to establish a persistent infection, while the Armstrong strain causes acute infection which is quickly cleared. This single amino acid difference between the two strains was found to be responsible for the differential replicative capacity of the viral isolates *in vivo*, with the persistent strain showing higher replication rates. In addition to higher levels of viremia, this single mutation resulted in higher levels of RNA replication intracellularly as well as

resulting in a generalized immune suppression [107]. Taken together, these data suggest that viral replicative capacity can serve as a good determinant of increased severity in arenavirus infection.

Through systematic mutagenesis, we were able to map virulence determinants to the C terminus of the PICV L polymerase that include a combination of N1906D, N1889D, and L1839V mutations which produced a virus that was able to confer similar levels of attenuation as observed for the fragment swapping rS18L18(D2) virus (Figure 2.3.1 and Figure 2.3.2). This suggests that these residues work in concert and are likely positioned in close proximity to one another in the tertiary structure of the protein that can modulate the polymerase catalytic function.

Structural information on negative strand virus polymerases is currently scarce. While the crystal structures of the C terminal domain of the PB2 subunit of the influenza polymerase [258] as well as a complex of the N terminus of influenza PB1 with the C terminus of PA [259] have been determined, the RNA-dependent RNA polymerases (RdRps) of other negative-strand RNA viruses have proven difficult to crystallize. These proteins are extremely large (e.g., ~250 kDa for arenaviral L polymerase) and contain multiple functional domains. Sequence analysis has indicated that there are at least 4 conserved domains within the arenaviral L polymerase that are connected by highly variable linker regions [54]. Domain III contains the RdRp, as evidenced by conserved motifs consistent with the RdRps of other negative-strand RNA viruses. Recently, the structure of the L1 domain of the LCMV polymerase, which consists of the first 196 amino acids, has successfully been solved and shown to fold into an endonuclease domain that is thought to be involved in the cap snatching process of viral transcription

[55]. However, the structure of the other domains of L polymerase remains elusive. Domains I and III of the Tacaribe L polymerase have been shown to be involved in binding the Z matrix protein, allowing Z to inhibit viral transcription [60]. Many negative-strand viral polymerases, including the arenaviral RdRp, are known to oligomerize, which may be a requirement for transcription [260-263]. Recently, studies have shown that the N terminus of the L protein may bind to the N terminus of another L subunit via domain I in a head-to-head conformation [54]. Conversely, domains III and IV at the C terminus of one subunit may bind to the C terminus of another subunit [54]. In addition, the N terminus of one subunit may also bind to the C terminus of another in a head-to-tail orientation [54]. How these different conformations of oligomerization contribute to the function of the polymerase is yet to be understood. Currently, the exact residues involved in oligomerization of L are unknown. One possibility is that the residues identified in the current study as being important for the replicative differences between the two strains of PICV may affect the oligomerization state of the polymerase, although we have not formally tested this hypothesis. Also, the functions of domains II and IV of the polymerase remain unknown. Of note, the residues that we have identified in this study (N1906, N1889, and L1839) as critical for development of highly pathogenic PICV infection are located in domain IV. The sequence of this domain is unique, and does not resemble any other known protein structures. While the residues identified here may potentially be involved in oligomerization of the polymerase, it is also possible that they might contribute to other unknown function(s) of domain IV. One such function that this domain could potentially contribute to is polymerase processivity.

The rP2 and rP18 viruses exhibit different rates of replication in tissue cultures with the rP18 virus growing at a faster rate than the rP2 virus (Figure 2.3.4) [234]. Analysis of reassortant viruses have determined that the L segment is responsible for the observed differences in growth rate as the sequences of the Z protein are identical between the two strains. We confirmed by real-time RT-PCR that the P18 virus is more efficient at catalyzing viral genomic RNA replication than its P2 counterpart (Figure 2.3.5). We have introduced various natural sequence changes into the P18 polymerase and tested the effects of the mutations on viral genome replication. Once again, while individual mutations showed little effect on the rate of genome replication, a combination of the point mutations in the C terminus of L reduced the levels of RNA replication, more closely resembling the levels seen in the P2 virus. Because these mutations in domain IV affected the efficiency of the polymerase function, we propose that this domain may be involved in determining the rate of polymerase activity. Taken together, these data suggest that rapid virus replication as a result of enhanced polymerase activity plays an important role in determining the degree of virulence in arenavirus-induced VHFs. Other viral polymerases, such as that of influenza, have also been shown to contribute to disease virulence [264-266].

While we have shown in the current study that sequence variations in arenaviral L polymerase play an important role in determining the degree of virulence, it is important to note that the pathogenic nature of arenavirus VHFs may involve other factors. For example, reassortant analysis of P2 and P18 PICV viruses has indicated that additional viral virulence determinants may also be localized to the GPC and NP genes encoded by the S segment of the viral genome [257]. Therefore, we would not expect introduction of

the critical residues for the pathogenesis of P18 to the P2 reverse genetics system to result in complete rescue of the P18 virulence phenotype. This would require introduction of the residues critical for virulence in the S segment as well. The binding affinity of the viral glycoprotein (GPC) to its receptor has been implicated as an important factor for viral pathogenesis [30, 88]. While the receptor used by PICV is currently unknown, several New World arenaviruses that cause hemorrhagic fevers are known to use the human transferrin receptor 1 (TfR1) as their cellular receptor [45, 47], while the nonpathogenic viruses Tacaribe and Amapari use TfR1 orthologs but cannot gain entry into cells via the human TfR1 [48]. Old world arenaviruses such as LASV utilize alpha-dystroglycan (αDG) as their cellular receptor [29, 30]. LCMV Clone 13, which causes chronic infection of mice, has a high affinity for αDG as it is able to displace laminin, the natural cellular ligand for αDG [30]. Meanwhile, LCMV Armstrong, which causes an acute infection, is unable to displace laminin [30, 88]. This evidence denotes the contribution of the GPC gene in arenavirus pathogenicity. Recent data from our laboratory and others have indicated that the nucleoprotein (NP) gene, which is encoded in the S segment, is involved in suppressing type I interferon (IFN) [99, 104, 220]. Arenaviral hemorrhagic fever has been shown to be associated with a generalized immune suppression, thereby enhancing viral replication and disease pathogenesis [134, 163, 165, 168, 176, 267, 268], and NP may contribute to this mechanism of host innate immune suppression. While most viral proteins that inhibit IFN production do so by inhibiting steps in the signal transduction pathway, the arenaviral NP functions in a unique manner. The C terminus of the protein contains an exoribunuclease domain, which has been shown to be responsible for the IFN inhibition function of the protein by

possibly degrading RNA substrates that can be recognized as viral pathogen-associated molecular patterns (PAMPs) by the host [103, 104, 269]. Taken together, while the pathogenesis of severe arenaviral infections does appear to be multigenic, we show here that differences in the viral L polymerase gene alone can greatly influence the degree of disease pathogenesis *in vivo*. Unique regions of the polymerase identified in this study to be involved in viral replication efficiency may provide novel targets for effective antiviral development and therapy.

Acknowledgements

We thank Dr. J. Aronson (University of Texas Medical Branch) for providing P2 and P18 viruses and Dr. T. G. Parslow and Dr. V. Adsay for providing expert consultation on liver pathology. This work was supported by NIH grants R01AI083409 to Y.L. and R01AI093580 and R56AI091805 to H.L.

Table 2.3.1:

Table 1: Macroscopic pathology observed in animals infected with combination point mutant viruses*

Combination point mutant virus	Animals with moderate to severe pathology	
N1906D/N1889D	4/6	67%
N1906D/L1839V	4/6	67%
N1906D/N1889D/ L1839V	1/6	17%
N1906D/N1889D/ L1839V/T1808A	1/6	17%

*Upon necropsy at terminal points, organs were visually inspected for signs of pathology. Organs where moderate to severe pathology was noted included the liver and lungs. One animal in the N1906D/L1839V infected group developed rectal prolapse.

Figure 2.3.1:

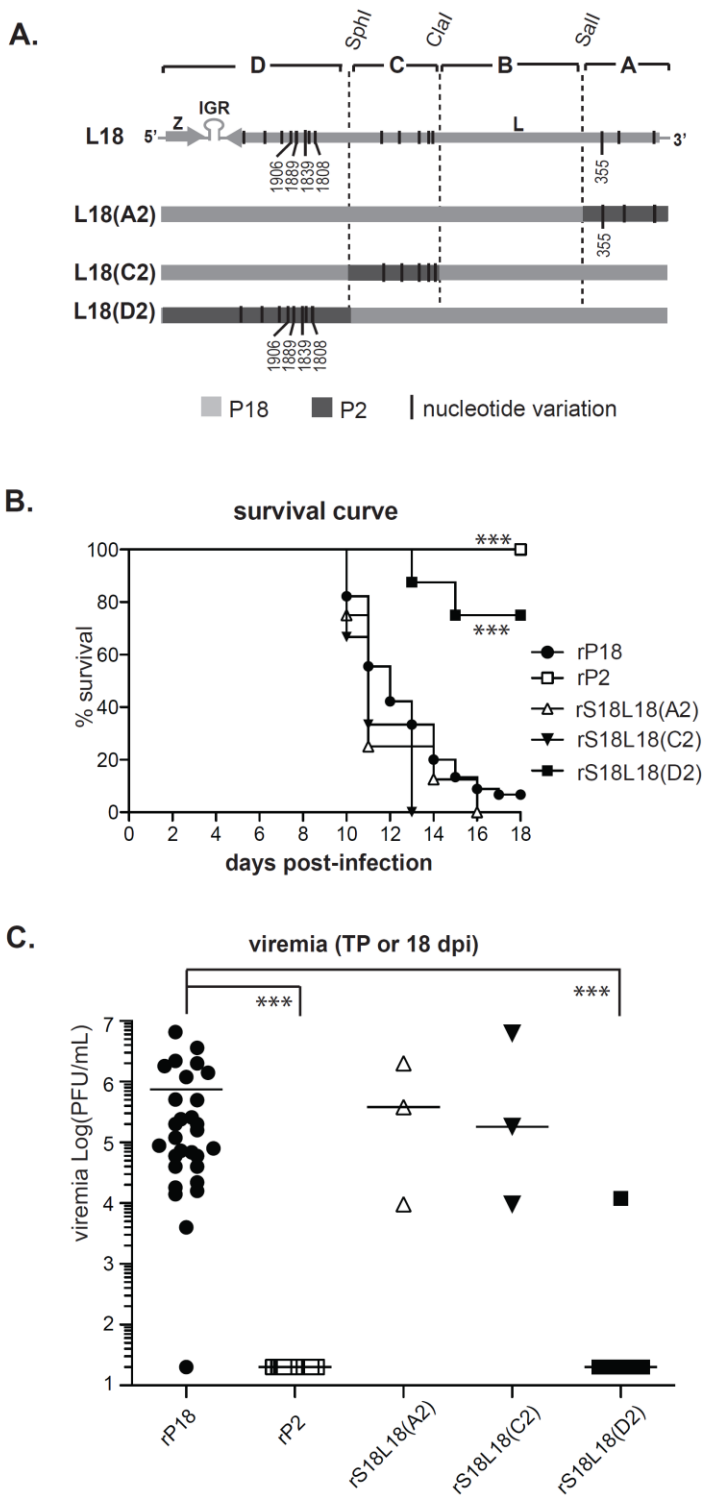
A.
SphI
ClaI
SalI
D
C
B
A
IGR
Z
L18
5'
3'
L
1906
1889
1839
1808
355
L18(A2)
L18(C2)
L18(D2)
P18
P2
nucleotide variation
B.
survival curve
% survival
days post-infection
***
rP18
rP2
rS18L18(A2)
rS18L18(C2)
rS18L18(D2)
C.
viremia (TP or 18 dpi)
viremia Log(PFU/mL)
rP18
rP2
rS18L18(A2)
rS18L18(C2)
rS18L18(D2)

Figure 2.3.2:

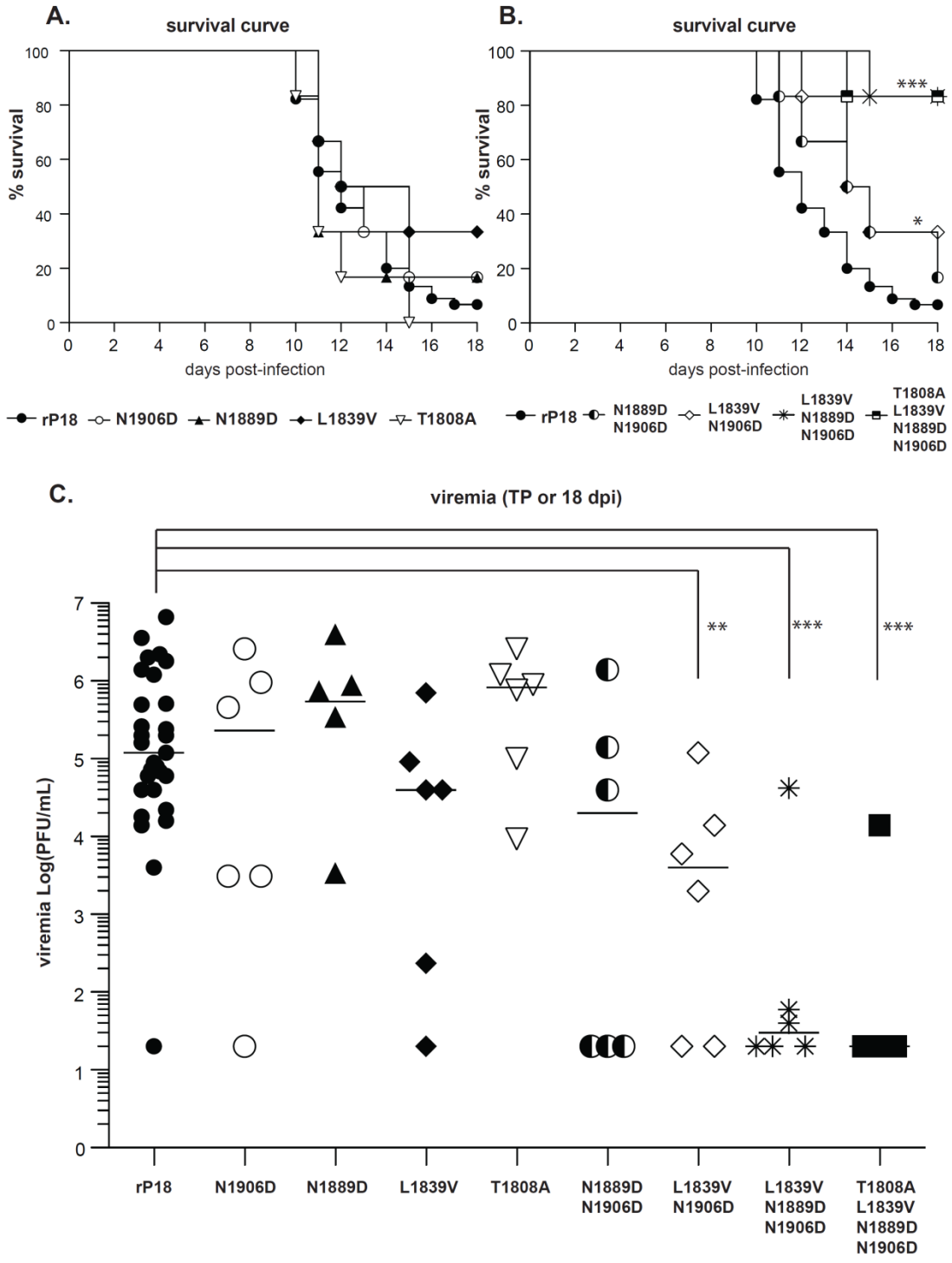
A.
survival curve
% survival
days post-infection
rP18
N1906D
N1889D
L1839V
T1808A
B.
survival curve
% survival
days post-infection
***
*
rP18
N1889D N1906D
L1839V N1906D
L1839V N1889D N1906D
T1808A L1839V N1889D N1906D
C.
viremia (TP or 18 dpi)
viremia Log(PFU/mL)
**
***
***
rP18
N1906D
N1889D
L1839V
T1808A
N1889D N1906D
L1839V N1906D
L1839V N1889D N1906D
T1808A L1839V N1889D N1906D

Figure 2.3.3:

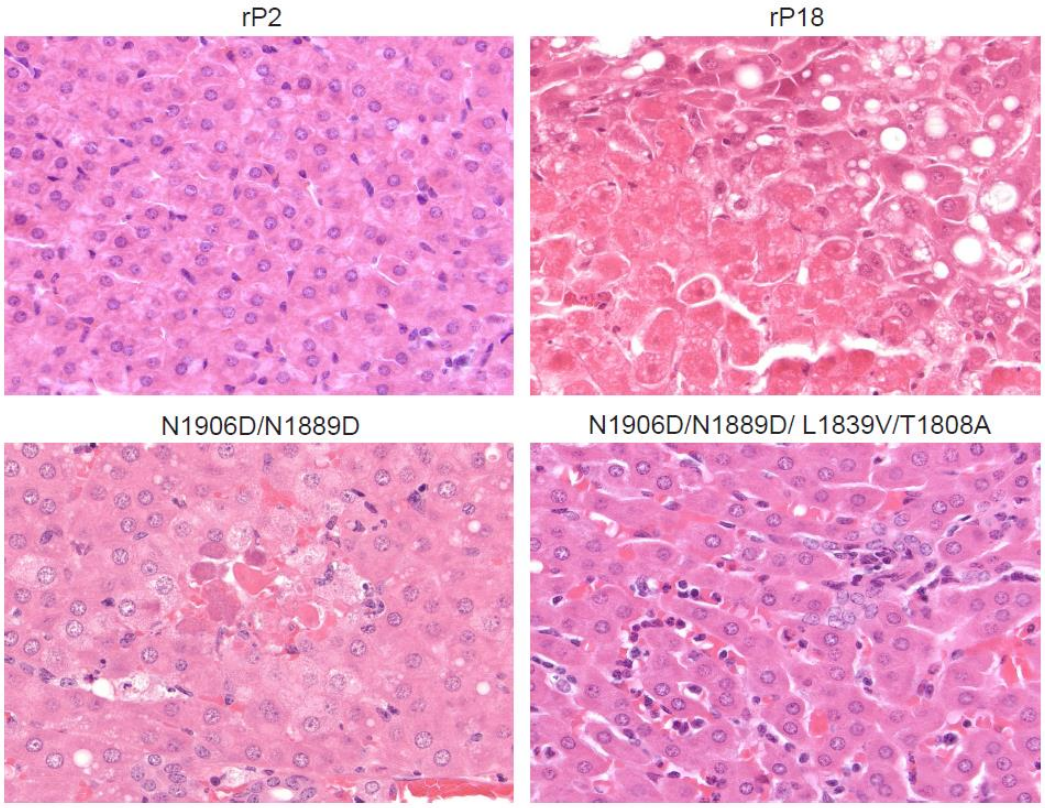

Figure 2.3.4:

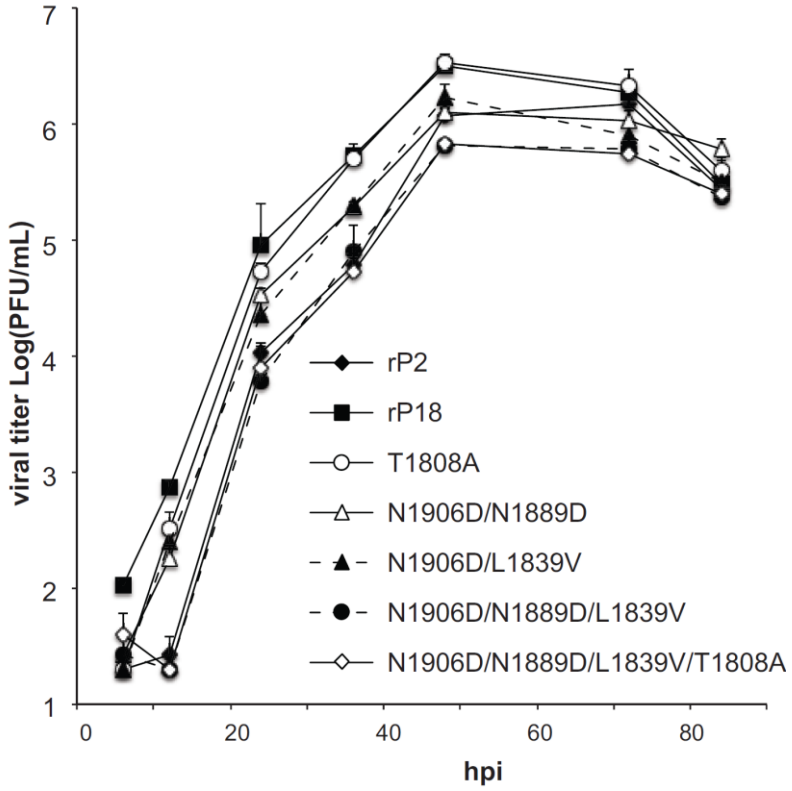
viral titer Log(PFU/mL)
hpi
rP2
rP18
T1808A
N1906D/N1889D
N1906D/L1839V
N1906D/N1889D/L1839V
N1906D/N1889D/L1839V/T1808A

Figure 2.3.5:

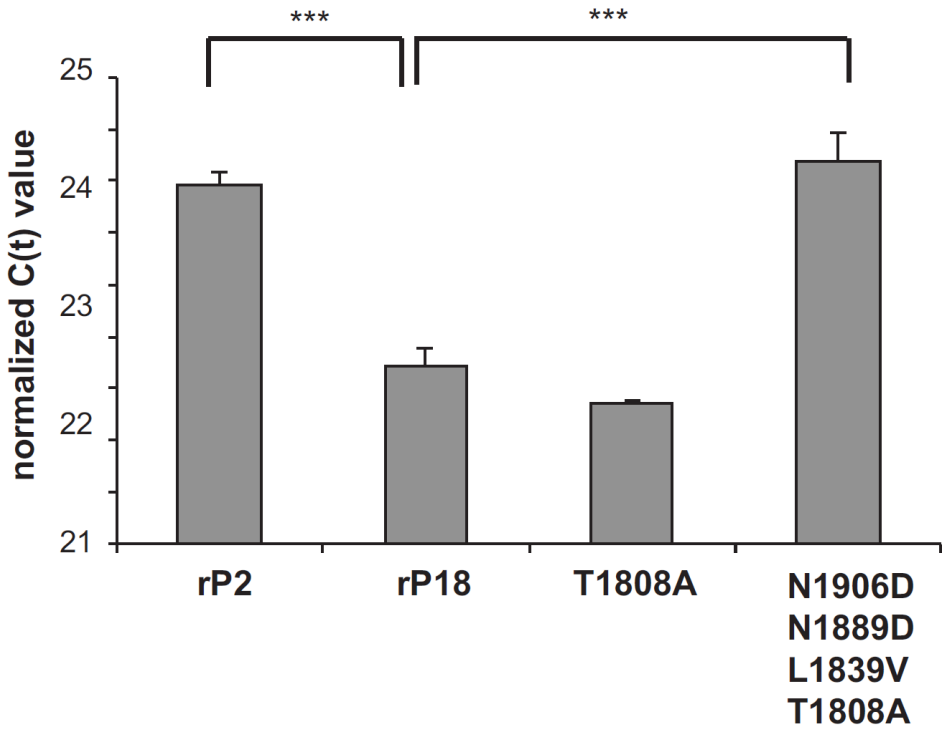
***
***
25
24
23
22
21
normalized C(t) value
rP2
rP18
T1808A
N1906D
N1889D
L1839V
T1808A

Figure legends:

Figure 2.3.1. (A) Generation of recombinant P2/P18 L segment fragment swapping mutants. Based on available unique restriction enzyme sites, 3 fragment swapping mutants were generated, replacing a fragment of the P18 L segment with the corresponding sequence of P2 genome. Sequence changes are highlighted in black, and changes that result in amino acid differences between the two strains are flagged. (B) Mortality of guinea pigs infected with L segment P2/P18 fragment swapping mutant recombinant viruses. Percentage of mortality was defined as the number of animals reaching terminal points (>30% weight loss as compared to a nomogram or rectal temperature < 38°C in addition to a marked decrease in the weight of the animal) within the course of an 18-day infection. Number of infected animals are as follows: rP18 (n=45), rP2 (n=24), rS18L18(A2) (n=8), rS18L18(C2) (n=3), rS18L18(D2) (n=8). (C) Viremia levels of guinea pigs infected with L segment P2/P18 fragment swapping mutant recombinant viruses. Serum samples collected at terminal points from animals infected with rS18L18(D2), rS18L18(C2), or rS18L18(A2) were analyzed by plaque assay to determine viral titers. Each data point represents one animal: rP18 (n=29), rP2 (n=12), rS18L18(A2) (n=3), rS18L18(C2) (n=3), rS18L18(D2) (n=6). * $p<0.05$, ** $p<0.01$, *** $p<0.001$.

Figure 2.3.2. Mortality and viremia levels at terminal point of guinea pigs infected with single or combination point-mutant viruses. (A) Mortality of animals infected with

single-point mutant viruses. Number of infected animals: rP18 (n=45), recombinant mutant viruses (n=6) (B) Mortality of animals infected with combination-point mutant viruses. Number of infected animals: rP18 (n=45), recombinant mutant viruses (n=6) (C) Viremia levels at terminal points (or end of experiment for recovered animals) of guinea pigs infected with single and combination point-mutant viruses. Each data point represents one animal: rP18 (n=29), N1889D (n=5), all other mutants (n=6). * $p<0.05$, ** $p<0.01$, *** $p<0.001$.

Figure 2.3.3. Liver pathology of infected animals. Representative H&E staining of livers from guinea pigs infected with rP2, rP18, N1906D/N1889D, & N1906D/N1889D/L1839V/T1808A mutants.

Figure. 2.3.4. Growth curves of recombinant single (A) or combination (B) point-mutant viruses. Vero cells were infected with various mutant viruses at MOI=0.01 and virus titers at various time points were determined by plaque assay.

Figure. 2.3.5. Real time RT-PCR analysis of genome replication in Vero cells infected with recombinant viruses. Vero cells were infected at MOI=1 with virus, RNA collected, and RT performed with primer specific for the 3' end of the genomic S segment. Real time RT-PCR was performed with primers specific to the NP gene, and values were normalized with values for GAPDH transcripts. * $p<0.05$, ** $p<0.01$, *** $p<0.001$.

CHAPTER 3:

Cap binding and immune evasion revealed by Lassa nucleoprotein structure [104]

Xiaoxuan Qi[1], Shuiyun Lan[2], Wenjian Wang[3], Lisa McLay Schelde[2], Haohao Dong[1], Gregor D. Wallat[1], Hinh Ly[2], Yuying Liang[2] & Changjiang Dong[1]

[1]Biomedical Sciences Research Complex, School of Chemistry, University of St Andrews, North Haugh, St Andrews UK. [2]Department of Pathology and Laboratory Medicine, Emory University School of Medicine, Atlanta, Georgia USA. [3]Laboratory of Department of Surgery, The First Affiliated Hospital, Sun Yat-Sen University, Guangzhou, Guangdong China.

Abstract

Lassa virus, the causative agent of Lassa fever, causes thousands of deaths annually and is a biological threat agent, for which there is no vaccine and limited therapy. The nucleoprotein (NP) of Lassa virus has essential roles in viral RNA synthesis and immune suppression, the molecular mechanisms of which are poorly understood. Here we report the crystal structure of Lassa virus NP at 1.80Å resolution, which reveals amino (N)- and carboxy (C)-terminal domains with structures unlike any of the reported viral NPs. The N domain folds into a novel structure with a deep cavity for binding the m7GpppN cap structure that is required for viral RNA transcription, whereas the C domain contains 3'–5' exoribonuclease activity involved in suppressing interferon induction. To our knowledge this is the first X-ray crystal structure solved for an arenaviral NP, which reveals its unexpected functions and indicates unique mechanisms in cap binding and immune evasion. These findings provide great potential for vaccine and drug development.

Introduction

Several arenaviruses, including Lassa virus (LASV), can cause severe viral haemorrhagic fevers in humans with high morbidity and mortality, to which there is no vaccine and limited treatment [7, 17, 270, 271]. These pathogenic arenaviruses are public health threats and potential biological threat agents. LASV, like other arenaviruses, is a single-stranded ambisense RNA virus with two genomic RNA segments encoding four genes [270]. The NP encapsidates viral genomic RNAs into ribonucleoprotein (RNP) complexes and is required for both RNA replication and transcription [62, 209, 254]. Like bunyaviruses and orthomyxoviruses, arenaviruses snatch the cap structure of cellular mRNAs to use as primers to initiate viral transcription, the exact mechanism of which is unknown. The cap-snatching mechanism of arenaviruses seems to be unique, as evidenced by the cytoplasmic localization and the much shorter 5' non-templated mRNA sequences [57, 272-274]. Severe arenavirus infections including lethal Lassa cases are associated with a generalized immune suppression in the infected hosts [134, 163, 165, 168, 176, 267, 268], the exact mechanism of which is unclear but is thought to involve NP's ability to suppress the induction of type I interferon (IFN) [99, 220]. To address the functional mechanisms of NP in viral RNA synthesis and host immune suppression, we set out to determine the crystal structure for LASV NP, knowledge derived from which can be extended to other arenavirus NP proteins, as all known arenaviral NP proteins share high sequence identity.

Results

Structure determination

The full-length 569-residue LASV NP protein (Josiah strain) was expressed and purified as a recombinant MBP fusion protein in Escherichia coli as described in Methods. The purified protein exists mainly in two forms, with a majority in trimeric and some in hexameric form. Both forms bind random RNAs, which are longer and more abundant in the hexamers than in the trimers, a feature that is similar to known NPs from negative-strand RNA viruses [275-278]. We attempted to crystallize both forms, but only the trimeric NP formed crystals. The crystals showed heavy twining with a twin fraction of ~0.43 and the reflection intensity statistic |E2-1| 0.681/0.681. Initial phases were obtained in a space group of P321 using the multiple wavelength anomalous diffraction (MAD) with Samarium derivative. The true space group was P3 with three subunits in an asymmetric unit. The structure was refined to a resolution of 1.80Å with de-twining. The crystal structures do not contain RNA, indicating that only RNA-free NP was able to form crystals. The final structural model of the native LASV NP has an R_{factor} of 0.18 and an R_{free} of 0.20.

Overall structure of LASV NP protein

In the NP protomer structure, 514 residues of the 569-residue LASV NP protein were built into the model (Fig. 3.1a). The electron densities for residues 1–6, 147–157, 339–363, 518–521, 562–569 were not well defined. LASV NP protomer, like other viral NPs [62, 272-274], is composed of the N- and the C-terminal domains, but neither

domain shows structural similarity to any known viral NPs. The large N domain (residues 7–338) consists mainly of α-helices and coils, whereas the C domain (residues 364–561) forms a typical α/β/α sandwich architecture. In the trimeric form, three subunits lie in a head-to-tail orientation to form a ring-shaped structure with a three-fold symmetry (Fig. 3.1b). Surface rendering reveals a deep cavity located near the bottom of the N domain and a large cavity at the top of the C domain (Fig.3.1c, d), which are the cap-binding site and the 3'–5' exoribonuclease active site (see below), respectively. The interface area between the subunits is 455Å^2, representing 1.9% of total surface area of a subunit (23,343Å^2). The central hole of the trimeric structure is 23Å in diameter, whereas the head ring is 98Å and the body ring is 118Å.

LASV NP is a 3'–5' exoribunuclease

A Dali search(http://ekhidna.biocenter.helsinki.fi/dali_server) identified several structures similar to the C domain of NP, including several known 3'–5' exonucleases/exoribonucleases in bacteria and humans (for example, human TREX1), all of which belong to the DEDDH subfamily of the DEDD (DnaQ) superfamily [279-281]. The humanTREX1 structure shows two Mn^{2+} cations in the active site [281]. We identified one Mn^{2+} in each subunit of LASV NP by crystal fluorescent scanning, but could not identify the second Mn^{2+}, possibly because it was not well ordered in the absence of the RNA substrate. The C domain of NP superimposes well with the portion of TREX1 that coordinates the Mn^{2+} cations (Fig. 3.2a), in particular the β5, β6, β7, β8 and β9 strands of NP completely overlap with the central β-sheets of TREX1. The

putative exonuclease catalytic residues D389, E391, D466, D533 and H528 are absolutely conserved in all known arenavirus NP proteins and are located at identical positions as in the TREX1 active cavity (Fig. 3.2b). Taken together, the structural evidence indicates that LASVNP is a new member of the DEDD 3'–5' exonuclease superfamily. We conducted *in vitro* assays to characterize the 3'–5' exonuclease activity of the wild-type LASV NP, as well as NP mutants at putative catalytic sites. We showed that the wild-type protein, in its trimeric or hexameric form, could digest both DNA and RNA substrates (Figures 3.3 and 3.4). As divalent cations are essential for exonuclease activity[279], we determined what divalent cation was most effective for NP exonuclease to digest various single-stranded RNA (ssRNA) species that are based on the NP gene in the viral genomic sense (60 nucleotides, vRNA), complementary antigenomic sense (30 nucleotides, cRNA), or in capped mRNA form (126 nucleotides, mRNA) (Methods). We showed the order of efficiency as $Mn^{2+} > Co^{2+} > Mg^{2+} > Ca^{2+} > Zn^{2+} > Fe^{2+} > Ni^{2+} > Cu^{2+}$ (Figure 3.5). Wild-type NP could cleave various ssRNA species efficiently (Fig. 3.2c), regardless of whether they contained a hydroxyl (5'OH) group, triphosphate (5'ppp), or a cap at the 5' termini (Methods). In contrast, the NP catalytic mutants (D389A, E391A and D466A) showed markedly reduced RNase activity (Fig. 3.2c and Fig. 3.4). We also demonstrated that wild-type NP, but not its catalytic mutants (D389A, E391A and D466A), can efficiently degrade various dsRNA molecules with 5'-hydroxyl (5'OH), single 5'-triphosphorylate (5'ppp/5'OH) and double 5'-triphosphorylate (5'ppp/5'ppp) (Fig. 3.2d).

Fluorescence scanning analysis identified a zinc ion in the NP structure, despite the fact that no typical zinc finger motif was predicted from the amino acid sequence and

that no zinc compounds were used during the purification and crystallization processes. Although the residues C506, C529, H509 and E399 that coordinate the zinc ion are not of the typical zinc-binding motif [282], they appear to adopt a zinc finger fold in structure [282, 283]. The CCHE zinc-binding site is located in the C domain near the 3'–5' exonuclease active site (Figure 3.6). We speculate that zinc binding may be required to stabilize the structure of the C domain and/or contribute to the substrate binding and specificity of the exonuclease activity [282, 283]. A highly positively charged groove located between the N and C domains is predicted as the genomic RNA-binding site (Figure 3.7). An *in vitro* assay confirmed that RNAs are bound within the purified NP oligomers and protected from its intrinsic exonuclease activity (Figure 3.7).

Exonuclease and immune evasion

To determine whether the exoribonuclease activity is important for the transcriptional function of NP, we generated alanine substitution at five putative catalytic sites, D389A, E391A, D466A, D533A and H528A, in the mammalian cell expression vectors of either native or Myc-tagged NP gene, and examined the activity of each mutant in transcribing the LASV minigenome RNA that encodes a *Renilla* luciferase (RLuc) reporter gene [220]. As shown in Fig. 3.8a, each NP mutant expressed comparable protein levels to the wild type, and led to similar folds of increase in RLuc activity, indicating that these mutations did not alter the overall structure or affect the basic function of NP in mediating viral RNA transcription.

We next examined whether the exoribonuclease activity is required for NP's function in the suppression of IFN [99, 220]. As expected, wildtype NP strongly inhibited Sendai-virus-induced IFN-β activation by a promoter assay (Methods), whereas all the catalytic mutants D389A, E391A, D466A, D533A and H528A showed a complete loss of function at a low level of transfected expression vectors (10 ng) and showed various levels of deficiency at higher levels (Fig. 3.8b and 3.9). Our results confirm a previous study showing that the D389 residue of LASV NP, as well as its corresponding residue D382 in the prototypic arenavirus lymphocytic choriomeningitis virus (LCMV), is required for IFN suppression but not for viral RNA transcription [255], and may help to explain the loss of IFN suppression for Tacaribe virus NP. In summary, these data provide strong genetic evidence for an important role of the NP exoribonuclease activity in suppressing the IFN induction.

Viral infections are usually detected by the cellular pattern-recognition receptors (PRRs) such as toll-like receptors (TLRs) and cytosolic RNA sensors, retinoid-acid-inducible gene-I-like helicase (RIG-I) and melanoma differentiation-associated protein 5 (MDA5), which recognize the pathogen-associated molecular patterns (PAMP) RNA ligands and initiate signalling pathways to induce the production of type I IFNs [284, 285]. We hypothesize that NP prevents the virus-induced IFN induction by degrading the PAMP RNA ligands that otherwise would trigger the viral sensors in the cells.

We examined whether the NP RNase function is essential for suppressing the IFN production induced by the immunostimulatory RNAs, that is, poly(I:C) and the virion RNAs extracted from Pichinde virus, which is a prototypic arenavirus [234]. We found that whereas wild-type NP efficiently inhibited the IFN-β activation induced by poly(I:C)

or by Pichinde-virion-associated RNAs, none of the five catalytic mutants (D389A, E391A, D466A, D533A and H528A) exhibited any suppressive activity (Fig. 3.8c). Similar results had been reported for LCMV NP [101].

We have shown that the NP exoribonuclease activity is essential for suppressing both viral-infection-induced and immunostimulatory- RNA-induced IFN production. A good example of exonuclease meditated suppression of IFN production has been demonstrated for human TREX1 protein, which degrades small ssDNAs and dsDNAs accumulated during cellular apoptosis. Failure to clear these DNA fragments by TREX1 natural mutants leads to the activation of cellular DNA receptors to trigger a persistent production of IFNs that contributes to human autoimmune diseases [281, 286-289]. How does the NP RNase activity function in suppressing the virus-induced IFN production? A simplistic but reasonable model is that the NP RNase activity is able to remove viral PAMP RNAs that are otherwise recognized by the cellular PRRs. Although we have shown that LASV NP protein can degrade various RNA templates *in vitro*, we believe that the NP RNase activity must be highly regulated *in vivo*, as NP does not cause a generalized nonspecific RNA degradation process of cellular or viral RNAs in the cells (data not shown). We propose that the NP RNase activity in the cells is restricted to viral PAMP RNAs through a yet-to-be characterized regulatory mechanism. A recent publication has shown a direct protein–protein interaction of NP with RIG-I and MDA5 [101], which may be one possible mechanism for the specific nuclease activity of NP against these PRR-associated PAMP RNAs.

LASV NP is a cap-binding protein

The N domain adopts a completely novel fold not found in the Dali server. To identify the cap-binding residues in the deep cavity of then domain, we attempted to soak and perform co-crystallization of LASV NP with m7GpppG, triphosphorylated, diphosphorylated or monophosphorylated ribonucleotides. We could observe the clear density for the triphosphate and partial density for uridine from the triphosphorylated ribonucleotide complex structures. We also visualized the structure of NP in complex with dTTP with a clear original $F_o - F_c$ electron density contoured at 2.5σ for dTTP (Fig. 3.10a). The triphosphate group of dTTP was bound in the middle of the cavity in an identical manner as that of UTP, in which it was anchored by salt bonds formed with the side chains of the conserved residues K309, R300, R323 and K253. In the deep end of the cavity, thymidine occupied a hydrophobic pocket that is composed of residues F176, W164, L172, M54, L120, L239 and I241. We propose that this dTTP-binding pocket is the binding site for the cap structure m7GTP and that the residues located within the pocket may have to change conformation to accommodate the cap moiety. Although the N domain of NP is not structurally similar to any of the cap-binding proteins, its hydrophobic thymidine-binding pocket shares common features for cap binding [290, 291]. Moreover, the NP cap-binding cavity has a unique feature in that its entrance contains another hydrophobic region that is composed of the hydrophobic residues Y319, Y209, Y213, L265 and the acidic residue E266, which can potentially act as the binding site for the second base of the m7GpppN (where N represents G, C, U or A) cap structure. The entrance of the cap-binding cavity has an oval shape with a diameter of 9–13Å , which is a perfect fit for the single-stranded mRNA. We propose that a loop

composed of residues K236 to S242 serves as a ‘gate’ for the capped template (primer) binding and that the entire structure of m7GpppN, including the cap m7G, the triphosphate, and at least one more nucleotide, is embedded within the deep cavity. This binding feature is unlike other known cap-binding proteins, in which only the m7G caps are locked in between the sandwich, whereas the rest of the RNA molecule is exposed [290, 291].

To characterize the role of the cap-binding residues in viral RNA transcription, we examined a panel of NP mutants with alanine substitution of residues located inside and at the entrance of the cavity and that are conserved among all known arenaviruses for their ability to mediate the cap-dependent viral RNA transcription using the LASV minigenome replicon assay. Wild-type NP (with or without Myc tag) produced up to a 1,000-fold increase in RLuc reporter activity over a control reaction, and more than 100-fold increase even when expressed at a low level (15 ng of transfected NP plasmid DNAs). All mutant proteins were expressed at similar levels as the wild type transfected with 15–30 ng of plasmid (Fig. 3.10b). Compared to the wild type, the K253A and E266A mutants completely lost the RNA transcription activity, and the Y319A, F176A, W164A, K309A and R323A mutants showed significantly decreased activity (Fig. 3.10c). R300A had a minor effect, whereas W12A and Y209A had no effect. It is worth noting that none of these mutants was found to impact the NP function in the suppression of IFN (Figure 3.11). These functional data correlate well with the proposed cap-binding function of some of these conserved residues.

The unique cap-binding feature of LASV NP, in that the entire cap structure m7GpppN is buried within the cavity, has significant implications in understanding the

distinctive cap-snatching mechanism of arenaviruses. Once NP binds and protects the 5’ cap m7GpppN, the rest of the mRNA molecule located outside of the cavity may be susceptible to viral and/or host exonuclease-mediated degradation and/or to endonuclease-mediated cleavage (Fig. 3.6). This may help to explain the relatively short (1–4 nucleotides) 5’ non-templated sequences in arenavirus mRNAs [270, 272, 273]. However, individual mutation of the NP exonuclease catalytic sites did not show any defect in viral cap-dependent RNA transcription (Fig. 3.3a), indicating that the NP exonuclease activity is not essential (required) for generating the capped primers. It is worth noting that we did not identify an influenza polymerase PA-like endonuclease structural motif [292, 293] within LASV NP structure (Supplementary Table 4). Instead, recent studies indicated that the LASV L polymerase protein contains an endonuclease domain in its N terminus that is crucial for the cap-dependent viral RNA transcription [55, 294].

Conclusion

Our structural analysis and functional assays have demonstrated that the C domain of LASV NP contains 3’–5’ exoribonuclease activity that is required for suppressing IFN-β induction. We have provided evidence to suggest that the NP RNase activity is highly regulated in cells and proposed a novel mechanism by which the NP RNase activity may specifically remove the viral PAMP RNA ligands to suppress the production of IFN. Another important feature of LASV NP protein is that its N domain contains a deep cavity to bind and shield the entire m7GpppN cap structure, which is

distinct from other known cap-binding proteins, and has shed light on the unique cap-snatching mechanism of arenaviruses. In addition, we have also identified an unusual zinc-binding site and the viral RNA-binding groove in the LASV NP structure. Taken together, these findings reveal several new and potentially vulnerable targets on NP for the development of antivirals and effective vaccines to combat LASV and other pathogenic arenaviruses that can cause severe haemorrhagic fever diseases in humans.

Methods

Protein expression and purification

The full-length LASV NP gene (Josiah strain) was cloned into the pMAL-c2X-derived pLou3 plasmid, downstream of the TEV cleavage site following the MBP gene. This construct, encoding the N-terminal MBP tagged NP protein, was transformed into Rosetta cells (Novagen). After IPTG induction at a final concentration of 0.03 mM overnight at 20 °C, the cells were harvested by centrifugation at 8,000 r.p.m. for 20 min and suspended in TEN buffer (20 mM Tris, pH 7.5; 0.2 M NaCl, 10% glycerol, 1 mM EDTA) with protease inhibitors (Roche), 1 μM DNase (Sigma) and 1 mM phenylmethylsulphonyl fluoride (Sigma). After cells were lysed by a cell disruptor (Constant System Ltd), the cell lysates were collected by centrifugation at 20,000 r.p.m. for 30 min and applied on an amylose column. The column was washed with >10-column volumes of the sample buffer. The MBP–NP fusion protein was eluted with the TEN buffer containing 10 mM maltose. The MBP–NP fusion protein was then cleaved by Tev proteinase. The MBP portion was removed through two amylose columns, and the NP

protein was purified to homogeneity by gel filtration column. Trypsin digestion coupled with mass spectroscopy confirmed that the purified LASV NP protein was homogenous (data not shown), with a final concentration of 7 mg ml^{-1}.

Crystallization and data collection

A Cartesian robot (Genomic solutions) was used to screen for optimal crystallization conditions. The native crystals were obtained in 0.2 M $LiCl_2$ and 20% PEG3350 in 1 week at 20 °C. To obtain the NP complex with m7GpppG, m7GTP, or m7GDP, the NP protein was incubated with individual compound at a concentration of 2 mM for 30 min on ice and the crystallization conditions were screened. The NP complex with other triphosphorylated, diphosphorylated or monophosphorylated nucleotides were formed by incubating the NP protein with 50 mM of the respective compounds for 30 min on ice and the crystallization conditions were screened. The crystallization conditions were optimized until the resolution of the data was better than 2.5 Å. All crystals grew in 0.2 M KCI or 0.2 M LiCl and 14–22% PEG3350. The NP complexed with manganese ion was obtained by crystallizing the NP protein in 0.2 M $MnCl_2$, 25% PEG3350 followed by soaking the crystals in 0.2 M $NaCl_2$, 20% PEG3350 and 15% glycerol three times for 15 min each. The presence of the manganese and the zinc ions was confirmed in all the crystals by fluorescence scanning at the Diamond light sources UK. All the crystals were protected by cryoprotectants that contain 15% to 20% glycerol in the crystallization conditions before data collection in IO2 or IO3 at the Diamond light sources UK. The Samarium derivative crystals were obtained by soaking

the crystals overnight in 100 mM Samarium acetate, 0.2 M LiCl and 16% PEG3350, and was protected in a cryoprotectant of 0.2 M LiCl, 16% PEG3350 and 20% glycerol. The Samarium derivative MAD data were collected at a wavelength of 1.83 Å for peak data, 1.84 Å for inflection data and 1.45 Å for remote data from a single crystal. All the data were indexed, integrated and scaled by HKL2000 or Mosflm and Scale.

Structure determination

The crystals were heavily twined with a twining fraction of 0.43. The initial phases were obtained from a space group of *P*321 using the MAD data and SOLVE [295]. The initial model was built using RESOLVE[295], Buccaneer and Coot [296]. It was found that the true space group of the crystals was *P*3 during the structure refinement. The structures were refined using REFMAC5 [297], and the water molecules were added into the structure by ARP/wARP [298]. The $F_o - F_c$ maps for ligands (dTTP, UTP, zinc and manganese) were calculated before any ligand was added into the structures. The structures were de-twinned at last using REFMAC5, and the structures were evaluated using Molprobity [299].

In vitro RNA synthesis

The 30-nucleotide cRNA (sense) sequence 5′-CUGGGCUUACCUAUUCUCAGCUGAUGACCC-3′ was derived from the LASV NP (Josiah strain) S segment (nucleotides 2186–2215 in antigenomic orientation) and

chemically synthesized by Eurogentic. The 30-nucleotide vRNA (in genomic orientation) sequence 5′-GGGUCAUCAGCUGAGAAUAGGUAAGCCCAG-3′ was complementary to the cRNA. The cRNA (30 nucleotides) was used as one of the three substrates for 3′–5′ exoribonuclease assay. To obtain the blunted dsRNA, both cRNA and vRNA oligonucleotides were dissolved into 0.1 M NaCl, 1 mM EDTA and 0.1 M Tris pH 8.0 at the final concentration of 200 mM, and an equal amount of the two oligonucleotides was mixed together and annealed in a thermocycler as follows: 95 °C for 3 min, 68 °C for 1 min and then 4 °C.

The 5′-triphosphorylated vRNA was generated by *in vitro* transcription of the partial dsDNA template formed by the T7 promoter sequence 5′-AATTTAATACGACTCACTATAGG-3′ and the reverse complement of the T7 promoter sequence and of the LASV (Josiah strain) S segment (nucleotides 2186–2215) 5′-CTGGGCTTACCTATTCTCAGCTGATGACCCTATAGTGAG TCGTATTAAATT-3′ using the T7 MEGAshortscript kit following the manufacturer's instructions (Ambion). A similar strategy was use to generate the 32-nucleotide triphosphorylated cRNA with the T7 primer and LASV (Josiah strain) S segment (nucleotides 2186–2213) 5′-GGGTCATCAGCTGAGAATAGGTAAGCCCAGCCTATAGTGAGTCGTATTAAAT T-3′. A similar strategy was used to generate the 60-nucleotide vRNA corresponding to LASV (Josiah strain) S segment (nucleotides 2186–2213), using the partial dsDNA template formed by 5′-AATTTAATACGACTCACTATAGG-3′ and 5′-GTAAATCCCTGCAGTCGGCAGGGTTTACCGCTGGGCTTACCTATTCTCAGCTG ATGACCCTATAGTGAG TCGTATTAAATT-3′ as a template. To generate the doubly 5′-triphosphorylated dsRNA, equal amounts of the triphosphorylated 5′ppp-vRNA and

5′ppp-cRNA were annealed *in vitro*. To make the singly 5′-triphosphorylated dsRNA, equal amounts of the *in vitro* synthesized 32-nucleotide 5′ppp-vRNA and the chemically synthesized 30-nucleotide unphosphorylated cRNA were annealed *in vitro*. The human 18S rRNA fragment (128 nucleotides) was generated by a T7 RNA polymerase-directed *in vitro* RNA synthesis reaction, using the pTRI-RNA 18S control plasmid (Ambion), following the manufacturer's instruction.

To synthesize the capped viral mRNA transcripts corresponding to nucleotides 992–1117 of the LASV NP gene, the DNA template was PCR amplified from the NP expression plasmid with a forward primer 5′-AATTTAATACGACTCACTATAGGGAAAACACTGTCGTTGATCTGGAATC-3′ (underlined are T7 promoter sequences) and a reverse primer 5′-GGGTCATCAGCTGAGAATAGGTAAGCCCAGCGG-3′, and subjected to *in vitro* RNA synthesis using the mMESSAGE mMACHINE T7 Ultra kit (Ambion) following the manufacturer's instruction, except that no poly(A) tail was added.

A plasmid phRL-CMV that encodes the T7 promoter (T7p)-directed human β-globin gene was provided by R. Elliott and G. Blakqori. The T7p-globin DNA fragment was purified by agarose electrophoresis after digestion of the phRL-CMV plasmid with HindIII and Smal. The capped human globin mRNA transcripts were generated using the T7p-globin fragment as a template and the mMESSAGE mMACHINE T7 Ultra kit from Ambion, and the poly(A) tail was added following the manufacturer's instruction.

The ssRNA markers (perfect RNA markers, 0.1–1 kb) were purchased from Novagen. The low molecular mass ssRNA marker (10–100 nucleotides) was purchased from USB. The dsRNA ladder (21–500 bp) was purchased from New England Biolabs.

In vitro 3′–5′ exoribonuclease assays

The *in vitro* 3′–5′ exoribonuclease assays were carried out in 10 μl of the reaction solution containing 0.3 M NaCl, 10% glycerol, 20 mM Tris pH 7.5, 10 mM $MnCl_2$, 7 μg of either wild-type or mutant NP proteins, and 8 units of the RNaseIN inhibitor (Promega), in the presence of various substrate(s), at 37 °C for 60–100 min. The control reactions included all but $MnCl_2$, which was substituted by 20 mM EDTA. All the reactions, each in triplicate, were stopped by the addition of EDTA to a final concentration of 20 mM. The samples were mixed with equal volumes of RNA loading buffer (Ambion), heated at 95 °C for 3 min, cooled on ice for 5 min, and separated in 15% or 6% urea-polyacrylamide gel, or 2% agarose gel. The gels were stained in 0.05% ethidium bromide for 25 min, visualized using the 2UV transilluminator (UVP).

The luciferase-based assay to quantify virus-induced and immunostimulatory RNA-induced interferon-β activation

The Sendai-virus-induced IFN-β activation assay was conducted as described previously [200]. In brief, 293T cells were co-transfected using calcium phosphate with 100 ng of a vector that expresses the firefly luciferase (FLuc) reporter gene from a known functional

promoter sequence of the IFN-β gene (pIFNβ-LUC), variable amounts of either wild-type or mutant LASV NP vectors, and 50 ng of a β-gal-expressing plasmid for transfection normalization. At 24 h after transfection, cells were infected with Sendai virus (at multiplicity of infection = 1) to induce IFN-β expression. At 24 h after infection, cell lysates were prepared for luciferase and β-gal assays. FLuc activities were normalized by the β-gal values. Each transfection was conducted in triplicate and repeated in at least two independent experiments.

To determine whether NP can suppress the immunostimulatory RNA-induced IFN production, HEK293 cells were transfected with pIFNβ-LUC, variable amounts of either wild-type or mutant LASV NP vectors, and a β-gal-expressing plasmid for transfection normalization. Eighteen hours later, cells were transfected with either 1 μg of poly(I:C) or 250 ng of Pichinde virion RNA by lipofectamine 2000. Luciferase activity was determined at 18 h after the immunostimulatory RNA transfection and normalized by the β-gal activity.

Pichinde virion RNA preparation

Pichinde viruses were purified by 20% sucrose gradient ultracentrifugation at 50,000*g* for 2 h. Virus RNA was extracted with RNABee (Tel Test) according to the manufacturer's protocol.

LASV minigenome (MG) transcription assay

The full-length LASV L and NP genes (Josiah strain) were cloned into the pCAGGS vector for expression in mammalian cells. The LASV MG construct contains the T7 promoter-directed LASV S-segment-like sequences that include all the important cis-acting elements required for viral RNA synthesis (5′ UTR, intergenic region and 3′ UTR) and encode a *Renilla* luciferase (RLuc) gene in place of the viral NP coding sequence. This LASV-based LUC-encoding minigenome (MG) RNA was transcribed *in vitro* by the T7 MEGAScript kit (Ambion) and transfected into 293T cells, together with the LASV L expression plasmid, and wild-type or mutant NP expression plasmid. A β-gal expression vector was included in each transfection to normalize for cell transfection efficiency. LUC activity was determined at 24 h after transfection, normalized by β-gal activity, and shown as fold increase over a control sample that lacked the L expression plasmid. Each reaction was conducted in triplicate and in at least two independent experiments.

LAVS NP cannot degrade bound RNAs from the expression cells.

The purified NP contains RNAs from the expression cells, but the intrinsic exoribonuclease could not degrade the bound RNAs. The experiment was carried out in 20 mM Tris pH7.5, 10% glycerol, 0.3 M NaCl and 20 mM MnCl2 with two controls, one with 20 mM EDTA and no MnCl2, and another with no MnCl2. All the reactions contain 20 ul of the purified trimeric NP and were carried out in 37 degree for 1 hour. After the reactions, all the samples were added EDTA to final

concentration of 20 mM. All the samples were mixed with DNA loading buffer (Promega) and loaded on 2% agarose gel containing 0.005% EB. The electrophoresis was carried out at 100 V for 30 mins, and the gel was visualised under a UV transilluminator.

Figure 3.1:

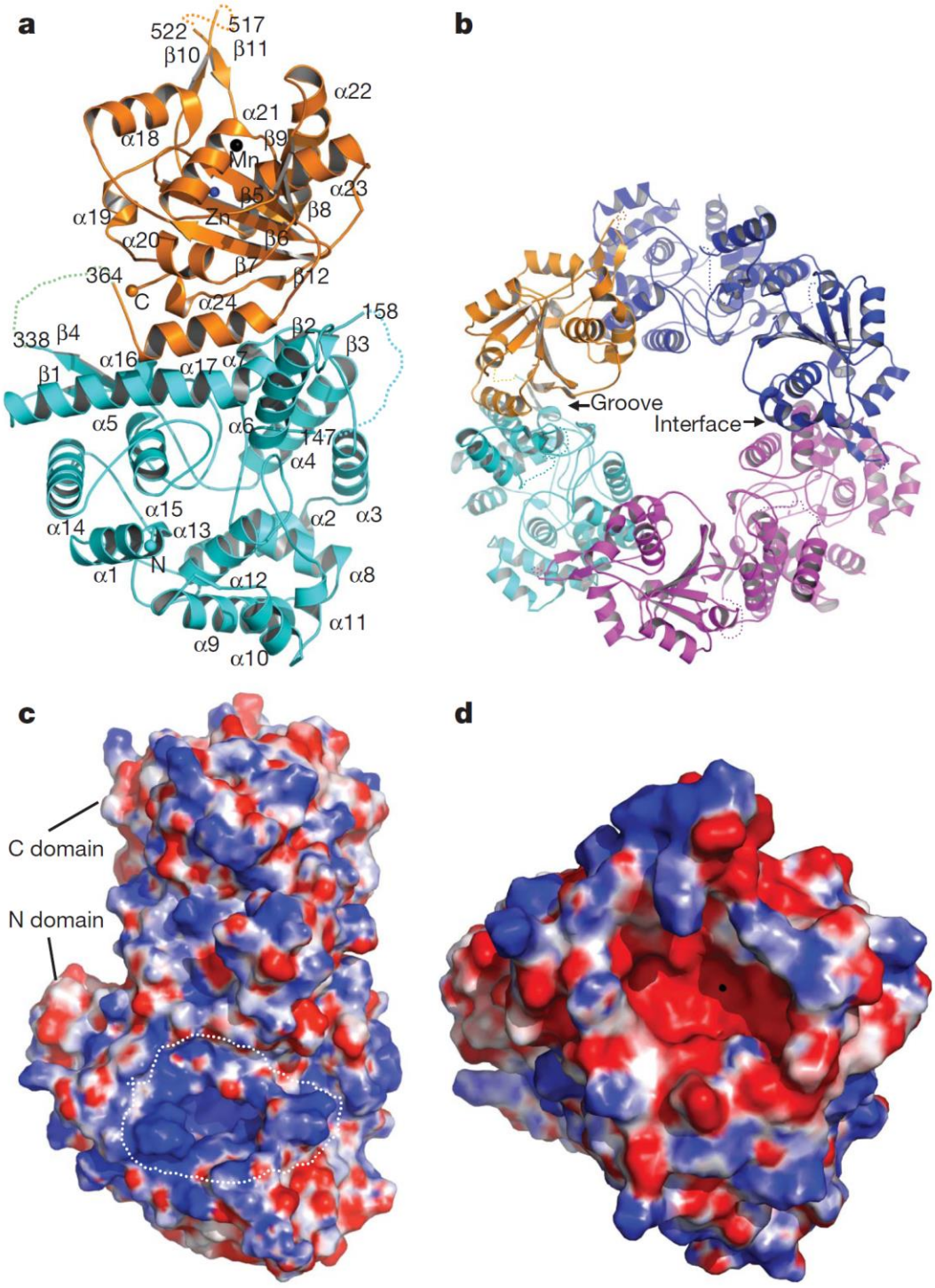
a
522
517
β10
β11
α22
α21
α18
β9
Mn
α23
β5
β8
α19
Zn
α20
β6
β7
β12
364
C
α24
158
338 β4
β2
β3
α16
α17
β1
α5
α6
147
α4
α15
α2
α3
α14
α13
N
α1
α12
α8
α11
α9
α10
b
Groove
Interface
c
C domain
N domain
d

Figure 3.2:

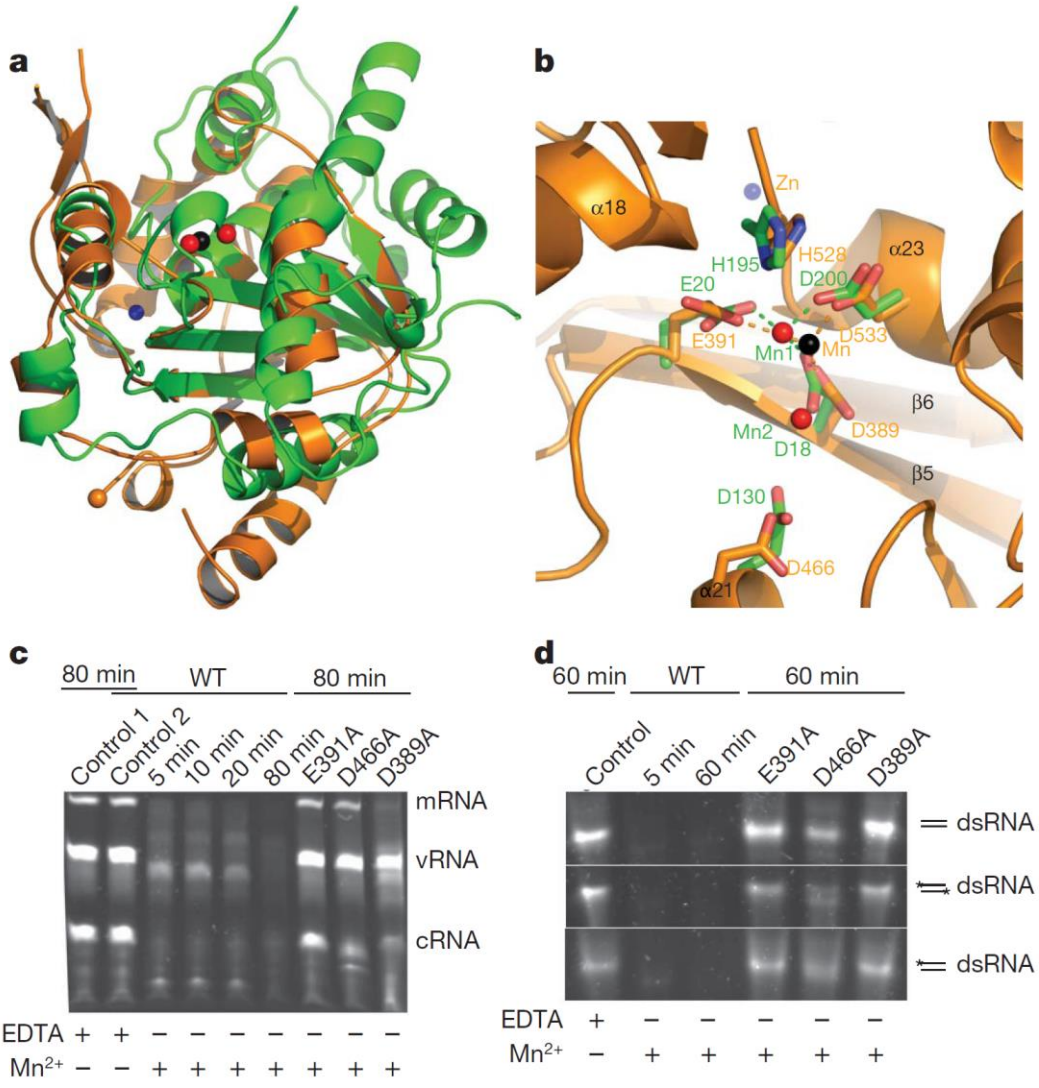
a
b
α18
Zn
H195
H528
α23
E20
D200
E391
Mn1
Mn
D533
β6
Mn2
D389
D18
β5
D130
D466
α21
c
80 min
WT
80 min
Control 1
Control 2
5 min
10 min
20 min
80 min
E391A
D466A
D389A
mRNA
vRNA
cRNA
EDTA + + − − − − − − −
Mn2+ − − + + + + + + +
d
60 min
WT
60 min
Control
5 min
60 min
E391A
D466A
D389A
dsRNA
dsRNA
dsRNA
EDTA + − − − − − −
Mn2+ − + + + + + +

Figure 3.3:

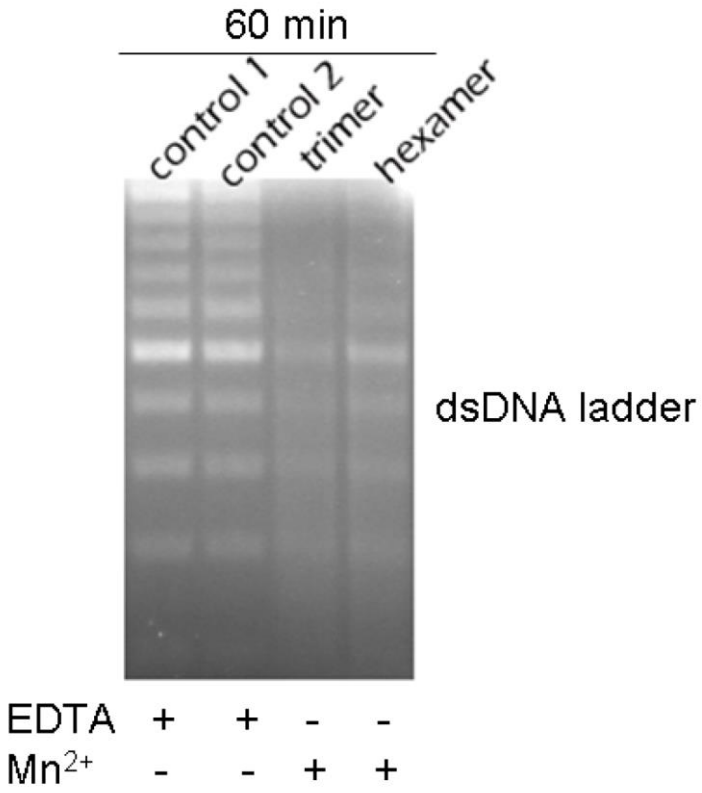
60 min
control 1
control 2
trimer
hexamer
dsDNA ladder
EDTA + + - -
Mn2+ - - + +

Figure 3.4:

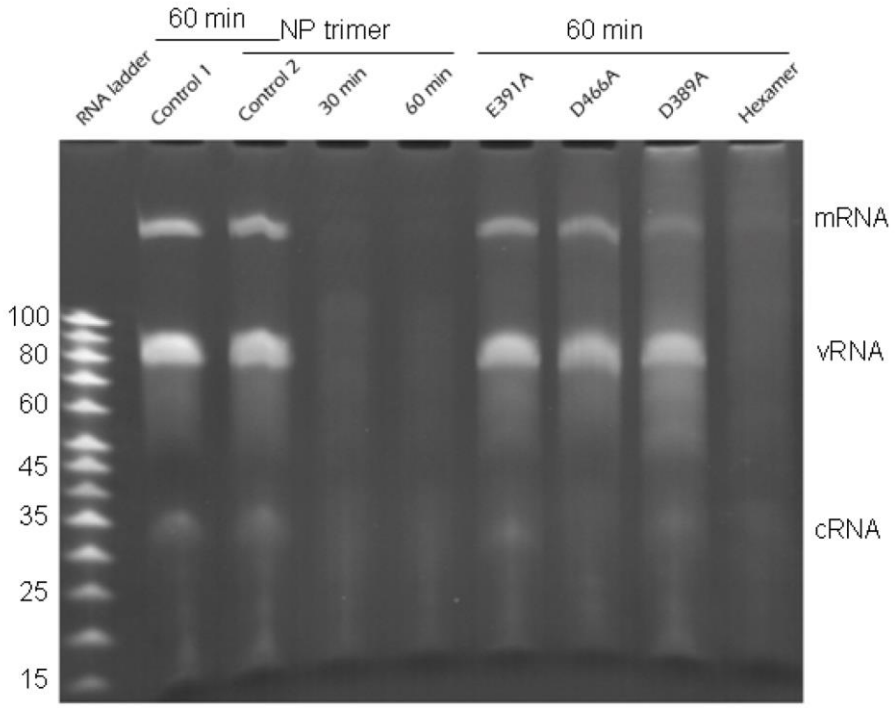
60 min
NP trimer
60 min
RNA ladder
Control 1
Control 2
30 min
60 min
E391A
D466A
D389A
Hexamer
mRNA
vRNA
cRNA
100
80
60
45
35
25
15

Figure 3.5:

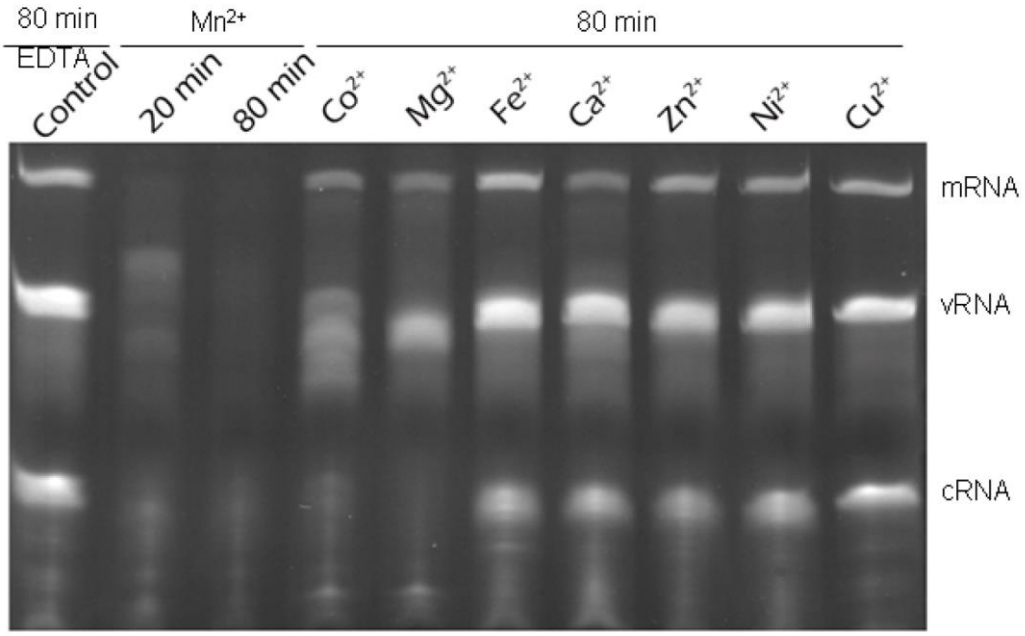
80 min
EDTA
Mn2+
80 min
Control
20 min
80 min
Co2+
Mg2+
Fe2+
Ca2+
Zn2+
Ni2+
Cu2+
mRNA
vRNA
cRNA

Figure 3.6:

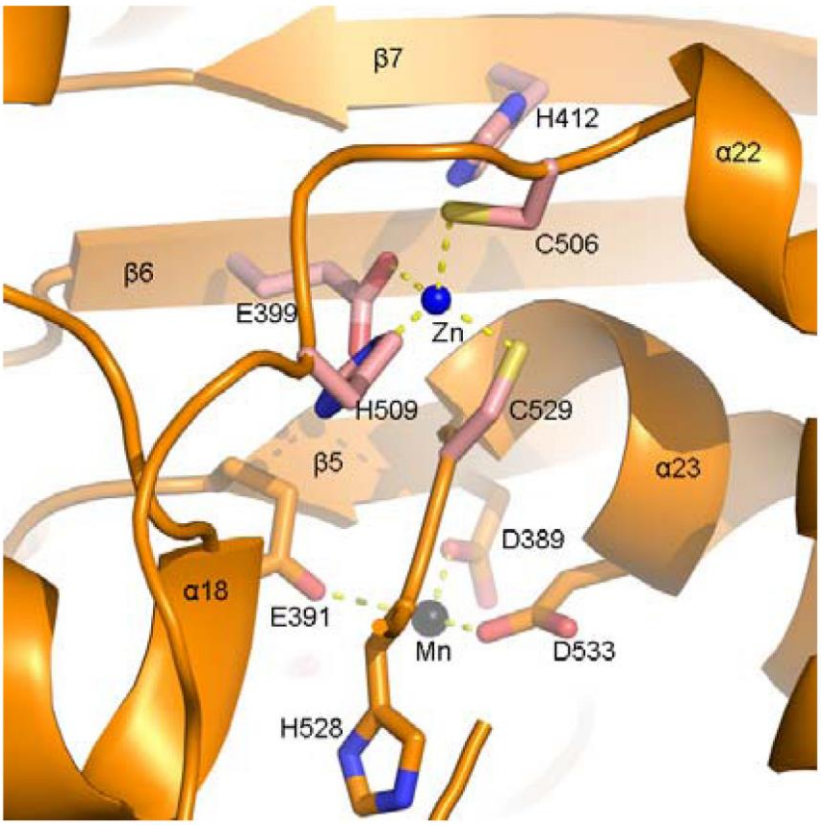
β7
H412
α22
C506
β6
E399
Zn
H509
C529
β5
α23
D389
α18
E391
Mn
D533
H528

Figure 3.7:

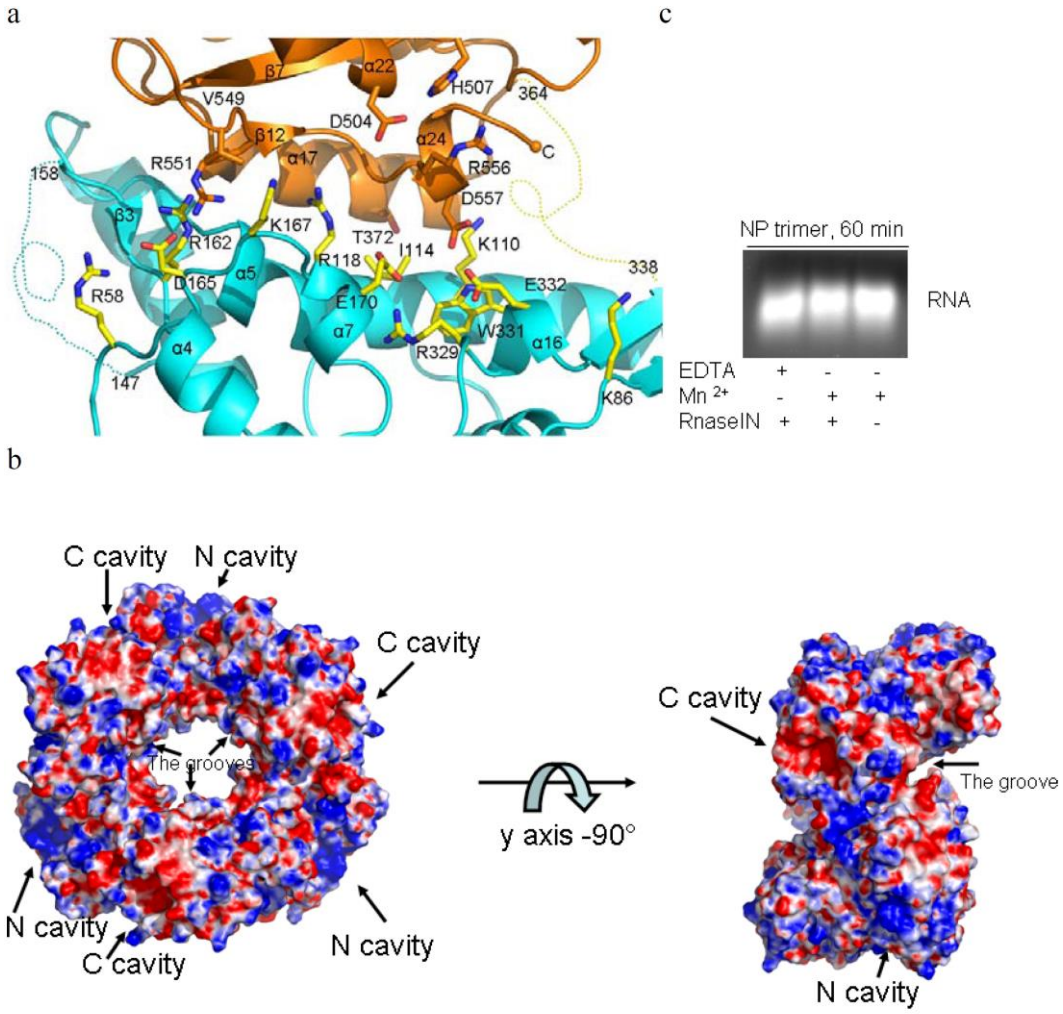
a
β7
α22
V549
H507
364
D504
β12
α24
C
R551
α17
R556
158
D557
β3
K167
T372
K110
R162
R118
I114
338
D165
α5
E332
R58
E170
α7
W331
α16
α4
R329
147
K86
c
NP trimer, 60 min
RNA
EDTA + - -
Mn 2+ - + +
RnaseIN + + -
b
C cavity
N cavity
C cavity
The grooves
N cavity
C cavity
N cavity
y axis -90°
C cavity
The groove
N cavity

Figure 3.8:

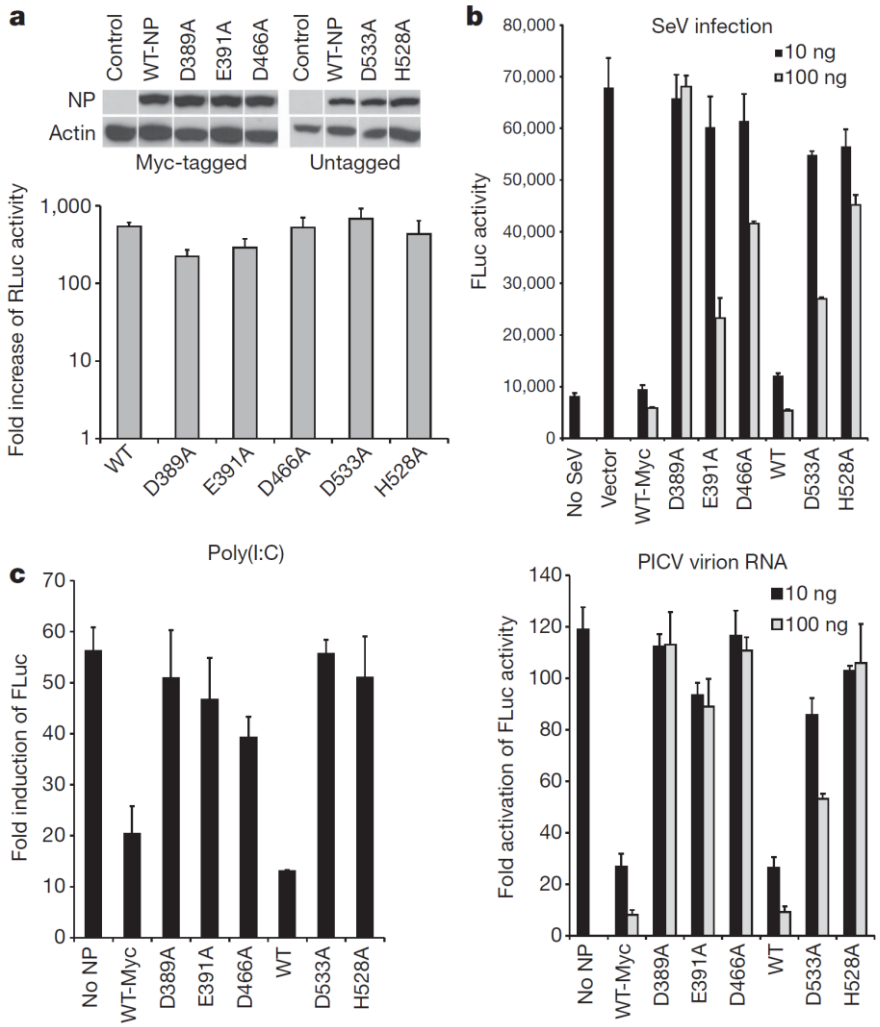
a
Control
WT-NP
D389A
E391A
D466A
Control
WT-NP
D533A
H528A
NP
Actin
Myc-tagged
Untagged
Fold increase of RLuc activity
1,000
100
10
1
WT
D389A
E391A
D466A
D533A
H528A
b
SeV infection
10 ng
100 ng
FLuc activity
80,000
70,000
60,000
50,000
40,000
30,000
20,000
10,000
0
No SeV
Vector
WT-Myc
D389A
E391A
D466A
WT
D533A
H528A
c
Poly(I:C)
Fold induction of FLuc
70
60
50
40
30
20
10
0
No NP
WT-Myc
D389A
E391A
D466A
WT
D533A
H528A
PICV virion RNA
10 ng
100 ng
Fold activation of FLuc activity
140
120
100
80
60
40
20
0
No NP
WT-Myc
D389A
E391A
D466A
WT
D533A
H528A

Figure 3.9:

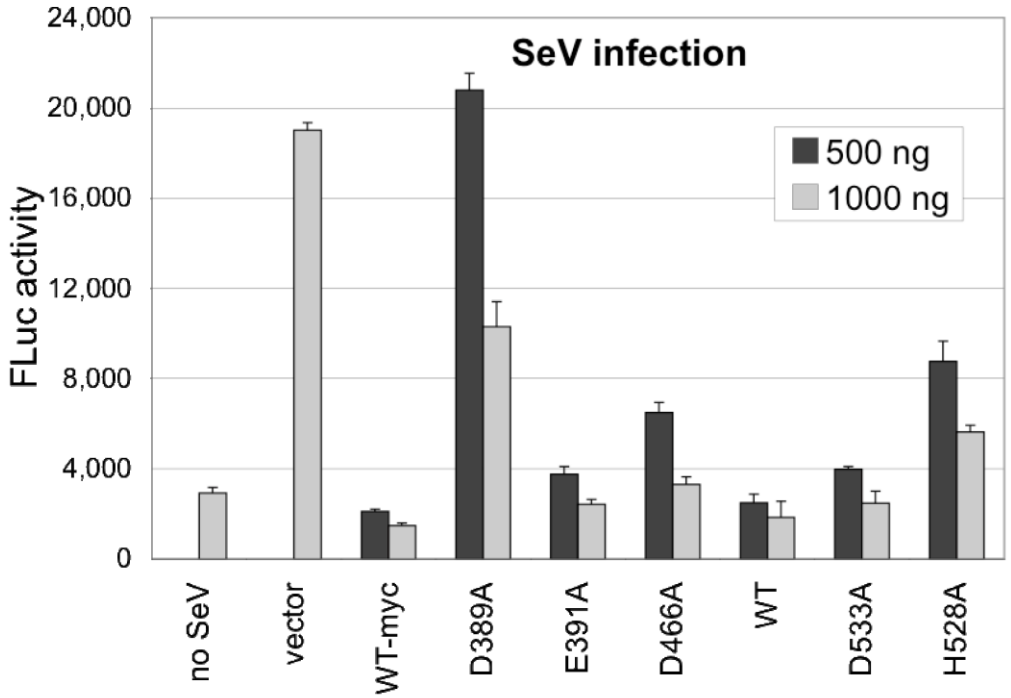
SeV infection
500 ng
1000 ng
FLuc activity
24,000
20,000
16,000
12,000
8,000
4,000
0
no SeV
vector
WT-myc
D389A
E391A
D466A
WT
D533A
H528A

Figure 3.10:

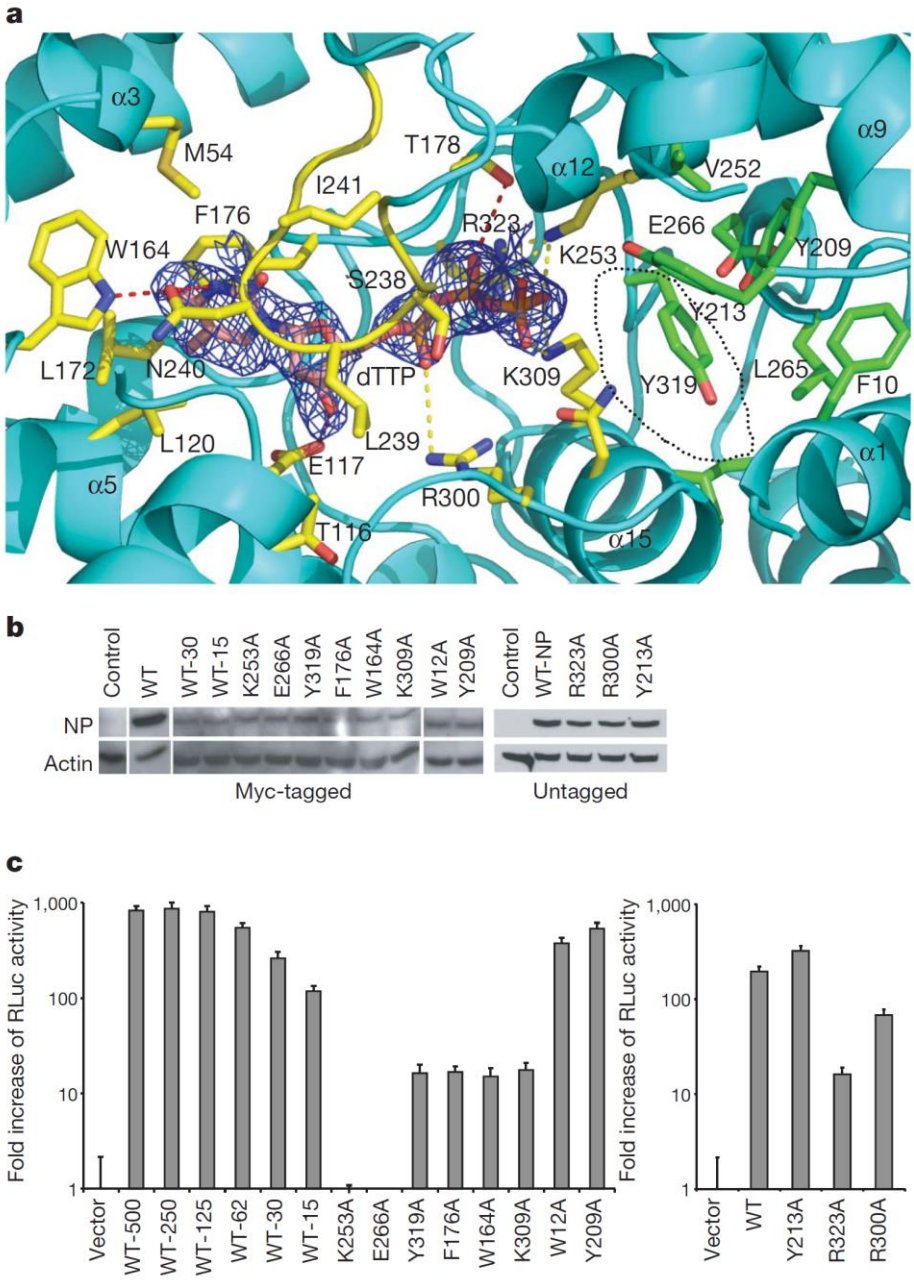
a
α3
M54
T178
α12
V252
α9
I241
F176
R323
E266
W164
K253
Y209
S238
Y213
L172
N240
dTTP
K309
Y319
L265
F10
L120
L239
α1
E117
α5
R300
T116
α15
b
Control
WT
WT-30
WT-15
K253A
E266A
Y319A
F176A
W164A
K309A
W12A
Y209A
Control
WT-NP
R323A
R300A
Y213A
NP
Actin
Myc-tagged
Untagged
c
Fold increase of RLuc activity
1,000
100
10
1
Vector
WT-500
WT-250
WT-125
WT-62
WT-30
WT-15
K253A
E266A
Y319A
F176A
W164A
K309A
W12A
Y209A
Fold increase of RLuc activity
1,000
100
10
1
Vector
WT
Y213A
R323A
R300A

Figure 3.11:

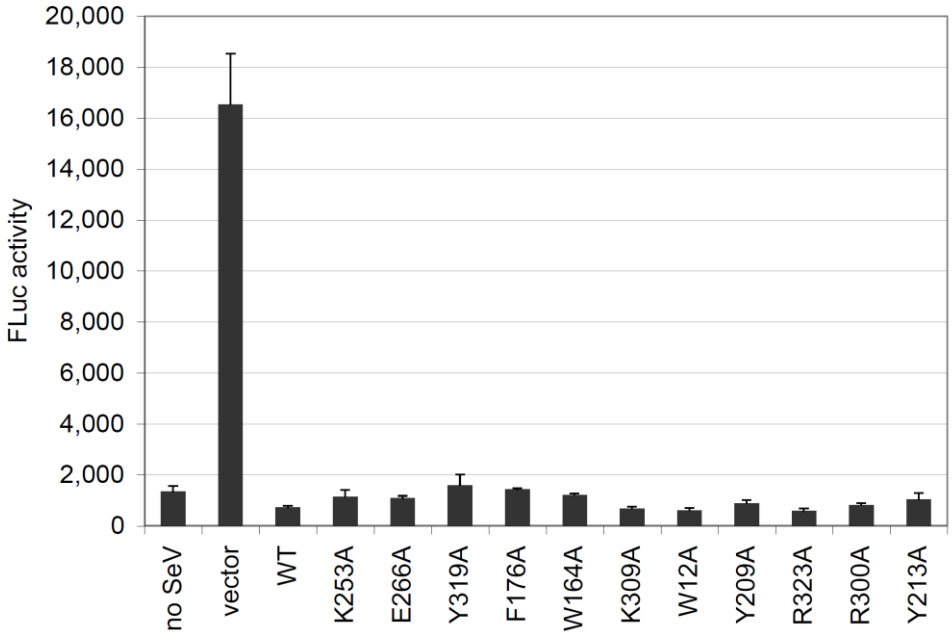
20,000
18,000
16,000
14,000
12,000
10,000
8,000
6,000
4,000
2,000
0
FLuc activity
no SeV
vector
WT
K253A
E266A
Y319A
F176A
W164A
K309A
W12A
Y209A
R323A
R300A
Y213A

Figure Legends

Figure 3.1: The crystal structure of LASV NP protein. A. Cartoon diagram of the LASV NP protomer. The N domain is in cyan with the cyan sphere indicating the N terminus; the C domain is in orange with the orange sphere indicating the C terminus. The black sphere shows $Mn2^{+}$, whereas the blue sphere shows $Zn2^{+}$. The dotted lines represent the disordered loops. **B.** The ring-shaped structure of LASV NP trimer. The first protomer is coloured as in A, the second protomer is in blue and the third is in magenta. The groove and the interface are indicated by arrows. **C**. Electrostatic surface potential map of the NP protomer. The entrance of the cap-binding cavity is shown as a white dotted circle. The blue area represents positively charged residues and the red area represents negatively charged residues. **D**. Electrostatic surface potential map of the 3'–5' exoribonuclease cavity. The black sphere represents $Mn2^{+}$.

Figure 3.2: The C domain of LASV NP is a 3'–5' exoribonuclease.

A. Superimposition of the C domain (orange) with human TREX1 protein (green) reveals a high degree of similarity between the two structures. $Mn2^{+}$ is in black in LASV NP and red in TREX1; $Zn2^{+}$ is in blue. **B**. The exonuclease catalytic residues of LASV NP and TREX1 are located in identical positions, and are shown in orange for NP and green for TREX1. **C**. The exoribunuclease activities of the wild-type (WT) and mutant LASVNP with different ssRNAs as substrates. Control 1 contains 10mM EDTA and no NP. Control 2 contains 10mM EDTA and NP. **D**. Comparison of the wild-type and NP catalytic mutants in degrading the dsRNA substrates, the 5'-hydroxyl dsRNA (top),

double 5'-triphosphorylated dsRNA (middle), and the single 5'- triphosphorylated dsRNA (bottom).

Figure 3.3: Both trimeric and hexameic forms of LASV NP degrade dsDNAs. The 1kb dsDNA ladder (Promega) was incubated at 37 °C for 1 h in the presence of 10 mM EDTA (control 1), or 10 mM EDTA together with the trimeric NP proteins (control 2), or 10 mM MnCl2 together with the trimeric NP proteins (trimer), or 10 mM MnCl2 together with the hexameric NP proteins (hexamer). The DNA ladder were separated on 1% agarose gel and visualized by ethidium bromide staining.

Figure 3.4: Both trimeric and hexameric NPs degrade ssRNAs. The three ss RNA oligos corresponding to LASV NP sequences (capped mRNA, vRNA, and cRNA) were prepared as described in the online Methods. The ssRNA substrates were incubated at 37 °C for 1 h (unless otherwise stated) with empty (no NP) control (control 1), or with WT LASV NP proteins of trimeric (trimer) or hexameric (hexamer) form, or with respective NP mutants (E391A, D466A, or D389A). Control 2 shows the ssRNA substrates incubated with the trimeric WT NP protein in the presence of 10 mM EDTA. The reactions were separated on 15% PAGE gel containing 8M urea.

Figure 3.5: The NP exonuclease activity is a divalent cation-dependent 3'-5' exoribonuclease. The three ssRNA substrates were incubated with the WT LASV NP protein at 37°C for 80 min (unless otherwise stated) in the presence of 10 mM EDTA (control) or 10 mM of the respective divalent cations.

Figure 3.6: The zinc-binding site of LASV NP. The zinc ion is coordinated by residues E399, H509, C506, and C529. The zinc ion-binding site is very close to the Mn-binding site. $Zn2^{+}$ is shown as a blue sphere and $Mn2^{+}$ in black.

Figure 3.7: LASV NP encapsidates and protects viral RNA from its exonuclease activity. A. The predicted viral genomic RNA-binding residues within the groove that is located between the N (shown in cyan) and C (shown in orange) domains. The disordered loops are shown as dotted lines. **B.** The electrostatic surface potential map of the trimeric NP structure shows that the viral genomic RNA-binding site (the groove) and the exoribonuclease active site (C cavity) are on different surfaces, indicating that the exoribonuclease catalytic sites cannot access the NP-bound viral genomic RNA. **C.** The RNAs associated with the purified trimeric NP proteins were not degraded by the NP exoribonuclease activity even under the optimal conditions for ribonuclease activity in vitro.

Figure 3.8: The exonuclease activity of NP is important for blocking the IFN induction. Results shown are the average (n53) with error bars indicating the standard deviations. **A**. The NP catalytic mutants were expressed at similar levels to the wild type in mammalian cells and had similar transcriptional activities in the LASV minigenome assay. **B**. The NP catalytic mutants were defective in suppressing the Sendai-virus (SeV)-induced IFN induction by a LUC-based IFN-β promoter assay. **C**. The NP catalytic

mutants were defective in suppressing the IFN production induced by the immunostimulatory RNAs poly(I:C) and Pichinde-virion-associated RNAs.

Figure 3.9: The ability of WT and catalytic mutants (D389A, D391A, D466A, D533A, and H528A) to suppress Sendai virus-induced IFNβ activation at high protein expression levels. Results shown are the average (n=3) with error bars indicating the standard deviations. The 293T cells were transfected with 500 or 1000 ng of control vector or each NP construct (WT or individual mutant), together with the IFNβ-LUC and β-Gal expression vectors, followed by mock infection (no SeV) or infection with Sendai virus (SeV). LUC activities were measured at 24 h post-infection and normalized by β-gal expression.

Figure 3.10: The cap-binding residues and their roles in viral RNA transcription. Results shown are the average (n53) with error bars indicating the standard deviations. **A**. A cap analogue dTTP is bound within the deep cavity of the N domain of LASV NP. Original $F_o - F_c$ map for the dTTP in blue contoured at 2.5σ. The F176 and W164 or L172 (L120) residues form a typical cap-binding sandwich structure. The middle cavity binds the triphosphate moiety and the hydrophobic cavity entrance can accommodate the second base of the cap structure. The carbon atoms are in pink for the dTTP, in yellow for the deep cavity residues and in green for the cavity entrance residues. **B.** The NP mutants were expressed at similar levels as the wild type at 15–30 ng plasmid (WT-15, WT-30) in the transfected mammalian cells. **C.** Mutational analyses of the residues

within the cap-binding cavity for the transcriptional activity using the LASV minigenome assay.

Figure 3.11: LASV NP mutants of potential cap-binding sites are functional in suppressing Sendai virus-induced IFN-beta activation. Results shown are the average (n=3) with error bars indicating the standard deviations. This result suggests that these mutations do not overly alter the NP structure or affect its IFN suppression activity.

CHAPTER 4: DISCUSSION

Arenaviruses are arguably one of the most neglected groups of tropical pathogens, and much still remains to be understood about their pathogenesis. Currently, the options for prevention and treatment of arenavirus hemorrhagic fevers are limited. The Candid#1 vaccine, which is largely effective against Argentine HF, has safety concerns, and therefore has not been approved for use by the FDA. The arenavirus responsible for the largest amount of human morbidity and mortality is LASV, and currently no vaccine is available for prevention of LASV infection, and therapy against Lassa HF is extremely limited. Additionally, the mechanism by which arenaviruses cause severe HF is poorly understood. Therefore, understanding the pathological mechanisms of these viruses is critical to the development of novel treatment options and vaccines. By studying the viral biology and determining which viral components are responsible for generating severe disease in infected individuals, we may uncover new targets for antiviral therapy.

While there are demonstrable differences between receptor usage, immune responses, and cellular entry pathways by different arenaviruses, their genome replication strategy and structures are quite similar. They share the same genome structure, cellular targets, type I IFN suppression, and viral proteins (Z, NP, L, and GP). PICV produces a syndrome in guinea pigs that mimics the disease symptoms observed in human patients suffering from severe Lassa fever. Due to the similar genome structure and disease characteristics, PICV offers an ideal model for understanding viral pathogenesis through mutagenesis of its genome. This type of analysis allows for the determination of which viral components are responsible for the vastly different disease phenotypes observed

between the avirulent P2 and virulent P18 strains of PICV in infected guinea pigs. Likewise, sequence heterogeneity has been observed in LASV strains, and some of these have proven to be more virulent than others in animal models [252, 253].

In order to study the determinants that define the differential disease outcomes between the two strains of PICV, we first sequenced the P2 and P18 viruses. Interestingly, while these two PICV strains have such widely divergent disease phenotypes, relatively few sequence differences exist between the viral genomes. We found that while the Z proteins remain unchanged between the two strains, the L gene contains 16 nucleotide differences, 5 of which result in amino acid changes. In the S segment, 14 nucleotide differences are found within the GPC gene, with 3 resulting in amino acid changes to the glycoprotein. Additionally, a total of 19 sequence changes are located in NP, but only one of these results in a change in the protein coding sequence. With only 9 amino acid differences occurring between the P2 and P18 strains of PICV, the difference in disease phenotypes in infected guinea pigs is fairly remarkable. Because of this, this arenaviral hemorrhagic fever model provides an excellent opportunity to study which viral components can contribute to severe disease in arenaviral hemorrhagic fever. Identification of virulence determinants within the PICV genome would provide insight into the mechanisms by which arenaviruses mediate severe pathology in infected hosts.

The generation of a reverse genetics system for both the P2 and P18 PICV strains was essential for the determination of which viral genome components contribute to the pathogenesis of P18 mediated disease. Reverse genetics systems are powerful tools. They allow for the generation of recombinant viruses, and minimize the chance for the

introduction of aberrant mutations, which may accumulate over time with the passage of viruses. Moreover, they allow for convenient manipulation of the viral genome. For example, recombinant viruses with reassorted viral genomes or with targeted mutations can be easily generated using reverse genetics. This powerful system allows for mutational analysis of the P2 and P18 strains of PICV to discern what sequence changes contribute to increased disease pathogenesis.

One of the hallmarks of LASV infection in humans is the correlation between viremia and outcome. Those patients displaying high viral titers are given a poor prognosis [105, 156]. We noted a similar trend in our PICV infection model. The plaques formed by P18 virus were larger than those formed by P2, suggesting that the P18 virus likely replicated faster than P2. Indeed, we have generated *in vitro* growth curves for both P2 and P18 in different cell types and shown that P18 consistently replicates at a faster rate than the P2 virus. As expected, the recombinant viruses generated through our reverse genetics systems mimicked the growth patterns of the parental (stock) viruses. The recombinant viruses not only mirrored their respective parental virus phenotypes *in vitro* but also *in vivo*. Guinea pigs infected with P2 and rP2 experienced mild disease with mild weight loss and fever lasting 1-2 days, followed by recovery. The P18 and rP18 infected animals, on the other hand, developed severe disease with prolonged fever and dramatic weight loss that eventually reached terminal points where all of the infected animals had to be euthanized. Likewise, the P18 and rP18 infected animals developed high levels of viremia up to terminal points, while viremia was undetectable in the P2 and rP2 infected animals. The inability to detect virus in the serum of P2 and rP2 infected animals implicated very low to no replication of the

avirulent strains during the course of animal infection. However, the P2 and rP2 viruses proved replication competent *in vivo*, as determined by detection of virus in the spleens, which was quickly cleared. Once again, this further bolsters the observation that increased viral replication is a strong determinant of pathogenesis in arenavirus mediated disease.

We generated reassortant viruses expressing the L segment from P18 and the S segment from P2 as well as the reverse reassortant viruses that comprised the L segment from P2 and the S segment from P18 [257]. The expectation was that reassortant viruses bearing any of the P2 genomic segments would lose pathogenicity in the infected animals. Interestingly, both reassortant viruses were found to be highly attenuated in infected guinea pigs, indicating the both the L and S segment carry virulence factors, and that the severe disease phenotype must, in fact, be multigenic. This is not unexpected, as arenaviruses encode a small number of gene products. Because so few viral proteins are present, it follows reason that these proteins would be multifunctional, and with additional functionality comes increased opportunity for modification of disease pathogenesis. While the virulent phenotype is indeed multigenic, *in vitro* analysis of viral growth did reveal that the L segment of P18 is responsible for the faster replication rate of the more virulent virus. The reassortant virus containing the L segment of P18 in combination with the S segment of P2 displayed the faster replication rate associated with P18, while the reverse reassortant more closely mirrored the growth curve of P2 [257]. This indicates that factors within the L segment, most likely the viral polymerase, are responsible for the increased replication rate of P18. The high viral titers observed in patients with severe Lassa fever implicate the rate of viral replication as an important

factor in disease pathogenesis. Therefore, the L segment provides an intuitive target for further analysis.

In order to further narrow down which sequence changes in the L segment were responsible for increased disease severity and faster replicative potential associated with P18, we generated a series of P2/P18 fragment swapping mutations within the L segment. Through analysis of the virulence of these fragment-swapping mutants in infected guinea pigs, we were able to narrow down which section of the L segment contained the sequence changes responsible for the increased disease severity of P18. The C terminal domain of the viral polymerase contains a cluster of 4 amino acid changes between P2 and P18. In the fragment of the L segment that encodes this region of the polymerase we were able to identify a correlation with increased disease severity with P18. This fragment of the L segment also contained the Z protein sequence, as well as the IGR. However, the sequences in these regions are identical between P2 and P18, allowing us to eliminate those regions as contributors to pathogenic differences between the viral strains.

While this region also contained a number of silent nucleotide changes between P2 and P18, the sequence differences that resulted in amino acid changes within the C terminus of the L polymerase were the most likely candidates for virulence factors. Therefore, we created individual point mutations in the P18 L segment backbone and introduced these point mutations into the P18 reverse genetics system. However, when we infected guinea pigs with the recombinant mutant viruses, none of them showed the dramatic levels of attenuation observed with the fragment-swapping mutant in this

region. Therefore, we theorized that a combination of these mutations was required to attenuate the rP18 virus.

Next we generated a series of combinations of these point mutations in the P18 reverse genetics system. We found that three amino acid changes (i.e., triple mutation) were required to create a highly attenuated virus: N1906D, N1889D, and L1839V. The combination of these 3 sequence changes resulted in a highly attenuated disease phenotype in infected animals. The level of attenuation observed for the triple mutant mirrored the levels of attenuation seen in the fragment-swapping mutant in this region, suggesting that these three residues play a major role in conferring viral virulence within this region of the genome. Additionally, these mutations also resulted in a drop in the rate of virus growth *in vivo*, causing the virus to mimic the growth rate of rP2 virus rather than rP18. This implies that the drop in levels of viral replication is related to the pathogenicity of the virus, which is not unexpected given the association between levels of viremia in LASV infected patients and disease severity. Likewise, the animals infected with the triple mutant virus also demonstrated significant drops in viremia levels.

We postulated that because these mutations resided in the viral polymerase, that the slower rate of viral growth *in vitro* may be a result of slower viral genome replication. In order to test this hypothesis, we infected cells *in vitro* with the WT virus as well as with the triple mutant virus, and performed real time RT-PCR to measure the levels of RNA genome replication. We found that the rP18 virus did indeed show higher levels of genome replication than rP2, and that the triple mutant virus mirrored the genome replication levels of rP2. While statistically significant, the differences in RNA genome replication were not dramatic, indicating that a modest difference in viral genome

replication can result in a significant difference in viral growth kinetics, which may be partly responsible for the vastly different disease phenotypes noted between P2 and P18.

Similar results have been found in studies analyzing the differences in replication between LCMV Cl13 and Armstrong strains. Cl13 is able to establish a chronic infection in mice, while Armstrong results in an acute infection, which is quickly cleared. Position 1079 of the viral polymerase was found to be responsible for determining the chronicity of the disease [107]. Likewise, Cl13 replicates at a faster rate than Armstrong, and this same residue was found to be responsible for the disparity in the viral replication rates. This study also looked into the rate of intracellular RNA replication, which is also higher for Cl13, and this residue was once again implicated in the higher level of RNA replication, which was also tied to immune suppression [107]. This discovery in concert with our own findings in the PICV model support the hypothesis that polymerase mutations that result in higher levels of intracellular RNA replication result in increased viral growth kinetics, which correlate with increased disease severity in arenavirus infection. This ties in well with patient data linking high viremia levels with poor disease prognosis. Also, this serves as an example of a shared mechanism of viral pathogenesis between NW and OW arenaviruses.

Unfortunately, structural information on the arenaviral polymerase is limited. These viral polymerase proteins are extremely large (~250kD) and have proven difficult to crystallize. Based on sequence analysis, the L polymerase is predicted to contain 4 conserved domains. Domain I has been crystallized, and has been shown to contain an endonuclease activity which has been implicated in cap-snatching, a process necessary for arenaviral mRNA transcription [55]. Domain III contains the RNA-dependent RNA

polymerase, a structure which is fairly conserved among negative-strand RNA viruses [54]. However, the function of domains II and IV remain unknown, and the residues that we have identified as important to the increased pathogenicity of P18 lie within domain IV. The arenaviral polymerase has been shown to oligomerize, and this may be a requirement for transcription [260]. Possibly, domain IV may be involved in this oligomerization, which could result in different efficiencies of RNA replication among different viral strains. Studies have shown that domains III and IV at the C terminus of L may bind to the C terminus of another subunit of L. The C terminus is also capable of binding the N terminus [54]. How the oligomerization conformations are involved in the function of the L polymerase is not yet understood. Alternatively, the residues we have identified in this study may be involved in some unknown function of L. Arenaviruses have very few viral gene products, therefore necessitating their ability to carry out multiple functions. The viral polymerase likely contains functions that are as of yet undiscovered. However, based on our data and the location of the residues that are implicated in increased genome transcription, we hypothesize that domain IV may be involved in increased polymerase processivity.

While our data indicates that the residues we have identified in the L polymerase show the most significant contribution to the increased disease severity of P18, these residues are not the only factors involved in this phenotype. As previously mentioned, protein determinants encoded on the S segment have also been implicated in viral pathogenicity. Other studies from our lab have shown that a change in the residue at position 140 of the GPC protein sequence contributes to increased efficiency of viral entry noted for P18, which is partially responsible for the increased pathogenicity of P18

[96]. Likewise, the single amino acid change in the NP protein also seems to contribute to this phenotype (our unpublished data).

As mutations in viral glycoprotein can alter receptor binding, they have been implicated in contributing to increased disease pathogenesis. The New World arenaviruses that are responsible for causing human hemorrhagic fever use the human TfR1 as the cellular receptor [47], and those that are apathogenic bind to TfR1 orthologs, but cannot mediate entry via hTfR1 [48]. Likewise, LCMV Cl13 demonstrates high affinity for αDG, the cellular receptor for OW arenaviruses. The binding affinity is high enough that the glycoprotein of Cl13 is able to displace laminin, the natural ligand for αDG. Conversely, LCMV Armstrong, which causes an acute infection rather than chronic, is unable to displace laminin [30, 87, 88].

Similarly, studies from our lab have shown that cellular entry by PICV P18 is more efficient than P2. The 3 nucleotide differences within the GPC gene that result in amino acid changes are located within the GP-1 subunit of the glycoprotein. GP-1 is the globular domain, which forms the receptor-binding site and is highly variable among arenaviruses. While all 3 sequence differences between P2 and P18 in the GPC gene appear to contribute to this increased efficiency, GPC 140 appears to be the critical mediator of this phenomenon [96]. Again, this mechanism correlates well with viral virulence in infected guinea pigs. Using the P18 reverse genetics system to change a single residue at position 140 to the corresponding residue of P2 (E140K) has resulted in an attenuated disease phenotype [96].

Unlike the sequence variation observed for GP-1, the arenaviral NP is highly conserved. Only one protein coding sequence change at position 374 was found between

P2 and P18, and it is located in a conserved domain of the protein, although the residue (374) is itself not conserved among arenaviruses. NP is critically involved in viral RNA replication as it encapsidates the viral genome. Additionally, NP is involved in suppression of innate immune signaling through inhibition of type I IFN. Therefore, any sequence changes in NP may have implications for disease pathogenesis. However, we found that both P2 NP and P18 NP efficiently inhibited IFNβ production, suggesting that the ability to inhibit type I IFN does not greatly contribute to the difference in disease severity noted between P2 and P18 PICV infection. Also, this residue does not map to the exoribonuclease domain of the protein (discussed further below), further suggesting that the contribution of PICV NP to the differential disease pathogenesis of P2 and P18 is likely not related to IFN inhibition. The role that this residue plays has yet to be determined, but one possibility is that it may be involved in modulating the rate of viral RNA transcription.

Preliminary data testing the effects of introducing the P2 residue at position 374 of NP into the P18 reverse genetics system show that this virus is in fact attenuated (data not shown). However, the levels of attenuation for the NP as well as GPC targeted mutants are not as dramatic as those seen for the triple mutant in the L polymerase described previously. This suggests that the efficiency of the L polymerase in viral replication as well as the rate of viral replication are the major contributors to PICV virulence. Additionally, changes in the GPC and NP proteins contribute to increased pathogenicity.

One of the hallmarks of LASV hemorrhagic fever is the generalized immune suppression observed in infected patients. The interplay of the viral infection and

immune response has yet to be worked out, but an important factor that seems to be involved is the viral NP. Arenaviral NPs are capable of inhibiting type I IFN production [99]. Through collaboration with Dr. Changjiang Dong's laboratory in England, we were able to elucidate the 3 dimensional structure of the LASV NP protein and to identify the domain within this protein that is responsible for IFNβ inhibition.

Interestingly, the crystal structure revealed a domain in the C terminus of the LASV NP protein that resembled other known 3'-5'exonucleases. The active site of LASV NP superimposed well with the active site of TREX1, a human 3'-5' exonuclease involved in degrading DNA during apoptosis [281, 286-289]. Information from the crystal structure allowed us to generate targeted mutations in this domain and to confirm that this region contained bona fide exoribonuclease enzymatic activity in vitro. The same NP mutants that abrogated exonuclease activity also prevented NP from inhibiting IFNβ production, as demonstrated by an *in vitro* IFNβ-promoter directed luciferase reporter assay. Mutations in this region, however, did not affect the ability of NP to support viral RNA transcription as shown by LASV minireplicon assay. Taken together, these data suggest that the mechanism by which LASV NP inhibits type I IFN is through digestion of dsRNA substrates that can function as pathogen-associated molecular patterns (PAMPs) and thus preventing recognition of virus infection by the pathogen recognition receptors (PRRs), which would otherwise stimulate type I IFN production. This is a novel mechanism for IFN inhibition by a viral protein. The TREX1 protein works in a similar fashion by degrading DNA fragments that accumulate during apoptosis. Natural TREX1 mutants that lack this exonuclease activity lead to persistent IFN production that results in autoimmune disease [281, 286-289]. It is important to note

that NP has also been implicated in binding cellular IKKε, to inhibit IRF3 phosphorylation and thereby inhibiting its nuclear translocation [100]. The same study also shows that mutation of the same residues in the exoribonuclease active site was able to abrogate this NP-IKKε interaction [100].

The idea of a virus degrading PAMPs that may consist of its own RNA seems counterintuitive. The virus must generate new viral RNAs in order to produce progeny virion particles. The crystal structure also identified putative RNA binding grooves within the ring structure of the NP trimers. The RNA binding grooves are located at the interior of the trimeric ring, while the exonuclease domain is positioned exteriorly. These grooves may provide protection for the viral RNA genomes from degradation by the NP's exoribonuclease function.

In addition to its role in type I IFN inhibition, arenaviral NP plays an important role in viral RNA transcription. It encapsidates the genome, and in conjunction with the L polymerase, is a necessary trans-acting factor required for transcription [51]. Arenaviral NPs are known to utilize a cap-snatching mechanism to generate primers for viral mRNA transcription [56], and the crystal structure revealed a putative cap binding domain in the N-terminus of the LASV NP protein. However, domain I located in the N terminus of the L polymerase has been shown to contain endonuclease activity, which is likely responsible for cleaving the cellular mRNA transcript from the cap structure. Mutation of residues in the putative cap-binding pocket of NP result in reduced RNA transcription, as demonstrated in a LASV minireplicon reporter assay. This supports the model in which NP binds the cap structure, whereas the endonuclease domain of the L polymerase cleaves the cap structure and uses it to prime viral mRNA transcription.

Taken together, this body of work consists of a detailed mutational analysis of the viral factors in order to determine the virulence mechanisms of arenavirus infection. The arenaviral proteins exhibit impressive multifunctionality, which is not unexpected given the limited number of viral gene products encoded on the viral bi-segmented genome. With this multifunctionality, it follows that the pathological mechanisms of the virus is also multigenic, as additional protein functions offer additional opportunities for increased viral replication efficiency and/or interactions with the host antiviral mechanisms. Identification of the residues and structures involved in mediating viral virulence is critical for not only understanding the viral biology but for the generation of new vaccines and therapeutics to combat deadly human arenaviral hemorrhagic fever.

REFERENCES

[1] McLay L, Ansari A, Liang Y and Ly H. Targeting virulence mechanisms for the prevention and therapy of arenaviral hemorrhagic fever. Antiviral Research 2013; 97: 81-92.

[2] Maiztegui JI, McKee KT, Oro JGB, Harrison LH, Gibbs PH, Feuillade MR, Enria DA, Briggiler AM, Levis SC, Ambrosio AM, Halsey NA, Peters CJ and Group tAS. Protective Efficacy of a Live Attenuated Vaccine against Argentine Hemorrhagic Fever. Journal of Infectious Diseases 1998; 177: 277-283.

[3] Gunther S and Lenz O. Lassa Virus. Crit Rev Clin Lab Sci 2004; 41: 339-390.

[4] McCormick JB. Lassa Fever. In: Saluzzo JF, Dodet B, editors. Emergence and control of rodent-borne viral diseases. Elsevier; 1999. p. 177-195.

[5] Moraz M-L and Kunz S. Pathogenesis of arenavirus hemorrhagic fevers. Expert Review of Anti-infective Therapy 2010; 9: 49-59.

[6] Cummins D MJBBD and et al. Acute sensorineural deafness in lassa fever. JAMA: The Journal of the American Medical Association 1990; 264: 2093-2096.

[7] Briese T, Paweska JT, McMullan LK, Hutchison SK, Street C, Palacios G, Khristova ML, Weyer J, Swanepoel R, Egholm M, Nichol ST and Lipkin WI. Genetic Detection and Characterization of Lujo Virus, a New Hemorrhagic Fever–Associated Arenavirus from Southern Africa. PLoS Pathog 2009; 5: e1000455.

[8] Paweska JT, Sewlall NH, Ksiazek TG, Blumberg LH, Hale MJ, Lipkin WI, Weyer J, Nichol ST, Rollin PE, McMullan LK, Paddock CD, Briese T, Mnyaluza

J, Dinh T-H, Mukonka V, Ching P, Duse A, Richards G, Jong Gd, Cohen C, Ikalafeng B, Mugero C, Asomugha C, Malotle MM, Nteo DM, Misiani E, Swanepoel R, Zaki SR and Team OCaI. Nosocomial outbreak of novel arenavirus infection, southern Africa. Emerging Infectious Disease 2009; 15: 1598-1602.

[9] Al-Zein N, Boyce TG, Correa AG and Rodriguez V. Meningitis Caused by Lymphocytic Choriomeningitis Virus in a Patient With Leukemia. Journal of Pediatric Hematology/Oncology 2008; 30: 781-784 710.1097/MPH.1090b1013e318182e318172b.

[10] Fischer SA, Graham MB, Kuehnert MJ, Kotton CN, Srinivasan A, Marty FM, Comer JA, Guarner J, Paddock CD, DeMeo DL, Shieh W-J, Erickson BR, Bandy U, DeMaria A, Davis JP, Delmonico FL, Pavlin B, Likos A, Vincent MJ, Sealy TK, Goldsmith CS, Jernigan DB, Rollin PE, Packard MM, Patel M, Rowland C, Helfand RF, Nichol ST, Fishman JA, Ksiazek T and Zaki SR. Transmission of Lymphocytic Choriomeningitis Virus by Organ Transplantation. New England Journal of Medicine 2006; 354: 2235-2249.

[11] MacNeil A, Stroher U, Farnon E, Campbell S, Cannon D, Paddock CD, Drew CP, Kuehnert M, Knust B, Gruenenfelder R, Zaki SR, Rollin PE, Nichol ST and team LTI. Solid organ transplant-associated lymphocytic choriomeningitis, United States, 2011. Emerging Infectious Disease 2012; 18: 1256-1262.

[12] Prevention CfDCa. Brief Report: lymphocytic choriomeningitis virus transmitted through solid organ transplantation - Massachussetts, 2008. MMWR Morb Mortal Wkly Rep 2008; 57: 799-801.

[13] Peters CJ. Lymphocytic Choriomeningitis Virus — An Old Enemy up to New Tricks. New England Journal of Medicine 2006; 354: 2208-2211.

[14] Rousseau MC, Saron MF, Brouqui P and Bourgeade A. Lymphocytic choriomeningitis virus in southern France: Four case reports and a review of the literature. European Journal of Epidemiology 1997; 13: 817-823.

[15] Bonthius DJ. Lymphocytic Choriomeningitis Virus: An Underrecognized Cause of Neurologic Disease in the Fetus, Child, and Adult. Seminars in Pediatric Neurology 2012; 19: 89-95.

[16] Wright R, Johnson D, Neumann M, Ksiazek TG, Rollin P, Keech RV, Bonthius DJ, Hitchon P, Grose CF, Bell WE and Bale JF. Congenital Lymphocytic Choriomeningitis Virus Syndrome: A Disease That Mimics Congenital Toxoplasmosis or Cytomegalovirus Infection. Pediatrics 1997; 100: e9.

[17] Delgado S, Erickson BR, Agudo R, Blair PJ, Vallejo E, Albariño CG, Vargas J, Comer JA, Rollin PE, Ksiazek TG, Olson JG and Nichol ST. Chapare Virus, a Newly Discovered Arenavirus Isolated from a Fatal Hemorrhagic Fever Case in Bolivia. PLoS Pathog 2008; 4: e1000047.

[18] Lisieux T, Coimbra M, Nassar ES, Burattini MN, Souza LTMd, Ferreira IB, Rocco IM, Rosa APATd, Vasconcelos PFC, Pinheiro FP, LeDuc JW, Rico-Hesse R, Gonzalez J-P, Jahrling PB and Tesh RB. New arenavirus isolated in Brazil. Lancet 1994; 343: 391-392.

[19] Aguilar PV, Camargo W, Vargas J, Guevara C, Roca Y, Felices V, Laguna-Torres VA, Tesh R, Ksiazek TG and Kochel TJ. Reemergence of Bolivian hemorrhagic fever, 2007-2008. Emerging Infectious Disease 2009; 15: 1526-1528.

[20] Ambrosio A, Saavedra M, Mariani M, Gamboa G and Maiza A. Argentine hemorrhagic fever vaccines. Human Vaccines 2011; 7: 694-700.

[21] Charrel RN and Lamballerie Xd. Arenaviruses other than Lassa virus. Antiviral Research 2003; 57: 89-100.

[22] Enria DA, Briggiler AM and Sánchez Z. Treatment of Argentine hemorrhagic fever. Antiviral Research 2008; 78: 132-139.

[23] Fulhorst CF, Cajimat MNB, Milazzo ML, Paredes H, de Manzione NMC, Salas RA, Rollin PE and Ksiazek TG. Genetic diversity between and within the arenavirus species indigenous to western Venezuela. Virology 2008; 378: 205-213.

[24] Harrison LH, Halsey NA, McKee KT, Peters CJ, Barrera Oro JG, Briggiler AM, Feuillade MR and Maiztegui JI. Clinical Case Definitions for Argentine Hemorrhagic Fever. Clinical Infectious Diseases 1999; 28: 1091-1094.

[25] Manzione Nd, Salas RA, Paredes H, Godoy O, Rojas L, Araoz F, Fulhorst CF, Ksiazek TG, Mills JN, Ellis BA, Peters CJ and Tesh RB. Venezuelan Hemorrhagic Fever: Clinical and Epidemiological Studies of 165 Cases. Clinical Infectious Diseases 1998; 26: 308-313.

[26] Pfau CJ. Arenaviruses. In: Baron S, editors. Medical Microbiology. 4th. Galveston, TX: The University of Texas Medical Branch at Galveston; 1996. p.

[27] Pinschewer DD, Perez M and de la Torre JC. Dual Role of the Lymphocytic Choriomeningitis Virus Intergenic Region in Transcription Termination and Virus Propagation. Journal of Virology 2005; 79: 4519-4526.

[28] Perez M and de la Torre JC. Characterization of the Genomic Promoter of the Prototypic Arenavirus Lymphocytic Choriomeningitis Virus. Journal of Virology 2003; 77: 1184-1194.

[29] Cao W, Henry M, Borrow P, Yamada H, Elder J, Ravkov E, Nichol S, Compans R, Campbell K and Oldstone M. Identification of alpha-dystroglycan as a receptor for lymphocytic choriomeningitis virus and Lassa fever virus. Science 1998; 282: 2079-2081.

[30] Kunz S, Sevilla N, McGavern DB, Campbell KP and Oldstone MBA. Molecular analysis of the interaction of LCMV with its cellular receptor α-dystroglycan. The Journal of Cell Biology 2001; 155: 301-310.

[31] Spiropoulou CF, Kunz S, Rollin PE, Campbell KP and Oldstone MBA. New World Arenavirus Clade C, but Not Clade A and B Viruses, Utilizes α-Dystroglycan as Its Major Receptor. Journal of Virology 2002; 76: 5140-5146.

[32] Sevilla N, Kunz S, Holz A, Lewicki H, Homann D, Yamada H, Campbell KP, de la Torre JC and Oldstone MBA. Immunosuppression and Resultant Viral Persistence by Specific Viral Targeting of Dendritic Cells. The Journal of Experimental Medicine 2000; 192: 1249-1260.

[33] Rojek JM, Moraz M-L, Pythoud C, Rothenberger S, Van der Goot FG, Campbell KP and Kunz S. Binding of Lassa virus perturbs extracellular matrix-induced signal transduction via dystroglycan. Cellular Microbiology 2012; 14: 1122-1134.

[34] Inamori K-i, Yoshida-Moriguchi T, Hara Y, Anderson ME, Yu L and Campbell KP. Dystroglycan Function Requires Xylosyl- and Glucuronyltransferase Activities of LARGE. Science 2012; 335: 93-96.

[35] Kunz S, Rojek JM, Kanagawa M, Spiropoulou CF, Barresi R, Campbell KP and Oldstone MBA. Posttranslational Modification of α-Dystroglycan, the Cellular Receptor for Arenaviruses, by the Glycosyltransferase LARGE Is Critical for Virus Binding. Journal of Virology 2005; 79: 14282-14296.

[36] Rojek JM, Spiropoulou CF, Campbell KP and Kunz S. Old World and Clade C New World Arenaviruses Mimic the Molecular Mechanism of Receptor Recognition Used by α-Dystroglycan's Host-Derived Ligands. Journal of Virology 2007; 81: 5685-5695.

[37] Imperiali M, Spörri R, Hewitt J and Oxenius A. Post-translational modification of α-dystroglycan is not critical for lymphocytic choriomeningitis virus receptor function in vivo. Journal of General Virology 2008; 89: 2713-2722.

[38] Shimojima M, Ströher U, Ebihara H, Feldmann H and Kawaoka Y. Identification of Cell Surface Molecules Involved in Dystroglycan-Independent Lassa Virus Cell Entry. Journal of Virology 2012; 86: 2067-2078.

[39] Bedossa P, Ferlicot S, Paradis V, Dargere D, Bonvoust F and Vidaud M. Dystroglycan Expression in Hepatic Stellate Cells: Role in Liver Fibrosis. Lab Invest 2002; 82: 1053-1061.

[40] Walker DH, McCormick JB, Johnson KM, Webb PA, Komba-Kono G, Elliot LH and Gardner JJ. Pathologic and virologic study of fatal Lassa fever in man. Am J Pathol 1982; 107: 249-356.

[41] Yamamoto T, Kato Y, Karita M, Kawaguchi M, Shibata N and Kobayashi M. Expression of genes related to muscular dystrophy with lissencephaly. Pediatric Neurology 2004; 31: 183-190.

[42] Alvarez CP, Lasala F, Carrillo J, Muñiz O, Corbí AL and Delgado R. C-Type Lectins DC-SIGN and L-SIGN Mediate Cellular Entry by Ebola Virus in cis and in trans. Journal of Virology 2002; 76: 6841-6844.

[43] Brindley MA, Hunt CL, Kondratowicz AS, Bowman J, Sinn PL, McCray Jr PB, Quinn K, Weller ML, Chiorini JA and Maury W. Tyrosine kinase receptor Axl enhances entry of Zaire ebolavirus without direct interactions with the viral glycoprotein. Virology 2011; 415: 83-94.

[44] Gramberg T, Hofmann H, Möller P, Lalor PF, Marzi A, Geier M, Krumbiegel M, Winkler T, Kirchhoff F, Adams DH, Becker S, Münch J and Pöhlmann S. LSECtin interacts with filovirus glycoproteins and the spike protein of SARS coronavirus. Virology 2005; 340: 224-236.

[45] Radoshitzky SR, Abraham J, Spiropoulou CF, Kuhn JH, Nguyen D, Li W, Nagel J, Schmidt PJ, Nunberg JH, Andrews NC, Farzan M and Choe H. Transferrin receptor 1 is a cellular receptor for New World haemorrhagic fever arenaviruses. Nature 2007; 446: 92-96.

[46] Andrews NC, Fleming MD and Levy JE. Molecular insights into mechanisms of iron transport. Current Opinion in Hematology 1999; 6: 61.

[47] Flanagan ML, Oldenburg J, Reignier T, Holt N, Hamilton GA, Martin VK and Cannon PM. New World Clade B Arenaviruses Can Use Transferrin Receptor 1 (TfR1)-Dependent and -Independent Entry Pathways, and Glycoproteins from Human Pathogenic Strains Are Associated with the Use of TfR1. Journal of Virology 2008; 82: 938-948.

[48] Abraham J, Kwong JA, Albariño CG, Lu JG, Radoshitzky SR, Salazar-Bravo J, Farzan M, Spiropoulou CF and Choe H. Host-Species Transferrin Receptor 1 Orthologs Are Cellular Receptors for Nonpathogenic New World Clade B Arenaviruses. PLoS Pathog 2009; 5: e1000358.

[49] Eschli B, Quirin K, Wepf A, Weber J, Zinkernagel R and Hengartner H. Identification of an N-Terminal Trimeric Coiled-Coil Core within Arenavirus Glycoprotein 2 Permits Assignment to Class I Viral Fusion Proteins. Journal of Virology 2006; 80: 5897-5907.

[50] Pasqual G, Rojek JM, Masin M, Chatton J-Y and Kunz S. Old World Arenaviruses Enter the Host Cell via the Multivesicular Body and Depend on the Endosomal Sorting Complex Required for Transport. PLoS Pathog 2011; 7: e1002232.

[51] Lee KJ, Novella IS, Teng MN, Oldstone MBA and de la Torre JC. NP and L Proteins of Lymphocytic Choriomeningitis Virus (LCMV) Are Sufficient for Efficient Transcription and Replication of LCMV Genomic RNA Analogs. Journal of Virology 2000; 74: 3470-3477.

[52] Vieth S, Torda AE, Asper M, Schmitz H and Günther S. Sequence analysis of L RNA of Lassa virus. Virology 2004; 318: 153-168.

[53] Hass M, Lelke M, Busch C, Becker-Ziaja B and Günther S. Mutational Evidence for a Structural Model of the Lassa Virus RNA Polymerase Domain and Identification of Two Residues, Gly1394 and Asp1395, That Are Critical for Transcription but Not Replication of the Genome. Journal of Virology 2008; 82: 10207-10217.

[54] Brunotte L, Lelke M, Hass M, Kleinsteuber K, Becker-Ziaja B and Günther S. Domain Structure of Lassa Virus L Protein. Journal of Virology 2011; 85: 324-333.

[55] Morin B, Coutard B, Lelke M, Ferron F, Kerber R, Jamal S, Frangeul A, Baronti C, Charrel R, de Lamballerie X, Vonrhein C, Lescar J, Bricogne G, Günther S and Canard B. The N-Terminal Domain of the Arenavirus L Protein Is an RNA Endonuclease Essential in mRNA Transcription. PLoS Pathog 2010; 6: e1001038.

[56] Raju R, Raju L, Hacker D, Garcin D, Compans R and Kolakofsky D. Nontemplated bases at the 5' ends of Tacaribe virus mRNAs. Virology 1990; 74: 53-59.

[57] Plotch SJ, Bouloy M, Ulmanen I and Krug RM. A unique cap(m7GpppXm)-dependent influenza virion endonuclease cleaves capped RNAs to generate the primers that initiate viral RNA transcription. Cell 1981; 23: 847-858.

[58] Jácamo R, López N, Wilda M and Franze-Fernández MT. Tacaribe Virus Z Protein Interacts with the L Polymerase Protein To Inhibit Viral RNA Synthesis. Journal of Virology 2003; 77: 10383-10393.

[59] Kerber R, Rieger T, Busch C, Flatz L, Pinschewer DD, Kümmerer BM and Günther S. Cross-Species Analysis of the Replication Complex of Old World Arenaviruses Reveals Two Nucleoprotein Sites Involved in L Protein Function. Journal of Virology 2011; 85: 12518-12528.

[60] Wilda M, Lopez N, Casabona JC and Franze-Fernandez MT. Mapping of the Tacaribe Arenavirus Z-Protein Binding Sites on the L Protein Identified both Amino Acids within the Putative Polymerase Domain and a Region at the N

Terminus of L That Are Critically Involved in Binding. Journal of Virology 2008; 82: 11454-11460.

[61] Cornu TI and de la Torre JC. RING Finger Z Protein of Lymphocytic Choriomeningitis Virus (LCMV) Inhibits Transcription and RNA Replication of an LCMV S-Segment Minigenome. Journal of Virology 2001; 75: 9415-9426.

[62] López N, Jácamo R and Franze-Fernández MaT. Transcription and RNA Replication of Tacaribe Virus Genome and Antigenome Analogs Require N and L Proteins: Z Protein Is an Inhibitor of These Processes. Journal of Virology 2001; 75: 12241-12251.

[63] Kranzusch PJ and Whelan SPJ. Arenavirus Z protein controls viral RNA synthesis by locking a polymerase–promoter complex. Proceedings of the National Academy of Sciences 2011; 108: 19743-19748.

[64] Eichler R, Lenz O, Strecker T and Garten W. Signal peptide of Lassa virus glycoprotein GP-C exhibits an unusual length. FEBS Letters 2003; 538: 203-206.

[65] York J and Nunberg JH. Distinct requirements for signal peptidase processing and function in the stable signal peptide subunit of the Junín virus envelope glycoprotein. Virology 2007; 359: 72-81.

[66] Beyer WR, Pöpplau D, Garten W, von Laer D and Lenz O. Endoproteolytic Processing of the Lymphocytic Choriomeningitis Virus Glycoprotein by the Subtilase SKI-1/S1P. Journal of Virology 2003; 77: 2866-2872.

[67] Eichler R, Lenz O, Strecker T, Eickmann M, Klenk H-D and Garten W. Identification of Lassa virus glycoprotein signal peptide as a trans-acting maturation factor. EMBO Rep 2003; 4: 1084-1088.

[68] Burri DJ, Pasqual G, Rochat C, Seidah NG, Pasquato A and Kunz S. Molecular Characterization of the Processing of Arenavirus Envelope Glycoprotein Precursors by Subtilisin Kexin Isozyme-1/Site-1 Protease. Journal of Virology 2012; 86: 4935-4946.

[69] Lenz O, ter Meulen J, Klenk H-D, Seidah NG and Garten W. The Lassa virus glycoprotein precursor GP-C is proteolytically processed by subtilase SKI-1/S1P. Proceedings of the National Academy of Sciences 2001; 98: 12701-12705.

[70] Wright KE, Spiro RC, Burns JW and Buchmeier MJ. Post-translational processing of the glycoproteins of lymphocytic choriomeningitis virus. Virology 1990; 177: 175-183.

[71] Bonhomme CJ, Capul AA, Lauron EJ, Bederka LH, Knopp KA and Buchmeier MJ. Glycosylation modulates arenavirus glycoprotein expression and function. Virology 2011; 409: 223-233.

[72] Eichler R, Lenz O, Garten W and Strecker T. The role of single N-glycans in proteolytic processing and cell surface transport of the Lassa virus glycoprotein GP-C. Virology Journal 2006; 3: 41.

[73] Messina EL, York J and Nunberg JH. Dissection of the Role of the Stable Signal Peptide of the Arenavirus Envelope Glycoprotein in Membrane Fusion. Journal of Virology 2012; 86: 6138-6145.

[74] Saunders AA, Ting JPC, Meisner J, Neuman BW, Perez M, de la Torre JC and Buchmeier MJ. Mapping the Landscape of the Lymphocytic Choriomeningitis Virus Stable Signal Peptide Reveals Novel Functional Domains. Journal of Virology 2007; 81: 5649-5657.

[75] Capul AA, Perez M, Burke E, Kunz S, Buchmeier MJ and de la Torre JC. Arenavirus Z-Glycoprotein Association Requires Z Myristoylation but Not Functional RING or Late Domains. Journal of Virology 2007; 81: 9451-9460.

[76] Perez M, Craven RC and de la Torre JC. The small RING finger protein Z drives arenavirus budding: Implications for antiviral strategies. Proceedings of the National Academy of Sciences 2003; 100: 12978-12983.

[77] Strecker T, Eichler R, Meulen Jt, Weissenhorn W, Dieter Klenk H, Garten W and Lenz O. Lassa Virus Z Protein Is a Matrix Protein Sufficient for the Release of Virus-Like Particles. Journal of Virology 2003; 77: 10700-10705.

[78] Loureiro ME, Wilda M, Levingston Macleod JM, D'Antuono A, Foscaldi S, Buslje CM and Lopez N. Molecular Determinants of Arenavirus Z Protein Homo-Oligomerization and L Polymerase Binding. Journal of Virology 2011; 85: 12304-12314.

[79] Casabona JC, Levingston Macleod JM, Loureiro ME, Gomez GA and Lopez N. The RING Domain and the L79 Residue of Z Protein Are Involved in both the Rescue of Nucleocapsids and the Incorporation of Glycoproteins into Infectious Chimeric Arenavirus-Like Particles. Journal of Virology 2009; 83: 7029-7039.

[80] Groseth A, Wolff S, Strecker T, Hoenen T and Becker S. Efficient Budding of the Tacaribe Virus Matrix Protein Z Requires the Nucleoprotein. Journal of Virology 2010; 84: 3603-3611.

[81] Levingston Macleod JM, D'Antuono A, Loureiro ME, Casabona JC, Gomez GA and Lopez N. Identification of Two Functional Domains within the Arenavirus Nucleoprotein. Journal of Virology 2011; 85: 2012-2023.

[82] Ortiz-Riaño E, Cheng BYH, de la Torre JC and Martínez-Sobrido L. The C-Terminal Region of Lymphocytic Choriomeningitis Virus Nucleoprotein Contains Distinct and Segregable Functional Domains Involved in NP-Z Interaction and Counteraction of the Type I Interferon Response. Journal of Virology 2011; 85: 13038-13048.

[83] Shtanko O, Imai M, Goto H, Lukashevich IS, Neumann G, Watanabe T and Kawaoka Y. A Role for the C Terminus of Mopeia Virus Nucleoprotein in Its Incorporation into Z Protein-Induced Virus-Like Particles. Journal of Virology 2010; 84: 5415-5422.

[84] Loureiro ME, D'Antuono A, Levingston Macleod JM and López N. Uncovering Viral Protein-Protein Interactions and their Role in Arenavirus Life Cycle. Viruses 2012; 4: 1651-1667.

[85] Shtanko O, Watanabe S, Jasenosky LD, Watanabe T and Kawaoka Y. ALIX/AIP1 Is Required for NP Incorporation into Mopeia Virus Z-Induced Virus-Like Particles. Journal of Virology 2011; 85: 3631-3641.

[86] Kentsis A, Gordon RE and Borden KLB. Self-assembly properties of a model RING domain. Proceedings of the National Academy of Sciences 2002; 99: 667-672.

[87] Sullivan BM, Emonet SF, Welch MJ, Lee AM, Campbell KP, de la Torre JC and Oldstone MB. Point mutation in the glycoprotein of lymphocytic choriomeningitis virus is necessary for receptor binding, dendritic cell infection, and long-term persistence. Proceedings of the National Academy of Sciences 2011; 108: 2969-2974.

[88] Smelt SC, Borrow P, Kunz S, Cao W, Tishon A, Lewicki H, Campbell KP and Oldstone MBA. Differences in Affinity of Binding of Lymphocytic Choriomeningitis Virus Strains to the Cellular Receptor α-Dystroglycan Correlate with Viral Tropism and Disease Kinetics. Journal of Virology 2001; 75: 448-457.

[89] Rojek JM, Campbell KP, Oldstone MBA and Kunz S. Old World Arenavirus Infection Interferes with the Expression of Functional α-Dystroglycan in the Host Cell. Molecular Biology of the Cell 2007; 18: 4493-4507.

[90] Andersen KG, Shylakhter I, Tabrizi S, Grossman SR, Happi CT and Sabeti PC. Genome-wide scans provide evidence for positive selection of genes implicated in Lassa fever. Philosophical Transactions of the Royal Society B: Biological Sciences 2012; 367: 868-877.

[91] Sabeti PC, Varilly P, Fry B, Lohmueller J, Hostetter E, Cotsapas C, Xie X, Byrne EH, McCarroll SA, Gaudet R, Schaffner SF and Lander ES. Genome-wide detection and characterization of positive selection in human populations. Nature 2007; 449: 913-918.

[92] Choe H, Jemielity S, Abraham J, Radoshitzky SR and Farzan M. Transferrin receptor 1 in the zoonosis and pathogenesis of New World hemorrhagic fever arenaviruses. Current Opinion in Microbiology 2011; 14: 476-482.

[93] Reignier T, Oldenburg J, Flanagan ML, Hamilton GA, Martin VK and Cannon PM. Receptor use by the Whitewater Arroyo virus glycoprotein. Virology 2008; 371: 439-446.

[94] Aronson J, Herzog N and Jerrells T. Pathological and virological features of arenavirus disease in guinea pigs. Comparison of two Pichinde virus strains. Am J Pathol 1994; 145: 228-235.

[95] Jahrling PB, Hesse RA, Rhoderick JB, Elwell MA and Moe JB. Pathogenesis of a Pichinde Virus Strain Adapted to Produce Lethal Infections in Guinea Pigs. Infection and Immunity 1981; 32: 872-880.

[96] Kumar N, Wang J, Lan S, Danzy S, McLay Schelde L, Seladi-Schulman J, Ly H and Liang Y. Characterization of virulence-associated determinants in the envelope glycoprotein of Pichinde virus. Virology 2012; 433: 97-103.

[97] Albariño CG, Bird BH, Chakrabarti AK, Dodd KA, Flint M, Bergeron É, White DM and Nichol ST. The Major Determinant of Attenuation in Mice of the Candid1 Vaccine for Argentine Hemorrhagic Fever Is Located in the G2 Glycoprotein Transmembrane Domain. Journal of Virology 2011; 85: 10404-10408.

[98] Droniou-Bonzom ME, Reignier T, Oldenburg JE, Cox AU, Exline CM, Rathbun JY and Cannon PM. Substitutions in the Glycoprotein (GP) of the Candid#1 Vaccine Strain of Junin Virus Increase Dependence on Human Transferrin Receptor 1 for Entry and Destabilize the Metastable Conformation of GP. Journal of Virology 2011; 85: 13457-13462.

[99] Martínez-Sobrido L, Giannakas P, Cubitt B, García-Sastre A and de la Torre JC. Differential Inhibition of Type I Interferon Induction by Arenavirus Nucleoproteins. Journal of Virology 2007; 81: 12696-12703.

[100] Pythoud C, Rodrigo WWSI, Pasqual G, Rothenberger S, Martínez-Sobrido L, de la Torre JC and Kunz S. Arenavirus Nucleoprotein Targets Interferon Regulatory Factor-Activating Kinase IKKε. Journal of Virology 2012; 86: 7728-7738.

[101] Zhou S, Cerny AM, Zacharia A, Fitzgerald KA, Kurt-Jones EA and Finberg RW. Induction and Inhibition of Type I Interferon Responses by Distinct Components of Lymphocytic Choriomeningitis Virus. Journal of Virology 2010; 84: 9452-9462.

[102] Rodrigo WWSI, Ortiz-Riaño E, Pythoud C, Kunz S, de la Torre JC and Martínez-Sobrido L. Arenavirus Nucleoproteins Prevent Activation of Nuclear Factor Kappa B. Journal of Virology 2012; 86: 8185-8197.

[103] Hastie KM, Kimberlin CR, Zandonatti MA, MacRae IJ and Saphire EO. Structure of the Lassa virus nucleoprotein reveals a dsRNA-specific 3′ to 5′ exonuclease activity essential for immune suppression. Proceedings of the National Academy of Sciences 2011; 108: 2396-2401.

[104] Qi X, Lan S, Wang W, Schelde LM, Dong H, Wallat GD, Ly H, Liang Y and Dong C. Cap binding and immune evasion revealed by Lassa nucleoprotein structure. Nature 2010; 468: 779-783.

[105] Johnson KM, McCormick JB, Webb PA, Smith ES, Elliott LH and King IJ. Clinical Virology of Lassa Fever in Hospitalized Patients. Journal of Infectious Diseases 1987; 155: 456-464.

[106] Albariño CG, Bird BH, Chakrabarti AK, Dodd KA, Erickson BR and Nichol ST. Efficient Rescue of Recombinant Lassa Virus Reveals the Influence of S Segment

Noncoding Regions on Virus Replication and Virulence. Journal of Virology 2011; 85: 4020-4024.

[107] Bergthaler A, Flatz L, Hegazy AN, Johnson S, Horvath E, Löhning M and Pinschewer DD. Viral replicative capacity is the primary determinant of lymphocytic choriomeningitis virus persistence and immunosuppression. Proceedings of the National Academy of Sciences 2010; 107: 21641-21646.

[108] Matloubian M, Kolhekar SR, Somasundaram T and Ahmed R. Molecular determinants of macrophage tropism and viral persistence: importance of single amino acid changes in the polymerase and glycoprotein of lymphocytic choriomeningitis virus. Journal of Virology 1993; 67: 7340-7349.

[109] Salomoni P, Dvorkina M and Michod D. Role of the promyelocytic leukaemia protein in cell death regulation. Cell Death and Dis 2012; 3: e247.

[110] Kentsis A, Dwyer EC, Perez JM, Sharma M, Chen A, Pan ZQ and Borden KLB. The RING domains of the promyelocytic leukemia protein PML and the arenaviral protein Z repress translation by directly inhibiting translation initiation factor eIF4E. Journal of Molecular Biology 2001; 312: 609-623.

[111] Volpon L, Osborne MJ, Capul AA, de la Torre JC and Borden KLB. Structural characterization of the Z RING-eIF4E complex reveals a distinct mode of control for eIF4E. Proceedings of the National Academy of Sciences 2010; 107: 5441-5446.

[112] Fan L, Briese T and Lipkin WI. Z Proteins of New World Arenaviruses Bind RIG-I and Interfere with Type I Interferon Induction. Journal of Virology 2010; 84: 1785-1791.

[113] Lee AM, Rojek JM, Gundersen A, Ströher U, Juteau J-M, Vaillant A and Kunz S. Inhibition of cellular entry of lymphocytic choriomeningitis virus by amphipathic DNA polymers. Virology 2008; 372: 107-117.

[114] Lee AM, Rojek JM, Spiropoulou CF, Gundersen AT, Jin W, Shaginian A, York J, Nunberg JH, Boger DL, Oldstone MBA and Kunz S. Unique Small Molecule Entry Inhibitors of Hemorrhagic Fever Arenaviruses. Journal of Biological Chemistry 2008; 283: 18734-18742.

[115] York J, Dai D, Amberg SM and Nunberg JH. pH-Induced Activation of Arenavirus Membrane Fusion Is Antagonized by Small-Molecule Inhibitors. Journal of Virology 2008; 82: 10932-10939.

[116] Cashman KA, Smith MA, Twenhafel NA, Larson RA, Jones KF, Allen Iii RD, Dai D, Chinsangaram J, Bolken TC, Hruby DE, Amberg SM, Hensley LE and Guttieri MC. Evaluation of Lassa antiviral compound ST-193 in a guinea pig model. Antiviral Research 2011; 90: 70-79.

[117] Furuta Y, Takahashi K, Shiraki K, Sakamoto K, Smee DF, Barnard DL, Gowen BB, Julander JG and Morrey JD. T-705 (favipiravir) and related compounds: Novel broad-spectrum inhibitors of RNA viral infections. Antiviral Research 2009; 82: 95-102.

[118] Mendenhall M, Russell A, Smee DF, Hall JO, Skirpstunas R, Furuta Y and Gowen BB. Effective Oral Favipiravir (T-705) Therapy Initiated after the Onset of Clinical Disease in a Model of Arenavirus Hemorrhagic Fever. PLoS Negl Trop Dis 2011; 5: e1342.

[119] Mendenhall M, Russell A, Juelich T, Messina EL, Smee DF, Freiberg AN, Holbrook MR, Furuta Y, Torre Jdl, Nunberg JH and Gowen B. T-705 (Favipiravir) inhibition of arenavirus replication in cell culture. Antimicrob Agents Chemother 2011; 55: 782-787.

[120] Moreno H, Gallego I, Sevilla N, de la Torre JC, Domingo E and Martín V. Ribavirin Can Be Mutagenic for Arenaviruses. Journal of Virology 2011; 85: 7246-7255.

[121] Neuman B, Bederka L, Stein D, Ting J, Moulton H and Buchmeier M. Development of peptide-conjugated morpholino oligomers as pan-arenavirus inhibitors. Antimicrob Agents Chemother 2011; 55: 4631-4638.

[122] Sepúlveda CS, García CC, Fascio ML, D'Accorso NB, Docampo Palacios ML, Pellón RF and Damonte EB. Inhibition of Junin virus RNA synthesis by an antiviral acridone derivative. Antiviral Research 2012; 93: 16-22.

[123] Ferron F, Decroly E, Selisko B and Canard B. The viral RNA capping machinery as a target for antiviral drugs. Antiviral Research 2012; 96: 21-31.

[124] Maisa A, Ströher U, Klenk H-D, Garten W and Strecker T. Inhibition of Lassa Virus Glycoprotein Cleavage and Multicycle Replication by Site 1 Protease-Adapted α₁-Antitrypsin Variants. PLoS Negl Trop Dis 2009; 3: e446.

[125] Rojek JM, Pasqual G, Sanchez AB, Nguyen N-T, de la Torre J-C and Kunz S. Targeting the Proteolytic Processing of the Viral Glycoprotein Precursor Is a Promising Novel Antiviral Strategy against Arenaviruses. Journal of Virology 2010; 84: 573-584.

[126] Urata S, Yun N, Pasquato A, Paessler S, Kunz S and de la Torre JC. Antiviral Activity of a Small-Molecule Inhibitor of Arenavirus Glycoprotein Processing by the Cellular Site 1 Protease. Journal of Virology 2011; 85: 795-803.

[127] Pasquato A, Rochat C, Burri DJ, Pasqual G, la Torre JCd and Kunz S. Evaluation of the anti-arenaviral activity of the subtilisin kexin isozyme-1/site-1 protease inhibitor PF-429242. Virology 2012; 423: 14-22.

[128] Artuso MC, Ellenberg PC, Scolaro LA, Damonte EB and García CC. Inhibition of Junín virus replication by small interfering RNAs. Antiviral Research 2009; 84: 31-37.

[129] Strecker T, Maisa A, Daffis S, Eichler R, Lenz O and Garten W. The role of myristoylation in the membrane association of the Lassa virus matrix protein Z. Virology Journal 2006; 3: 93.

[130] Cordo SM, Candurra NA and Damonte EB. Myristic acid analogs are inhibitors of Junin virus replication. Microbes and Infection 1999; 1: 609-614.

[131] Sepúlveda CS, García CC and Damonte EB. Inhibition of arenavirus infection by thiuram and aromatic disulfides. Antiviral Research 2010; 87: 329-337.

[132] García CC, Djavani M, Topisirovic I, Borden KLB, Salvato MS and Damonte EB. Arenavirus Z protein as an antiviral target: virus inactivation and protein oligomerization by zinc finger-reactive compounds. Journal of General Virology 2006; 87: 1217-1228.

[133] García CC, Topisirovic I, Djavani M, Borden KLB, Damonte EB and Salvato MS. An antiviral disulfide compound blocks interaction between arenavirus Z

protein and cellular promyelocytic leukemia protein. Biochemical and Biophysical Research Communications 2010; 393: 625-630.

[134] Baize S, Kaplon J, Faure C, Pannetier D, Georges-Courbot M-C and Deubel V. Lassa Virus Infection of Human Dendritic Cells and Macrophages Is Productive but Fails to Activate Cells. The Journal of Immunology 2004; 172: 2861-2869.

[135] Althage A, Odermatt B, Moskophidis D, Kündig T, Hengartner UH-RH and Zinkernagel RM. Immunosuppression by lymphocytic choriomeningitis virus infection: competent effector T and B cells but impaired antigen presentation. European Journal of Immunology 1992; 22: 1803-1812.

[136] Sevilla N, McGavern DB, Teng C, Kunz S and Oldstone MBA. Viral targeting of hematopoietic progenitors and inhibition of DC maturation as a dual strategy for immune subversion. The Journal of Clinical Investigation 2004; 113: 737-745.

[137] Brooks DG, Trifilo MJ, Edelmann KH, Teyton L, McGavern DB and Oldstone MBA. Interleukin-10 determines viral clearance or persistence in vivo. Nat Med 2006; 12: 1301-1309.

[138] Barber DL, Wherry EJ, Masopust D, Zhu B, Allison JP, Sharpe AH, Freeman GJ and Ahmed R. Restoring function in exhausted CD8 T cells during chronic viral infection. Nature 2006; 439: 682-687.

[139] Blackburn SD, Shin H, Haining WN, Zou T, Workman CJ, Polley A, Betts MR, Freeman GJ, Vignali DAA and Wherry EJ. Coregulation of CD8+ T cell exhaustion by multiple inhibitory receptors during chronic viral infection. Nat Immunol 2009; 10: 29-37.

[140] Fisher-Hoch SP, Hutwagner L, Brown B and McCormick JB. Effective Vaccine for Lassa Fever. Journal of Virology 2000; 74: 6777-6783.

[141] Pannetier D, Faure C, Georges-Courbot M-C, Deubel V and Baize S. Human Macrophages, but Not Dendritic Cells, Are Activated and Produce Alpha/Beta Interferons in Response to Mopeia Virus Infection. Journal of Virology 2004; 78: 10516-10524.

[142] Pannetier D, Reynard S, Russier M, Journeaux A, Tordo N, Deubel V and Baize S. Human Dendritic Cells Infected with the Nonpathogenic Mopeia Virus Induce Stronger T-Cell Responses than Those Infected with Lassa Virus. Journal of Virology 2011; 85: 8293-8306.

[143] Heller MV, Saavedra MC, Falcoff R, Maiztegui JI and Molinas FC. Increased Tumor Necrosis Factor-α Levels in Argentine Hemorrhagic Fever. Journal of Infectious Diseases 1992; 166: 1203-1204.

[144] Levis SC, Saavedra MC, Ceccoli C, Feuillade MR, Enria DA, Maiztequi JI and Falcoff R. Correlation between endogenous interferon and the clinical evolution of patients with Argentine hemorrhagic fever. Journal of Interferon Research 1985; 5: 383-389.

[145] Marta RF, Montero VS, Hack CE, Sturk A, Maiztegui JI and Molinas FC. Proinflammatory cytokines and elastase-alpha-1-antitrypsin in Argentine hemorrhagic fever. The American Journal of Tropical Medicine and Hygiene 1999; 60: 85-89.

[146] Groseth A, Hoenen T, Weber M, Wolff S, Herwig A, Kaufmann A and Becker S. Tacaribe Virus but Not Junin Virus Infection Induces Cytokine Release from

Primary Human Monocytes and Macrophages. PLoS Negl Trop Dis 2011; 5: e1137.

[147] Huang C, Kolokoltsova OA, Yun NE, Seregin AV, Poussard AL, Walker AG, Brasier AR, Zhao Y, Tian B, de la Torre JC and Paessler S. Junín Virus Infection Activates the Type I Interferon Pathway in a RIG-I-Dependent Manner. PLoS Negl Trop Dis 2012; 6: e1659.

[148] York J, Romanowski V, Lu M and Nunberg JH. The Signal Peptide of the Junín Arenavirus Envelope Glycoprotein Is Myristoylated and Forms an Essential Subunit of the Mature G1-G2 Complex. Journal of Virology 2004; 78: 10783-10792.

[149] Buchmeier M, Bowen M and Peters C. Arenaviridae: The Viruses and Their Replication. In: Knipe D, Howley P, editors. Field's Virology 4th. Philadelphia, PA: Lippincott-Raven Publisher; 2001. p. 1635-1668.

[150] Mills JN, Ellis BA, McKee KT, Ksiazek TG, Barrera Oro JG, Maiztegui JI, Calderon GE, Peters CJ and Childs JE. Junin Virus Activity in Rodents from Endemic and Nonendemic Loci in Central Argentina. The American Journal of Tropical Medicine and Hygiene 1991; 44: 589-597.

[151] Fulhorst CF, Bowen MD, Salas RA, De Manzione NMC, Duno G, Utrera A, Ksiazek TG, Peters CJ, Nichol ST, De Miller E, Tovar D, Ramos B, Vasquez C and Tesh RB. Isolation and Characterization of Pirital Virus, a Newly Discovered South American Arenavirus. The American Journal of Tropical Medicine and Hygiene 1997; 56: 548-553.

[152] Johnson KM, Kuns ML, Mackenzie RB, Webb PA and Yunker CE. Isolation of Machupo Virus from Wild Rodent Calomys callosus. The American Journal of Tropical Medicine and Hygiene 1966; 15: 103-106.

[153] Lukashevich IS, Clegg JCS and Sidibe K. Lassa virus activity in Guinea: Distribution of human antiviral antibody defined using enzyme-linked immunosorbent assay with recombinant antigen. Journal of Medical Virology 1993; 40: 210-217.

[154] McCormick JB, King IJ, Webb PA, Johnson KM, O'Sullivan R, Smith ES, Trippel S and Tong TC. A Case-Control Study of the Clinical Diagnosis and Course of Lassa Fever. Journal of Infectious Diseases 1987; 155: 445-455.

[155] Monath TP and Casals J. Diagnosis of Lassa fever and the isolation and management of patients. Bull World Health Organ 1975; 52: 707-715.

[156] Oldstone MBA and Campbell KP. Decoding arenavirus pathogenesis: Essential roles for alpha-dystroglycan-virus interactions and the immune response. Virology 2011; 411: 170-179.

[157] Walker D, McCormick J, Johnson K, Webb P, Komba-Kono G, Elliott L and Gardner J. Pathologic and virologic study of fatal Lassa fever in man. Am J Pathol 1982; 107: 349-356.

[158] Maiztegui JI, Laguens RP, Cossio PM, Casanova MB, de la Vega MT, Ritacco V, Segal A, Fernández NJ and Arana RM. Ultrastructural and Immunohistochemical Studies in Five Cases of Argentine Hemorrhagic Fever. Journal of Infectious Diseases 1975; 132: 35-43.

[159] Elsner B, Schwarz E, Mando OG, Maiztegui J and Vilches A. Pathology of 12 fatal cases of Argentine hemorrhagic fever. The American Journal of Tropical Medicine and Hygiene 1973; 22: 229-236.

[160] Johnson KM, Halstead SB and Cohen SN. Hemorrhagic fevers of Southeast Asia and South America: a comparative appraisal. 1967.

[161] Stinebaugh BJ, Schloeder FX, Johnson KM, Mackenzie RB, Entwisle G and De Alba E. Bolivian hemorrhagic fever: A report of four cases. The American Journal of Medicine 1966; 40: 217-230.

[162] Tesh RB, Jahrling PB, Salas R and Shope RE. Description of Guanarito Virus (Arenaviridae: Arenavirus), the Etiologic Agent of Venezuelan Hemorrhagic Fever. The American Journal of Tropical Medicine and Hygiene 1994; 50: 452-459.

[163] McCormick J and Fisher-Hoch S. Lassa Fever. Curr Top Microbiol Immunol 2002; 262: 75-109.

[164] Cummins D, Fisher-Hoch SP, Walshe KJ, Mackie IJ, McCormick JB, Bennett D, Perez G, Farrar B and Machin SJ. A plasma inhibitor of platelet aggregation in patients with Lassa fever. British Journal of Haematology 1989; 72: 543-548.

[165] Fisher-Hoch S, McCormick J, Sasso D and Craven R. Hematologic dysfunction in Lassa fever. J Med Virol 1988; 26: 127-135.

[166] Lukashevich IS, Maryankova R, Vladyko AS, Nashkevich N, Koleda S, Djavani M, Horejsh D, Voitenok NN and Salvato MS. Lassa and mopeia virus replication in human monocytes/macrophages and in endothelial cells: Different effects on IL-8 and TNF-α gene expression. Journal of Medical Virology 1999; 59: 552-560.

[167] Mahanty S, Bausch DG, Thomas RL, Goba A, Bah A, Peters CJ and Rollin PE. Low Levels of Interleukin-8 and Interferon-Inducible Protein–10 in Serum Are Associated with Fatal Infections in Acute Lassa Fever. Journal of Infectious Diseases 2001; 183: 1713-1721.

[168] Mahanty S, Hutchinson K, Agarwal S, Mcrae M, Rollin PE and Pulendran B. Cutting Edge: Impairment of Dendritic Cells and Adaptive Immunity by Ebola and Lassa Viruses. The Journal of Immunology 2003; 170: 2797-2801.

[169] Weissenbacher MC, Laquens RP and Coto CE. Argentine hemorrhagic fever. Curr Top Microbiol Immunol 1987; 134: 79-116.

[170] Andrews BS, Theofilopoulos AN, Peters CJ, Loskutoff DJ, Brandt WE and Dixon FJ. Replication of dengue and junin viruses in cultured rabbit and human endothelial cells. Infection and Immunity 1978; 20: 776-781.

[171] Gomez RM, Pozner RG, Lazzari MA, D'Atri LP, Negrotto S, Chudzinski-Tavassi AM, Berría MI and Schattner M. Endothelial cell function alteration after Junin virus infection. Thrombosis and haemostasis 2003; 90: 326-333.

[172] Molinas FC, Bracco MMEd and Maiztegui JI. Hemostasis and the Complement System in Argentine Hemorrhagic Fever. Review of Infectious Diseases 1989; 11: S762-S770.

[173] Cummins D, Molinas FC, Lerer G, Maiztegui JI, Faint R and Machin SJ. A plasma inhibitor of platelet aggregation in patients with Argentine hemorrhagic fever. The American Journal of Tropical Medicine and Hygiene 1990; 42: 470-475.

[174] de Bracco MME, Rimoldi MT, Cossio PM, Rabinovich A, Maiztegui JI, Carballal G and Arana RM. Argentine Hemorrhagic Fever. New England Journal of Medicine 1978; 299: 216-221.

[175] Heller MV, Marta RF, Sturk A, Maiztegui JI, Hack CE, Cate JW and Molinas FC. Early markers of blood coagulation and fibrinolysis activation in Argentine hemorrhagic fever. Thrombosis and haemostasis 1995; 73: 368-373.

[176] Baize S, Marianneau P, Loth P, Reynard S, Journeaux A, Chevallier M, Tordo N, Deubel V and Contamin H. Early and Strong Immune Responses Are Associated with Control of Viral Replication and Recovery in Lassa Virus-Infected Cynomolgus Monkeys. Journal of Virology 2009; 83: 5890-5903.

[177] Maiztegui J, Fernandez N and Damilano Ad. Efficacy of immune plasma in treatment of Argentine haemorrhagic fever and association between treatment and a late neurological syndrome. Lancet 1979; 2: 1216-1217.

[178] Enria DA and Maiztegui JI. Antiviral treatment of argentine hemorrhagic fever. Antiviral Research 1994; 23: 23-31.

[179] Montardit AI, Fernandez MJ, DeSensi MRF, Damilano AJ and Maiztegui JI. Neutralizacion de la viremia en enfermos de fiebre hemorragica Argentina tratados con plasma inmune. Medicina 1979; 39: 799.

[180] Enria DA, Briggiler AM, Levis S, Vallejos D, Maiztegui JI and Canonico PG. Tolerance and antiviral effect of ribavirin in patients with argentine hemorrhagic fever. Antiviral Research 1987; 7: 353-359.

[181] Vela EM, Zhang L, Colpitts TM, Davey RA and Aronson JF. Arenavirus entry occurs through a cholesterol-dependent, non-caveolar, clathrin-mediated endocytic mechanism. Virology 2007; 369: 1-11.

[182] Borrow P and Oldstone MBA. Mechanism of Lymphocytic Choriomeningitis Virus Entry into Cells. Virology 1994; 198: 1-9.

[183] Quirin K, Eschli B, Scheu I, Poort L, Kartenbeck J and Helenius A. Lymphocytic choriomeningitis virus uses a novel endocytic pathway for infectious entry via late endosomes. Virology 2008; 378: 21-33.

[184] Rojek JM, Perez M and Kunz S. Cellular Entry of Lymphocytic Choriomeningitis Virus. Journal of Virology 2008; 82: 1505-1517.

[185] Rojek JM, Sanchez AB, Nguyen NT, de la Torre J-C and Kunz S. Different Mechanisms of Cell Entry by Human-Pathogenic Old World and New World Arenaviruses. Journal of Virology 2008; 82: 7677-7687.

[186] Moraz M-L, Pythoud C, Turk R, Rothenberger S, Pasquato A, Campbell KP and Kunz S. Cell entry of Lassa virus induces tyrosine phosphorylation of dystroglycan. Cellular Microbiology 2013; n/a-n/a.

[187] Martinez MG, Cordo SM and Candurra NA. Characterization of Junín arenavirus cell entry. Journal of General Virology 2007; 88: 1776-1784.

[188] Martinez MG, Forlenza MB and Candurra NA. Involvement of cellular proteins in Junin arenavirus entry. Biotechnology Journal 2009; 4: 866-870.

[189] Marsh EW, Leopold PL, Jones NL and Maxfield FR. Oligomerized transferrin receptors are selectively retained by a lumenal sorting signal in a long-lived

endocytic recycling compartment. The Journal of Cell Biology 1995; 129: 1509-1522.

[190] Rojek JM and Kunz S. Cell entry by human pathogenic arenaviruses. Cellular Microbiology 2008; 10: 828-835.

[191] Harmon B, Kozina C, Maar D, Carpenter TS, Branda CS, Negrete OA and Carson BD. Identification of Critical Amino Acids within the Nucleoprotein of Tacaribe Virus Important for Anti-Interferon Activity. Journal of Biological Chemistry 2013;

[192] McCormick JB, Mitchell SW, Kiley MP, Ruo S and Fisher-Hoch SP. Inactivated Lassa virus elicits a non protective immune response in rhesus monkeys. J Med Virol 1992; 37: 1-7.

[193] Flatz L, Rieger T, Merkler D, Bergthaler A, Regen T, Schedensack M, Bestmann L, Verschoor A, Kreutzfeldt M, Brück W, Hanisch U-K, Günther S and Pinschewer DD. T Cell-Dependence of Lassa Fever Pathogenesis. PLoS Pathog 2010; 6: e1000836.

[194] Lukashevich IS, Carrion Jr R, Salvato MS, Mansfield K, Brasky K, Zapata J, Cairo C, Goicochea M, Hoosien GE, Ticer A, Bryant J, Davis H, Hammamieh R, Mayda M, Jett M and Patterson J. Safety, immunogenicity, and efficacy of the ML29 reassortant vaccine for Lassa fever in small non-human primates. Vaccine 2008; 26: 5246-5254.

[195] Geisbert TW, Jones S, Fritz EA, Shurtleff AC, Geisbert JB, Liebscher R, Grolla A, Ströher U, Fernando L, Daddario KM, Guttieri MC, Mothé BR, Larsen T,

Hensley LE, Jahrling PB and Feldmann H. Development of a New Vaccine for the Prevention of Lassa Fever. PLoS Med 2005; 2: e183.

[196] Bredenbeek PJ, Molenkamp R, Spaan WJM, Deubel V, Marianneau P, Salvato MS, Moshkoff D, Zapata J, Tikhonov I, Patterson J, Carrion R, Ticer A, Brasky K and Lukashevich IS. A recombinant Yellow Fever 17D vaccine expressing Lassa virus glycoproteins. Virology 2006; 345: 299-304.

[197] Jiang X, Dalebout TJ, Bredenbeek PJ, Carrion Jr R, Brasky K, Patterson J, Goicochea M, Bryant J, Salvato MS and Lukashevich IS. Yellow fever 17D-vectored vaccines expressing Lassa virus GP1 and GP2 glycoproteins provide protection against fatal disease in guinea pigs. Vaccine 2011; 29: 1248-1257.

[198] Goñi S, Iserte J, Ambrosio A, Romanowski V, Ghiringhelli P and Lozano M. Genomic Features of Attenuated Junín Virus Vaccine Strain Candidate. Virus Genes 2006; 32: 37-41.

[199] Emonet SF, Seregin AV, Yun NE, Poussard AL, Walker AG, de la Torre JC and Paessler S. Rescue from Cloned cDNAs and In Vivo Characterization of Recombinant Pathogenic Romero and Live-Attenuated Candid #1 Strains of Junin Virus, the Causative Agent of Argentine Hemorrhagic Fever Disease. Journal of Virology 2011; 85: 1473-1483.

[200] Lan S, McLay L, Aronson J, Ly H and Liang Y. Genome comparison of virulent and avirulent strains of the Pichinde arenavirus. Archives of Virology 2008; 153: 1241-1250.

[201] McCormick J, Webb P, Krebs J, Johnson K and Smith E. A prospective study of the epidemiology and ecology of Lassa Fever. Journal of Infectious Diseases 1987; 155: 437-444.

[202] Katz MA and Starr JF. Pichinde Virus Infection in Strain 13 Guinea Pigs Reduces Intestinal Protein Reflection Coefficient with Compensation. Journal of Infectious Diseases 1990; 162: 1304-1308.

[203] Connolly BM, Jenson AB, Peters CJ, Geyer SJ, Barth jF and McPherson RA. Pathogenesis of Pichinde Virus Infection in Strain 13 Guinea Pigs: an Immunocytochemical, Virologic, and Clinical Chemistry Study. The American Journal of Tropical Medicine and Hygiene 1993; 49: 10-24.

[204] Hass M, Westerkofsky M, Müller S, Becker-Ziaja B, Busch C and Günther S. Mutational Analysis of the Lassa Virus Promoter. Journal of Virology 2006; 80: 12414-12419.

[205] Wilson S and Clegg J. Sequence analysis of the S RNA of the African arenavirus Mopeia: an unusual secondary structure feature in the intergenic region. Virology 1991; 180: 543-552.

[206] Franze-Fernandez MT, Iapalucci S, Lopez N and Rossi C. Subgenomic RNAs of Tacaribe virus. New York: Plenum Press, 1993.

[207] Iapalucci S, López N and Franze-Fernández MT. The 3′ end termini of the tacaribe arenavirus subgenomic RNAs. Virology 1991; 182: 269-278.

[208] López N and Franze-Fernández MT. A single stem-loop structure in Tacaribe arenavirus intergenic region is essential for transcription termination but is not

required for a correct initiation of transcription and replication. Virus Research 2007; 124: 237-244.

[209] Pinschewer DD, Perez M and de la Torre JC. Role of the Virus Nucleoprotein in the Regulation of Lymphocytic Choriomeningitis Virus Transcription and RNA Replication. Journal of Virology 2003; 77: 3882-3887.

[210] Freed EO. The HIV–TSG101 interface: recent advances in a budding field. Trends in Microbiology 2003; 11: 56-59.

[211] Zhang L, Marriott K and Aronson JF. Sequence analysis of the small RNA segment of guinea pig-passaged Pichinde virus variants. The American Journal of Tropical Medicine and Hygiene 1999; 61: 220-225.

[212] Zhang L, Marriott KA, Harnish DG and Aronson JF. Reassortant Analysis of Guinea Pig Virulence of Pichinde Virus Variants. Virology 2001; 290: 30-38.

[213] Garcıa-Sastre A. Inhibition of Interferon-Mediated Antiviral Responses by Influenza A Viruses and Other Negative-Strand RNA Viruses. Virology 2001; 279: 375-384.

[214] Glaser L, Stevens J, Zamarin D, Wilson IA, García-Sastre A, Tumpey TM, Basler CF, Taubenberger JK and Palese P. A Single Amino Acid Substitution in 1918 Influenza Virus Hemagglutinin Changes Receptor Binding Specificity. Journal of Virology 2005; 79: 11533-11536.

[215] Rogers GN, Paulson JC, Daniels RS, Skehel JJ, Wilson IA and Wiley DC. Single amino acid substitutions in influenza haemagglutinin change receptor binding specificity. Nature 1983; 304: 76-78.

[216] Stevens J, Blixt O, Tumpey TM, Taubenberger JK, Paulson JC and Wilson IA. Structure and Receptor Specificity of the Hemagglutinin from an H5N1 Influenza Virus. Science 2006; 312: 404-410.

[217] Feldmann H, Volchkov VE, Volchkova VA and Klenk HD. The glycoproteins of Marburg and Ebola virus and their potential roles in pathogenesis. In: Calisher C, Horzinek MC, editors. 100 Years of Virology. Springer Vienna; 1999. p. 159-169.

[218] Feldmann H, Volchkov VE, Volchkova VA, Ströher U and Klenk H-D. Biosynthesis and role of filoviral glycoproteins. Journal of General Virology 2001; 82: 2839-2848.

[219] Wahl-Jensen VM, Afanasieva TA, Seebach J, Ströher U, Feldmann H and Schnittler H-J. Effects of Ebola Virus Glycoproteins on Endothelial Cell Activation and Barrier Function. Journal of Virology 2005; 79: 10442-10450.

[220] Martínez-Sobrido L, Zúñiga EI, Rosario D, García-Sastre A and de la Torre JC. Inhibition of the Type I Interferon Response by the Nucleoprotein of the Prototypic Arenavirus Lymphocytic Choriomeningitis Virus. Journal of Virology 2006; 80: 9192-9199.

[221] Eichler R, Strecker T, Kolesnikova L, ter Meulen J, Weissenhorn W, Becker S, Klenk HD, Garten W and Lenz O. Characterization of the Lassa virus matrix protein Z: electron microscopic study of virus-like particles and interaction with the nucleoprotein (NP). Virus Research 2004; 100: 249-255.

[222] Lee KJ, Perez M, Pinschewer DD and de la Torre JC. Identification of the Lymphocytic Choriomeningitis Virus (LCMV) Proteins Required To Rescue

LCMV RNA Analogs into LCMV-Like Particles. Journal of Virology 2002; 76: 6393-6397.

[223] Cornu TI and de la Torre JC. Characterization of the Arenavirus RING Finger Z Protein Regions Required for Z-Mediated Inhibition of Viral RNA Synthesis. Journal of Virology 2002; 76: 6678-6688.

[224] Garcin D, Rochat S and Kolakofsky D. The Tacaribe arenavirus small zinc finger protein is required for both mRNA synthesis and genome replication. Journal of Virology 1993; 67: 807-812.

[225] Poch O, Sauvaget I, Delarue M and Tordo N. Identification of four conserved motifs among the RNA-dependent polymerase encoding elements. The EMBO journal 1989; 8: 3867-3874.

[226] Kirk WE, Cash P, Peters CJ and Bishop DHL. Formation and Characterization of an Intertypic Lymphocytic Choriomeningitis Recombinant Virus. Journal of General Virology 1980; 51: 213-218.

[227] Riviere Y, Ahmed R, Southern PJ, Buchmeier MJ and Oldstone MB. Genetic mapping of lymphocytic choriomeningitis virus pathogenicity: virulence in guinea pigs is associated with the L RNA segment. Journal of Virology 1985; 55: 704-709.

[228] Salvato M, Borrow P, Shimomaye E and Oldstone MB. Molecular basis of viral persistence: a single amino acid change in the glycoprotein of lymphocytic choriomeningitis virus is associated with suppression of the antiviral cytotoxic T-lymphocyte response and establishment of persistence. Journal of Virology 1991; 65: 1863-1869.

[229] Hatta M, Gao P, Halfmann P and Kawaoka Y. Molecular Basis for High Virulence of Hong Kong H5N1 Influenza A Viruses. Science 2001; 293: 1840-1842.

[230] Aronson J, Herzog N and Jerrells T. Tumor necrosis factor and the pathogenesis of Pichinde virus infection in guinea pigs. Am J Trop Med Hyg 1995; 52: 262-269.

[231] Bowick GC, Fennewald SM, Elsom BL, Aronson JF, Luxon BA, Gorenstein DG and Herzog NK. Differential Signaling Networks Induced by Mild and Lethal Hemorrhagic Fever Virus Infections. Journal of Virology 2006; 80: 10248-10252.

[232] Bowick GC, Fennewald SM, Scott EP, Zhang L, Elsom BL, Aronson JF, Spratt HM, Luxon BA, Gorenstein DG and Herzog NK. Identification of Differentially Activated Cell-Signaling Networks Associated with Pichinde Virus Pathogenesis by Using Systems Kinomics. Journal of Virology 2007; 81: 1923-1933.

[233] Fennewald SM, Aronson JF, Zhang L and Herzog NK. Alterations in NF-κB and RBP-Jκ by Arenavirus Infection of Macrophages In Vitro and In Vivo. Journal of Virology 2002; 76: 1154-1162.

[234] Lan S, McLay Schelde L, Wang J, Kumar N, Ly H and Liang Y. Development of Infectious Clones for Virulent and Avirulent Pichinde Viruses: a Model Virus To Study Arenavirus-Induced Hemorrhagic Fevers. Journal of Virology 2009; 83: 6357-6362.

[235] Lee K and Torre Jdl. Reverse genetics of arenaviruses. Curr Top Microbiol Immunol 2002; 262: 175-193.

[236] Flatz L, Bergthaler A, de la Torre JC and Pinschewer DD. Recovery of an arenavirus entirely from RNA polymerase I/II-driven cDNA. Proceedings of the National Academy of Sciences of the United States of America 2006; 103: 4663-4668.

[237] Sánchez AB and de la Torre JC. Rescue of the prototypic Arenavirus LCMV entirely from plasmid. Virology 2006; 350: 370-380.

[238] Fisher-Hoch SP and McCormick JB. Lassa fever vaccine. Expert Review of Vaccines 2004; 3: 189-197.

[239] McCormick JB. Clinical, epidemiologic, and therapeutic aspects of Lassa fever. Med Microbiol Immunol 1986; 175: 153-155.

[240] Carrion R, Brasky K, Mansfield K, Johnson C, Gonzales M, Ticer A, Lukashevich I, Tardif S and Patterson J. Lassa Virus Infection in Experimentally Infected Marmosets: Liver Pathology and Immunophenotypic Alterations in Target Tissues. Journal of Virology 2007; 81: 6482-6490.

[241] Carrion Jr R, Patterson JL, Johnson C, Gonzales M, Moreira CR, Ticer A, Brasky K, Hubbard GB, Moshkoff D, Zapata J, Salvato MS and Lukashevich IS. A ML29 reassortant virus protects guinea pigs against a distantly related Nigerian strain of Lassa virus and can provide sterilizing immunity. Vaccine 2007; 25: 4093-4102.

[242] Jahrling PB, Hesse RA, Eddy GA, Johnson KM, Callis RT and Stephen EL. Lassa Virus Infection of Rhesus Monkeys: Pathogenesis and Treatment with Ribavirin. Journal of Infectious Diseases 1980; 141: 580-589.

[243] Jahrling PB, Smith S, Hesse RA and Rhoderick JB. Pathogenesis of Lassa virus infection in guinea pigs. Infection and Immunity 1982; 37: 771-778.

[244] Lukashevich IS, Patterson J, Carrion R, Moshkoff D, Ticer A, Zapata J, Brasky K, Geiger R, Hubbard GB, Bryant J and Salvato MS. A Live Attenuated Vaccine for Lassa Fever Made by Reassortment of Lassa and Mopeia Viruses. Journal of Virology 2005; 79: 13934-13942.

[245] Morrison HG, Bauer SP, Lange JV, Esposito JI, McCormick JB and Auperin DD. Protection of guinea pigs from lassa fever by vaccinia virus recombinants expressing the nucleoprotein or the envelope glycoproteins of lassa virus. Virology 1989; 171: 179-188.

[246] Peters CJ, Jahrling PB, Liu CT, H KR, McKee KT and Barrera Oro JG. Experimental studies of arenaviral hemorrhagic fevers. Curr Top Microbiol Immunol 1987; 134: 5-68.

[247] Pushko P, Geisbert J, Parker M, Jahrling P and Smith J. Individual and Bivalent Vaccines Based on Alphavirus Replicons Protect Guinea Pigs against Infection with Lassa and Ebola Viruses. Journal of Virology 2001; 75: 11677-11685.

[248] Qian C, Jahrling PB, Peters C and Liu C. Cardiovascular and pulmonary responses to Pichinde virus infection in strain 13 guinea pigs. Lab Anim Sci 1994; 44: 600-607.

[249] Lucia HL, Coppenhaver DH, Harrison RL and Baron S. The Effect of an Arenavirus Infection on Liver Morphology and Function. The American Journal of Tropical Medicine and Hygiene 1990; 43: 93-98.

[250] Peters C, Liu C, Anderson G, Morrill J and Jahrling P. Pathogenesis of viral hemorrhagic fevers: Rift Valley fever and Lassa fever contrasted. Rev Infect Dis 1989; 11 Suppl 4: S743-749.

[251] Murphy FA, Buchmeier MJ and Rawls WE. The reticuloendothelium as the target in a virus infection. Pichinde virus pathogenesis in two strains of hamsters. Laboratory investigation; a journal of technical methods and pathology 1977; 37: 502-515.

[252] Jahrling PB, Frame JD, Smith SB and Monson MH. Endemic Lassa fever in Liberia. III. Characterization of Lassa virus isolates. Transactions of the Royal Society of Tropical Medicine and Hygiene 1985; 79: 374-379.

[253] Bowen MD, Rollin PE, Ksiazek TG, Hustad HL, Bausch DG, Demby AH, Bajani MD, Peters CJ and Nichol ST. Genetic Diversity among Lassa Virus Strains. Journal of Virology 2000; 74: 6992-7004.

[254] Hass M, Gölnitz U, Müller S, Becker-Ziaja B and Günther S. Replicon System for Lassa Virus. Journal of Virology 2004; 78: 13793-13803.

[255] Martínez-Sobrido L, Emonet S, Giannakas P, Cubitt B, García-Sastre A and de la Torre JC. Identification of Amino Acid Residues Critical for the Anti-Interferon Activity of the Nucleoprotein of the Prototypic Arenavirus Lymphocytic Choriomeningitis Virus. Journal of Virology 2009; 83: 11330-11340.

[256] McCormick JB, King IJ, Webb PA, Scribner CL, Craven RB, Johnson KM, Elliott LH and Belmont-Williams R. Lassa Fever. New England Journal of Medicine 1986; 314: 20-26.

[257] Liang Y, Lan S and Ly H. Molecular Determinants of Pichinde Virus Infection of Guinea Pigs—a Small Animal Model System for Arenaviral Hemorrhagic Fevers. Annals of the New York Academy of Sciences 2009; 1171: E65-E74.

[258] Tarendeau F, Boudet J, Guilligay D, Mas PJ, Bougault CM, Boulo S, Baudin F, Ruigrok RWH, Daigle N, Ellenberg J, Cusack S, Simorre J-P and Hart DJ. Structure and nuclear import function of the C-terminal domain of influenza virus polymerase PB2 subunit. Nat Struct Mol Biol 2007; 14: 229-233.

[259] He X, Zhou J, Bartlam M, Zhang R, Ma J, Lou Z, Li X, Li J, Joachimiak A, Zeng Z, Ge R, Rao Z and Liu Y. Crystal structure of the polymerase PAC-PB1N complex from an avian influenza H5N1 virus. Nature 2008; 454: 1123-1126.

[260] Sánchez AB and de la Torre JC. Genetic and Biochemical Evidence for an Oligomeric Structure of the Functional L Polymerase of the Prototypic Arenavirus Lymphocytic Choriomeningitis Virus. Journal of Virology 2005; 79: 7262-7268.

[261] Smallwood S, Çevik B and Moyer SA. Intragenic Complementation and Oligomerization of the L Subunit of the Sendai Virus RNA Polymerase. Virology 2002; 304: 235-245.

[262] Smallwood S and Moyer SA. The L polymerase protein of parainfluenza virus 3 forms an oligomer and can interact with the heterologous Sendai virus L, P and C proteins. Virology 2004; 318: 439-450.

[263] Zamoto-Niikura A, Terasaki K, Ikegami T, Peters CJ and Makino S. Rift Valley Fever Virus L Protein Forms a Biologically Active Oligomer. Journal of Virology 2009; 83: 12779-12789.

[264] Tada T, Suzuki K, Sakurai Y, Kubo M, Okada H, Itoh T and Tsukamoto K. NP Body Domain and PB2 Contribute to Increased Virulence of H5N1 Highly Pathogenic Avian Influenza Viruses in Chickens. Journal of Virology 2011; 85: 1834-1846.

[265] Ping J, Dankar SK, Forbes NE, Keleta L, Zhou Y, Tyler S and Brown EG. PB2 and Hemagglutinin Mutations Are Major Determinants of Host Range and Virulence in Mouse-Adapted Influenza A Virus. Journal of Virology 2010; 84: 10606-10618.

[266] Xu L, Bao L, Zhou J, Wang D, Deng W, Lv Q, Ma Y, Li F, Sun H, Zhan L, Zhu H, Ma C, Shu Y and Qin C. Genomic Polymorphism of the Pandemic A (H1N1) Influenza Viruses Correlates with Viral Replication, Virulence, and Pathogenicity <italic>In Vitro</italic> and <italic>In Vivo</italic>. PLoS ONE 2011; 6: e20698.

[267] Edington G and White H. The pathology of Lassa fever. Trans R Soc Trop Med Hyg 1972; 66: 381-389.

[268] Müller S, Geffers R and Günther S. Analysis of gene expression in Lassa virus-infected HuH-7 cells. Journal of General Virology 2007; 88: 1568-1575.

[269] Brunotte L, Kerber R, Shang W, Hauer F, Hass M, Gabriel M, Lelke M, Busch C, Stark H, Svergun DI, Betzel C, Perbandt M and Günther S. Structure of the Lassa Virus Nucleoprotein Revealed by X-ray Crystallography, Small-angle X-ray Scattering, and Electron Microscopy. Journal of Biological Chemistry 2011; 286: 38748-38756.

[270] Buchmeier MJ, de la Torre JC and Peters CJ. Arenaviridae: the viruses and their replication. In: Knipe D, Howley P, editors. Field's Virology. Lippincott Williams & Wilkins; 2007. p. 1791-1827.

[271] Khan SH, Goba A, Chu M, Roth C, Healing T, Marx A, Fair J, Guttieri MC, Ferro P, Imes T, Monagin C, Garry RF and Bausch DG. New opportunities for field

research on the pathogenesis and treatment of Lassa fever. Antiviral Research 2008; 78: 103-115.

[272] Polyak SJ, Zheng S and Harnish DG. 5' termini of Pichinde arenavirus S RNAs and mRNAs contain nontemplated nucleotides. Journal of Virology 1995; 69: 3211-3215.

[273] Meyer BJ and Southern PJ. Concurrent sequence analysis of 5' and 3' RNA termini by intramolecular circularization reveals 5' nontemplated bases and 3' terminal heterogeneity for lymphocytic choriomeningitis virus mRNAs. Journal of Virology 1993; 67: 2621-2627.

[274] Jin H and Elliott RM. Characterization of Bunyamwera virus S RNA that is transcribed and replicated by the L protein expressed from recombinant vaccinia virus. Journal of Virology 1993; 67: 1396-1404.

[275] Green TJ, Zhang X, Wertz GW and Luo M. Structure of the Vesicular Stomatitis Virus Nucleoprotein-RNA Complex. Science 2006; 313: 357-360.

[276] Tawar RG, Duquerroy S, Vonrhein C, Varela PF, Damier-Piolle L, Castagné N, MacLellan K, Bedouelle H, Bricogne G, Bhella D, Eléouët J-F and Rey FA. Crystal Structure of a Nucleocapsid-Like Nucleoprotein-RNA Complex of Respiratory Syncytial Virus. Science 2009; 326: 1279-1283.

[277] Ye Q, Krug RM and Tao YJ. The mechanism by which influenza A virus nucleoprotein forms oligomers and binds RNA. Nature 2006; 444: 1078-1082.

[278] Albertini AAV, Wernimont AK, Muziol T, Ravelli RBG, Clapier CR, Schoehn G, Weissenhorn W and Ruigrok RWH. Crystal Structure of the Rabies Virus Nucleoprotein-RNA Complex. Science 2006; 313: 360-363.

[279] Cisneros GAs, Perera L, Schaaper RM, Pedersen LC, London RE, Pedersen LG and Darden TA. Reaction Mechanism of the ε Subunit of E. coli DNA Polymerase III: Insights into Active Site Metal Coordination and Catalytically Significant Residues. Journal of the American Chemical Society 2009; 131: 1550-1556.

[280] Zuo Y, Zheng H, Wang Y, Chruszcz M, Cymborowski M, Skarina T, Savchenko A, Malhotra A and Minor W. Crystal Structure of RNase T, an Exoribonuclease Involved in tRNA Maturation and End Turnover. Structure 2007; 15: 417-428.

[281] de Silva U, Choudhury S, Bailey SL, Harvey S, Perrino FW and Hollis T. The Crystal Structure of TREX1 Explains the 3′ Nucleotide Specificity and Reveals a Polyproline II Helix for Protein Partnering. Journal of Biological Chemistry 2007; 282: 10537-10543.

[282] Hall TMT. Multiple modes of RNA recognition by zinc finger proteins. Current Opinion in Structural Biology 2005; 15: 367-373.

[283] Matthews JM and Sunde M. Zinc Fingers--Folds for Many Occasions. IUBMB Life 2002; 54: 351-355.

[284] Kawai T and Akira S. Innate immune recognition of viral infection. Nat Immunol 2006; 7: 131-137.

[285] McCartney SA and Colonna M. Viral sensors: diversity in pathogen recognition. Immunological Reviews 2009; 227: 87-94.

[286] Crow YJ and Rehwinkel J. Aicardi-Goutières syndrome and related phenotypes: linking nucleic acid metabolism with autoimmunity. Human Molecular Genetics 2009; 18: R130-R136.

[287] Lee-Kirsch MA, Gong M, Chowdhury D, Senenko L, Engel K, Lee Y-A, de Silva U, Bailey SL, Witte T, Vyse TJ, Kere J, Pfeiffer C, Harvey S, Wong A, Koskenmies S, Hummel O, Rohde K, Schmidt RE, Dominiczak AF, Gahr M, Hollis T, Perrino FW, Lieberman J and Hubner N. Mutations in the gene encoding the 3[prime]-5[prime] DNA exonuclease TREX1 are associated with systemic lupus erythematosus. Nat Genet 2007; 39: 1065-1067.

[288] Lehtinen DA, Harvey S, Mulcahy MJ, Hollis T and Perrino FW. The TREX1 Double-stranded DNA Degradation Activity Is Defective in Dominant Mutations Associated with Autoimmune Disease. Journal of Biological Chemistry 2008; 283: 31649-31656.

[289] Stetson DB, Ko JS, Heidmann T and Medzhitov R. Trex1 Prevents Cell-Intrinsic Initiation of Autoimmunity. Cell 2008; 134: 587-598.

[290] Guilligay D, Tarendeau F, Resa-Infante P, Coloma R, Crepin T, Sehr P, Lewis J, Ruigrok RWH, Ortin J, Hart DJ and Cusack S. The structural basis for cap binding by influenza virus polymerase subunit PB2. Nat Struct Mol Biol 2008; 15: 500-506.

[291] Fechter P and Brownlee GG. Recognition of mRNA cap structures by viral and cellular proteins. Journal of General Virology 2005; 86: 1239-1249.

[292] Yuan P, Bartlam M, Lou Z, Chen S, Zhou J, He X, Lv Z, Ge R, Li X, Deng T, Fodor E, Rao Z and Liu Y. Crystal structure of an avian influenza polymerase PAN reveals an endonuclease active site. Nature 2009; 458: 909-913.

[293] Dias A, Bouvier D, Crepin T, McCarthy AA, Hart DJ, Baudin F, Cusack S and Ruigrok RWH. The cap-snatching endonuclease of influenza virus polymerase resides in the PA subunit. Nature 2009; 458: 914-918.

[294] Lelke M, Brunotte L, Busch C and Günther S. An N-Terminal Region of Lassa Virus L Protein Plays a Critical Role in Transcription but Not Replication of the Virus Genome. Journal of Virology 2010; 84: 1934-1944.

[295] Terwilliger TC and Berendzen J. Automated {MAD} and {MIR} structure solution. Acta Crystallogr. 1999; D55: 849-861.

[296] Emsley P and Cowtan K. Coot: model-building tools for molecular graphics. Acta crystallographica. Section D, Biological crystallography 2004; 60: 2126-2132.

[297] Vagin AA, Steiner RA, Lebedev AA, Potterton L, McNicholas S, Long F and Murshudov GN. {REFMAC5} dictionary: organization of prior chemical knowledge and guidelines for its use. Acta Cryst. 2004; D60: 2184-2195.

[298] Cohen SX, Morris RJ, Fernandez FJ, Ben Jelloul M, Kakaris M, Parthasarathy V, Lamzin VS, Kleywegt GJ and Perrakis A. Towards complete validated models in the next generation of ARP/wARP. Acta Crystallographica Section D 2004; 60: 2222-2229.

[299] Davis IW, Leaver-Fay A, Chen VB, Block JN, Kapral GJ, Wang X, Murray LW, Arendall III BW, Snoeyink J, Richardson JS and Richardson DC. MolProbity: all-atom contacts and structure validation for proteins and nucleic acids. Nucleic Acids Res 2007; 35: W375-W383.